

Fluid Powered Vehicle Challenge:
Team Soulenoid Cycle

A Senior Project
presented to
the Faculty of the Mechanical Engineering Department
California Polytechnic State University – San Luis Obispo

In Partial Fulfillment
of the Requirements for the Degree
Bachelor of Science

By

Kellen Giuliani
Jordan Kochavi
Cayla Quinn
Martin Reyes

May, 2021

Fluid Powered Vehicle Challenge

Team Soulenoid Cycle



Final Design Report 5/9/2021

Jordan Kochavi
jkochavi@calpoly.edu
Martin Reyes
mreyes46@calpoly.edu

Cayla Quinn
cquinn01@calpoly.edu
Kellen Giuliani
kgiulian@calpoly.edu

Instructor:
John Fabijanic
Sponsor:
Jim Widmann

Statement of Disclaimer

Since this project is a result of a class assignment, it has been graded and accepted as fulfillment of the course requirements. Acceptance does not imply technical accuracy or reliability. Any use of information in this report is done at the risk of the user. These risks may include catastrophic failure of the device or infringement of patent or copyright laws. California Polytechnic State University at San Luis Obispo and its staff cannot be held liable for any use or misuse of the project.



Special thanks to:

- Dr. Widmann
- Dr. Fabijanic
- Eric Pulse
- Junnior Rodriguez
- Christine Haas
- Chris Kolbe
- Mark Decklar

Table of Contents

1	Introduction	12
2	Background	13
2.1	Competitors & Current Designs	15
2.2	Vehicle Subsystems	18
2.3	System Identification	25
3	Objectives	29
3.1	Problem Statement	29
3.2	Boundary Diagram	29
3.3	Customer Requirements	30
3.4	Quality Function Deployment (QFD)	30
3.5	Engineering Specifications	30
4	Concept Design Development	35
4.1	Component Selection	35
4.2	Preliminary Hydraulic Circuit Design	46
4.3	Preliminary Frame Design	49
4.4	Preliminary Reservoir Design	53
4.5	Preliminary Circuit Board Design	54
4.6	Preliminary Graphical User Interface Design	55
4.7	Preliminary Electronics Schematic	60
4.8	Preliminary Electronics Enclosure Design	61
4.9	Steering Linkage	63
4.10	Simulated Performance of Concept Design	65
4.11	Risks, Challenges, and Unknowns.	69
5	Final Design	71
5.1	Final Circuit Board Design	71
5.2	Software Design	74
5.3	Final Electronics Enclosure Design	80
5.4	Hydraulic Circuit Design	84
5.5	Reservoir Design	85
5.6	Steering Linkage	86
5.7	Pneumatics	89
5.8	Frame Design	91

6	Manufacturing	95
6.1	Frame Manufacturing	95
6.2	Steering Manufacturing	98
6.3	Hydraulic Reservoir Manufacturing	100
6.4	Component Mounts Manufacturing	101
7	Design Verification	103
7.1	External Leakage	103
7.2	Bike Weight	103
7.3	Sprint Time	103
7.4	Efficiency Score	104
7.5	Endurance Time	105
7.6	Drive Mode Switch Time	106
7.7	Internal Leakage	107
7.8	Pneumatics Pressure	107
7.9	Pinching Points	108
7.10	Drag: Coast Down Time	108
7.11	Accumulator Charge Time	109
7.12	Presentation Score	109
7.13	Electronics Durability	110
7.14	Measurement Accuracy	113
7.15	Durability: Tipping Damage	113
8	Competition Results	115
8.1	Overview of the Virtual Competition	115
8.2	Virtual Competition Results	115
9	Project Management	117
9.1	Project Timeline	117
9.2	Project Management Reflection	117
10	Conclusions and Recommendations	119
	References	121
	Appendix	122

List of Figures

Figure 2.1 Cleveland State's recumbent tricycle, which won first place in 2019.	15
Figure 2.2 Purdue University's recumbent tricycle, 2019.	16
Figure 2.3 Cal Poly, San Luis Obispo's upright bicycle, 2020.	17
Figure 2.4 Milwaukee School of Engineering's upright bicycle, 2020.	18
Figure 2.5 Electrical wiring on the current upright bicycle.	19
Figure 2.6 HydraForce ECDR 0506-A Controller	20
Figure 2.7 Screen capture of existing valve driver software.	21
Figure 2.8 1.3-gallon reservoir designed by the Incompressibles in 2018.	21
Figure 2.9 Upright bicycle frame, built by The Incompressibles, 2019.	24
Figure 2.10 Recumbent tadpole (left), and delta trike (right), recumbent designs.	24
Figure 2.11 Simscape model of sprint challenge.	26
Figure 2.12 Simscape model of accumulator charge.	26
Figure 2.13 Predicted results of the spring challenge with a recumbent frame.	28
Figure 2.14 Predicted vehicle velocity with respect to time using a recumbent frame.	28
Figure 3.1 Vehicle system boundary diagram.	30
Figure 4.1 OPUS A3F Wachendorff display unit.	35
Figure 4.2 SparkFun CAN bus shield for the Arduino Uno.	36
Figure 4.3 Arduino Nano with ATmega328 (left) and STM32 Blue Pill (right).	36
Figure 4.4 ST-Link module used to program the STM32 Blue Pill development board.	37
Figure 4.5 MCP2551 (left) and TJA1050 (right) CAN transceivers.	37
Figure 4.6 MCP2515 and TJA1050 CAN bus breakout module.	38
Figure 4.7 2.8-inch TFT display with ILI9341 LCD driver.	38
Figure 4.8 Nextion LCD.	39
Figure 4.9 Nextion Editor HMI Software.	39
Figure 4.10 Predicted performance in sprint challenge using hydraulic hardlines.	40
Figure 4.11 Predicted maximum velocity using hydraulic hardlines.	40
Figure 4.12 Comparison of accumulator weights (lbs), varied by material.	41
Figure 4.13 Volumetric efficiency curve for Bosch pump/motor.	43
Figure 4.14 CAD render of the HydraForce manifold, installed on the 2019 vehicle.	44
Figure 4.15 Delta tricycle 3D printed model.	45
Figure 4.16 Tadpole tricycle 3D printed model.	45
Figure 4.17 3D printed steering linkage model.	46
Figure 4.18 Hydraulic circuit in Direct Drive mode, concept design.	46
Figure 4.19 Hydraulic circuit in Accumulator Discharge mode, concept design.	47
Figure 4.20 Hydraulic circuit in Regenerative Braking mode, concept design.	47
Figure 4.21 Hydraulic circuit in Coast mode, concept design.	48
Figure 4.22 Hydraulic circuit in Pedal Charge mode, concept design.	48
Figure 4.23 Preliminary recumbent frame design.	49
Figure 4.24 Orthographic profile of preliminary frame design.	50
Figure 4.25 Orthographic top view of preliminary frame design.	50
Figure 4.26 Preliminary mechatronics interface layout.	51
Figure 4.27 Predicted static loading on preliminary frame design.	51
Figure 4.28 Predicted frame displacement due to static loading.	52
Figure 4.29 Preliminary motor mount design.	52
Figure 4.30 Results of FEA of preliminary motor mount design.	53
Figure 4.31 Preliminary reservoir design.	53
Figure 4.32 PCB design with Arduino Nano.	54
Figure 4.33 JST-XH snap-fit wire connectors, 4-pin.	55
Figure 4.34 Preliminary home screen page.	56

Figure 4.35 Preliminary error diagnosis page.....	56
Figure 4.36 Preliminary pressure monitoring page.	57
Figure 4.37 Preliminary flowrate monitoring page.	57
Figure 4.38 Preliminary data plotting page.	58
Figure 4.39 Testing with preliminary touch screen interface.	58
Figure 4.40 Preliminary schematic of vehicle electronics.....	60
Figure 4.41 Preliminary enclosure design, exploded view.....	62
Figure 4.42 Preliminary button module enclosure, exploded view.	62
Figure 4.43 Preliminary component placement of electronics.	63
Figure 4.44 Direct vs. indirect steering linkages.	63
Figure 4.45 Diagram of Ackermann steering linkage geometry.	64
Figure 4.46 Preliminary steering design that implements center-point steering.	64
Figure 4.47 Preliminary steering design that implements a caster angle of 10 degrees.....	65
Figure 4.48 Orthographic view of preliminary steering design.....	65
Figure 4.49 Predicted performance of concept design in the sprint challenge.	66
Figure 4.50 Predicted performance of concept design in the endurance challenge.....	67
Figure 4.51 Predicted ability of the accumulator to meter its discharge.	67
Figure 4.52 Predicted performance of concept design in the efficiency challenge.	68
Figure 5.1 Complete render of final vehicle design.	71
Figure 5.2 Final PCB design that uses an STM32 development board.	72
Figure 5.3 Render of final PCB design, populated with 3D models of electrical components.	72
Figure 5.4 Breadboard prototype of CAN interface.	73
Figure 5.5 Photograph of final circuit board after assembly.	73
Figure 5.6 Inter-controller system boundary diagram.	74
Figure 5.7 High-level task diagram.	75
Figure 5.8 State transition diagram for hall effect sensor task.	76
Figure 5.9 Pressure transducer calibration curve.....	77
Figure 5.10 Screen captures of five pages from the interface's GUI.	78
Figure 5.11 USB to serial converter that is used to program the Nextion display.	78
Figure 5.12 Render of 3D printed enclosure for the printed circuit board.	80
Figure 5.13 Exploded view of 3D printed interface enclosure.....	80
Figure 5.14 Render of 3D printed button module enclosure.	81
Figure 5.15 Exploded view of 3D printed button module enclosure.....	81
Figure 5.16 3D printed screen stand.....	82
Figure 5.17 Photograph of the 3D printed interface enclosure.....	82
Figure 5.18 Photograph of the interface mounted on the right handlebar.....	83
Figure 5.19 Photograph of the location of the ECDR 0506-A and battery underneath the seat.	84
Figure 5.20 1/4" NPT aluminum weld-on fitting.....	85
Figure 5.21 JIC male to NPT male straight adapter.	85
Figure 5.22 Modified pump inlet port to join the pump return.	86
Figure 5.23 Front view of final steering linkage render.	86
Figure 5.24 Side view of final steering linkage render.....	87
Figure 5.25 The lowered tie rod avoids interference with the pump and chain.	87
Figure 5.26 Steering link with Ackerman geometry.	88
Figure 5.27 CAD render that demonstrates how the steering link connects to the frame.	88
Figure 5.28 Aluminum tie rod with threaded ends.	88
Figure 5.29 Steering link with mounted brake caliper.	89
Figure 5.30 Left steering link without a mounted brake caliper.....	89
Figure 5.31 Pneumatic circuit to actuate a parking brake.....	90
Figure 5.32 Bimba 171 single-acting air cylinder with a 1.5" bore diameter.....	91
Figure 5.33 Bimba D-5096-A-5 with an attached Schrader valve.	91

Figure 5.34 Profile view of final frame design, in CAD.	91
Figure 5.35 Hand-drawn sketch of seat angle and component room.	92
Figure 5.36 Profile of final frame design, in CAD with rider.	93
Figure 5.37 Estimated structural loading on final frame design.....	93
Figure 5.38 Benefits of switching some of the frame's square tubing to round tubing.	94
Figure 6.1 Annotated CAD render indicating material types on the frame.....	95
Figure 6.2 Using a chop saw to cut steel tubing stock.....	96
Figure 6.3 The two planes of the frame were welded separately.	96
Figure 6.4 MIG welding was used to weld all steel components on the frame.	96
Figure 6.5 A hole saw on a mill was used to notch the ends of the round tubing.	97
Figure 6.6 Completed frame welding, without the steering linkage.....	97
Figure 6.7 Vehicle stands on front wheels, without steering linkage.	99
Figure 6.8 Manufactured steering linkage with adjustable tie rod.	99
Figure 6.9 Photograph of completed steering linkage.	100
Figure 6.10 Waterjet cutting of the reservoir pieces.....	101
Figure 6.11 Fully assembled reservoir after welding.	101
Figure 6.12 Accumulator mounted vertically behind the seat.	102
Figure 6.13 Pump mounted underneath the seat.....	102
Figure 7.1 Google Earth aerial view of the 500-ft test course.....	104
Figure 7.2 Google Earth aerial view of the efficiency challenge test course.	105
Figure 7.3 Google Earth aerial view of the endurance challenge test course.	105
Figure 7.4 Google Earth aerial view of coast-down test location.....	108
Figure 7.5 Button module used for testing.	111
Figure 7.6 Button module after exposure to light splashing.....	111
Figure 7.7 Button module successfully protects circuitry after light splashing.	111
Figure 7.8 Button module turned on its side and exposed to direct flow.	112
Figure 7.9 Button module successfully protects circuitry after faucet flow directed at its profile.....	112
Figure 7.10 Button module exposed to direct faucet flow on the buttons.	112
Figure 7.11 Soaked contents of the button module after direct top-down faucet flow.	113

List of Tables

Table 2.1 Summary of NFPA's 2021 competition cash prizes.	14
Table 2.2 System parameters that were modified to model a recumbent frame.....	27
Table 3.1 Tabulated engineering specifications.	31
Table 4.1 Accumulator decision matrix.....	41
Table 4.2 Decision matrix to compare the current pump type (axial piston) to linear and gear pumps.....	42
Table 4.3 Estimated pressure loss for each drive mode at 1.3-gpm.	44
Table 4.4 Decision matrix comparing belt and gear drive methods.	44
Table 4.5 Results of speed testing conducted on ILI9341 TFT display.	59
Table 4.6 Comparison of model parameters used in the 2019 and 2020 vehicles.....	66
Table 4.7 Weight estimates of preliminary frame design.....	68
Table 4.8 Design hazard corrective action plan.....	70
Table 5.1 Table of variables defined in the Nextion's software with descriptions of their usage.....	79
Table 5.2 Measured component dimensions to determine the driving frame dimension.	92
Table 6.1 Stock material used for the vehicle frame.	95
Table 6.2 Stock components used to manufacture the reservoir.	100
Table 7.1 Accumulator charge times.	109
Table 8.1 Awards won at the 2021 competition.	116

Abstract

The National Fluid Power Association is a trade association that unifies customers and manufacturers within the hydraulics industry. Extending their partnership to universities, the annual Fluid Powered Vehicle Competition challenges college teams to design, build, and test a fluid-powered vehicle with the goal of educating students about the hydraulics industry and building career connections. Soulenoid Cycle produced the next iteration of Cal Poly's fluid powered vehicle for the 2021 competition.

This report summarizes research, ideation, component selection, initial and final design, manufacturing, and competition results conducted by Soulenoid Cycle. Relevant research includes successful current and past vehicles, the operation of a hydraulic propulsion system, and popular controller and sensor choices for hydraulic systems.

Based on the requirements of the competition, performance of competitors, and guidance from a previous Cal Poly team, Soulenoid Cycle identified three major areas of improvement for this year's competing vehicle: sprint time, hydraulic efficiency, and mechatronics.

Development of the goals and objectives discussed in this report were critical to the success of this project. By solidifying a foundation of preliminary research, defining the scope of work, and making initial design and component selections, Soulenoid Cycle was successful when approaching final vehicle design and manufacturing, and the 2021 Fluid Powered Vehicle Competition.

1 Introduction

This project includes the design and testing of a hydraulically powered vehicle to compete in the 2021 Fluid Powered Vehicle Challenge. The NFPA and Cal Poly SLO are responsible for providing the necessary funding for the production of this team's vehicle, and the team looks to the industry sponsor and the senior project advisor, Dr. Jim Widmann, for expertise and safety checks. This report serves to describe the project process from start to finish.

The Background section describes the Fluid Powered Vehicle Challenge, including its history, relevance, and objectives. This section also summarizes research conducted by the team including meetings and interviews, current competitors, descriptions of the various components within a typical fluid powered vehicle, and areas of interest within the scope of this project. The Objectives section describes what Soulenoid Cycle intends to accomplish, including engineering specifications, target goals, and means of measuring their success. The Concept Design section reviews additional research, decision making processes, and ultimate component choices. The Final Design section presents detailed descriptions of all design choices, as well as how each component and subsystem is manufactured. Engineering drawings are located in appendices but are referenced in this section.

2 Background

Background research was conducted on the challenge itself, Cal Poly's history in the competition, and vehicles from previous teams. After the Preliminary Design Review, this section was updated to include new rules and requirements for the 2021 competition. In addition, this section was updated to include descriptions of components and subsystems on the 2019 vehicle that will be improved upon by the 2020-21 vehicle.

The Fluid Powered Vehicle Challenge was initially started in 2004 by Parker Hannifin, a leading corporation in mechanical controls. It was called: The Chainless Challenge, where the primary competition goal was to design a bicycle that omits the use of power transmission via chains. The National Fluid Power Association (NFPA) took over the responsibilities in 2016. The NFPA now hosts the Fluid Powered Vehicle Challenge every year targeted as a college university senior capstone project. Its purpose is to challenge students to work as a team to apply their engineering skills to design, build, and test a fluid powered vehicle. By doing so, students are exposed to the hydraulic industry through hands-on learning and contact with industry representatives.

Soulenoid Cycle is designing with the initial 2020 competition rules in mind. These rules were modified after their initial release in response to the COVID-19 pandemic. They were adjusted so that students could still present their vehicle design process through a virtual video conference even if the vehicle was not complete. The official rules for 2021 competition will not be available until late Summer or early Fall of 2020. Since the event competition last year was canceled, Dr. Widman has assured the team that it is safe to assume the rules will not significantly change from previous years. An additional assumption is that the COVID-19 restriction will be cleared, and the competition event will happen in the Spring of 2021.

The single person vehicle must be fluid propelled by either hydraulics or pneumatics with human input as the only power to move the fluid. Electric or combustion motors are not allowed to propel the vehicle. Chains, belts, and gears are allowed but cannot directly transfer power from the user's input to the drive wheel. The vehicle must also contain an energy storage device, or accumulator. The maximum volume is 1 gallon (3.7854 liters), and its use must not exceed the manufacturer's recommendation. Regarding drive modes, the rules require a direct drive mode that uses a human powered pump to drive a motor, a boost mode that directly uses the accumulator discharge for propulsion, and a regenerative braking mode that recharges the accumulator while operating the vehicle. The vehicle weight limit (without rider) is set to 210 lbs with penalties for additional weight.

The competition consists of a midway review, final presentation, and three event challenges to judge the vehicle's sprint, endurance, and efficiency performance. The sprint challenge measures how fast the vehicle can travel a 400-600 foot straight-away. The quickest time is awarded first place. The efficiency challenge determines how efficiently the vehicle is able to use its stored energy to propel the total weight of the vehicle forward. The vehicle and rider are weighed, and the accumulator's size and pre-charge are noted before this challenge. The total distance the vehicle travels on accumulator discharge only is recorded and formulated with the other parameters to get an overall efficiency value. The highest efficiency value wins first place for the challenge. In the last challenge, the vehicle is tested for its durability and reliability. The vehicle is timed to see how fast it can complete a slalom style course about a mile long. Additionally, the regenerative braking is tested in this challenge by starting the vehicle off with no hydraulic fluid in the accumulator. At some point, it is expected that the vehicle would stop and travel a couple of feet on accumulator discharge only before continuing in direct drive mode to the end of the course. The team with the quickest time to complete the mile long course wins the endurance challenge. A new award was sponsored by industry partner, Bimba, last year for the team with the best use of pneumatics on their vehicle. The final and midway

presentations are evaluated along with the challenge performances to evaluate overall 1st, 2nd, and 3rd place winners.

Teams are given cash prizes for placing in the top three along with other events which are presented in Table 2.1. The biggest reward is given to the overall winners of the event along with the individual challenge winners. However, other areas like presentation, safety, and teamwork are also awarded totaling to \$13,500 to be awarded for the competition.

Table 2.1 Summary of NFPA's 2021 competition cash prizes.

AWARD	PRIZE	CONSIDERATIONS
Overall Champion 1 st place 2 nd place 3 rd Place	\$3,000 \$2,000 \$1,000	First place overall champion will not be eligible to win more than one of the following: sprint race, endurance or efficiency challenges. Funds will be distributed directly to team participants.
Best Presentations	\$2,000	Midway review score to be included in evaluating the winning presentation. Funds will be distributed directly to team participants.
Sprint Race	\$1,000	Top three scores to be considered for placement. Final 1st place will be determined by a number of factors, including Overall Champion.
Efficiency Challenge	\$1,000	Top three scores to be considered for placement. Final 1st place will be determined by a number of factors, including Overall Champion.
Endurance Challenge	\$1,000	Top three scores to be considered for placement. Final 1st place will be determined by a number of factors, including Overall Champion.
Best Use of Pneumatics, Sponsored by Bimba	\$500	To be considered for award, teams must display creativity, efficiency, and safety. Funds will be distributed directly to team participants.
Best Design	\$500	To be considered for award, teams must display innovation, uniqueness and originality of the design. Selected by Student Teams.
Best Reliability and Safety	\$500	To be considered for award, teams must take sufficient steps to prevent injuries from hardware and surpass a 1-year warranty.
Best Workmanship	\$500	Best degree of skill, expertise and quality in vehicle.
Best Teamwork	\$500	Best attitude and team cohesiveness.
11 Awards	\$13,500	

2.1 Competitors & Current Designs

Solenoid Cycle chose to investigate some of the top competitors from the last two years of competition, including Cleveland State University, Purdue University, Cal Poly's previous team, and the Milwaukee School of Engineering.

2.1.1 Cleveland State University [2018-2019]

The 2019 Cleveland State Team transitioned the previous year's vehicle from a standard bike design to a recumbent tricycle design. The main objectives, as designated by the team, were to increase the amount of stored energy and to make the vehicle easier to operate. The team replaced three main components after careful analysis and chose to use a bent axis displacement pump, a manual ball valve, and a 2.5-gallon accumulator. The accumulator was charged via chain and sprocket, which was powered by the pedals at the front of the vehicle.

With this design, Cleveland placed 1st overall in the 2019 competition. The team won the sprint challenge with a time of 14.71 seconds. The top competitors in the round had fast accelerations, which meant large accumulators and minimal weight. After the 2019 competition, accumulator sizes were limited to 1 gallon. Cleveland also placed second in the endurance challenge and the efficiency challenge. The efficiency score was calculated with an equation that has since changed, but the team did replace their 2.5-gallon accumulator with a 0.5-gallon accumulator for this challenge in an effort to increase their distance to weight ratio.

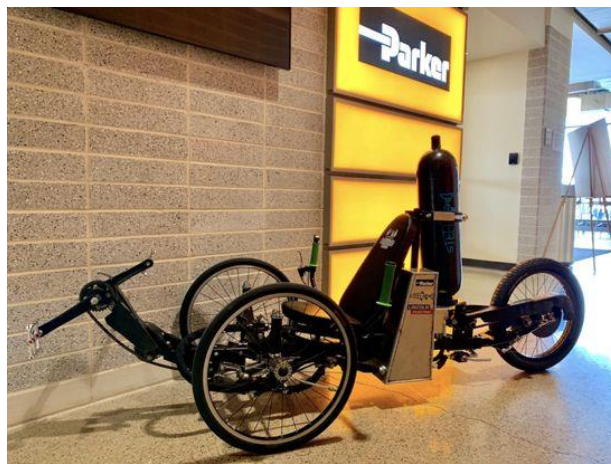


Figure 2.1 Cleveland State's recumbent tricycle, which won first place in 2019.

The 2018-2019 Cleveland team suggested that future teams should increase the back-end gear ratios for the hydraulic pump, adjust the motor operation, move the idler gear, and relocate the bearing housing.

2.1.2 Purdue University [2018-2019]

In the 2019 competition, Purdue University produced a recumbent tricycle, with the primary goal of reducing overall weight. Their hydraulic circuit used two 1.3-gallon accumulators, with a clutch system that engaged with the regenerative pump. The circuit also included two hand pumps that circulated fluid from the reservoir to the accumulators. Their selected hand pumps provided 7.5 cc/stroke, and their regenerative pump required 7.54 cc/rev. Their selected hydraulic motor provided 3.12 cc/rev.

The tricycle design is advantageous because it allows for larger, heavier components with greater energy storing capacity. In addition, in a recumbent vehicle, the rider's arms are free to contribute to propulsion by pumping or cranking, which provides more power to the vehicle. The vehicle includes three different drive modes: charging, boost, and regeneration.

The charging mode fills the accumulators with two hand pumps. The use of hand pumps allows for the vehicle to be charged in a stationary position. Most teams charge their vehicles by physically pushing them around or cranking the pedals in a stationary position. Though hand pumps likely contribute more weight to the vehicle, they provide an easy and efficient means of charging. The boost mode allows the accumulators to discharge directly to a hydraulic motor that drives the rear wheels. The pump mode powers the hydraulic motor, while also allowing the rider to use the hand pumps to recharge the accumulators. In regeneration, the clutch system routes fluid to a regenerative pump that is driven by the front wheel, which recharges the accumulators.



Figure 2.2 Purdue University's recumbent tricycle, 2019.

Purdue's vehicle reduced overall weight by building their frame entirely out of aluminum tubing. Their mechatronics system served to primarily control valves for each drive mode, though also measured the accumulator and mainline pressures. Extra features included measuring bike speed with a hall-effect speed sensor, and the user heart rate with a sensor mounted to the handlebars.

2.1.3 Cal Poly, San Luis Obispo [2019-2020]

The 2019-2020 Cap Poly team, Pump My Ride, did not place in the top three in the virtual competition. However, they were awarded Judge's Choice in Teamwork for exhibiting effective communication, quality answers to questions, participation in mentor meetings, and a cohesive final presentation. Pump My Ride believe their overall score would have ranked better if the competition were not changed to a virtual one since they designed for the competition events. The steel frame used by Pump my ride was reused from the 2018-2019 Cal Poly Team: The Incompressibles.

The custom-built frame was originally inspired by combining the benefits of mountain and road bicycles. For the hydraulic system, Pump My Ride designed a custom manifold from HydraForce to minimize the hydraulic line lengths and number of fittings reducing the overall pressure losses. Hard lines were originally planned to be implemented; however, Pump My Ride had to stay with soft lines due the delivery delay time of the manifold. The drive modes remained the same from the Incompressibles: boost, regenerative braking, direct drive, and coast. To control the drive modes, Pump My Ride switched to an ECDR-0506A industrial controller from HydraForce. After exposure to the elements ruined the custom PCB board built by the Incompressibles, Pump My Ride built a simple switch box to toggle between the drive modes. To deliver the power, they stayed with a bent-axis axial piston Bosch unit for both the pump and motor. The

accumulator Pump My Ride used was a 1-gallon composite bladder accumulator manufactured by Steelhead with a rated pressure of 3000 psi. They added tribars to decrease drag and improve the ergonomics of the vehicle at higher speeds. For safety, Pump My Ride had intended to add a front chain cover to eliminate pinching points and the possibility of the rider's pants or shoelaces getting tangled. The total vehicle weight increased from the Incompressibles' from 100 pounds to 103 pounds.



Figure 2.3 Cal Poly, San Luis Obispo's upright bicycle, 2020.

Pump My Ride performed several tests before stopping for the COVID-19 pandemic providing some benchmark scores regarding their vehicle's performance. Their sprint time was 21.96 seconds to complete their 600-foot test course by using the lightest rider and greatest pre-charge pressure (500 psi) in the accumulator. It took 5 minutes and 40 seconds to complete a 1-mile course that simulated the endurance challenge. Their result was 45 seconds slower than their simulated nominal value. Pump My Ride scored an efficiency score of 12.17% by traveling 1800 feet which fell short of their 18% goal.

The 2019-2020 Cal Poly team recommended implementing a pneumatic brake system along with completing their intended hydraulic hardlines. Regarding the mechatronics, a few recommendations were given: routing the wiring through cable lines is a safer and more aesthetic addition to the vehicle and installing an LCD screen along with refinement of the software to eliminate bugs or adjust drive modes is an essential addition for performance testing and vehicle ease of use.

2.1.4 Milwaukee School of Engineering [2019-2020]

The 2019-2020 Milwaukee team did not place in the top three in the virtual competition; however, they were awarded the Best Presentation award. This year was the second year Milwaukee competed, so they had a good foundation to build upon, and although their design is similar to the 2018-2019 team's, they almost completely rebuilt their vehicle, reusing only their manifold, pump, and motor.

Milwaukee's design revolved around creating a clean and compact vehicle while minimizing weight. One significant change from their 2018-2019 team involved a complete rebuild of their bike frame. They used a standard road bike frame as a base, modifying it only with two custom designed mounting plates for their motor and pump which they welded onto the frame. Other custom fabrication included a hydraulic fluid reservoir with a geometry designed to maximize fluid capacity based on their component layout. They intended to add one other piece of fabrication to the frame in order to mount a pneumatic cylinder which would act as a shock absorber for the seat. However, due to COVID-19, they were denied access to the machine shop before they could complete the addition.



Figure 2.4 Milwaukee School of Engineering's upright bicycle, 2020.

Milwaukee used a 1-quart accumulator with an assumed nitrogen pre-charge of 1500 psi and an assumed oil charge of 3000 psi, which they predicted would allow them to reach a top speed of around 20 mph during discharge in the sprint race. Lastly, their hydraulic circuit utilized hardlines everywhere except between the reservoir and pump. Milwaukee's control circuit allowed for four different drive modes: direct drive, regenerative braking, accumulator charging, and accumulator discharging. These modes were engaged by actuating three different solenoids controlled using an Arduino circuit that sent signals by mechanical switches. Their control system also integrated an LCD display and two pressure gauges to monitor drive mode and hydraulic conditions. Although Milwaukee's bike could not compete due to COVID-19, and therefore the efficacy of their design is still in question, one can assume that they would not have performed particularly well in the sprint challenge due to their smaller accumulator. Conversely, they most likely would have performed much better in the efficiency challenge due to their implementation of hardlines, and their lightweight and aerodynamic build.

2.2 Vehicle Subsystems

Designing for such a unique application requires extensive background knowledge about each of the components for the overall system. The following information allows Soulenoid Cycle to make design decisions based off of the components that Pump My Ride used on the previous vehicle.

2.2.1 Mechatronics

Most current designs use an electronic control system to actuate valves in the hydraulic system. Common microcontrollers such as Raspberry Pi and Arduino are effective in receiving sensor telemetry and outputting digital and analog commands to various electrical components. In the 2019 competition, Purdue University's vehicle was controlled with a Raspberry Pi, which controlled solenoid valves and logged data from a speed sensor and heart rate monitor.

The task of switching between drive modes by manipulating valves adds another degree of complexity to riding a bicycle. An effective control system would alleviate this complexity by either automating this process or making it effortless in the context of normal bicycle operation. In addition to controlling the hydraulic circuitry, feedback from sensors provides valuable insight into the real operation of the vehicle, which can be used to correct and improve models.

There are two possible routes to pursue with regard to selecting an appropriate main controller. Low-voltage, open-source microcontrollers, such as Arduino or Raspberry Pi, are effective for low-voltage sensors and outputs. However, hydraulic control applications in industry use Programmable Logic Controllers (PLCs). PLCs are larger controllers that can support a wide range of power outputs and inputs; some can output 12-24 Volt signals without external circuitry or other power supplies. These controllers are ubiquitous in industry applications because they are simple, self-contained assemblies that can be programmed with “Block Diagram Programming”, similar to MATLAB’s Simulink, rather than with line-code. In the 2020 competition, Cal Poly’s vehicle used a PLC to control valves. In contrast to Raspberry Pi and Arduino, PLCs are not open source, and are more difficult to interface with other controllers, thereby limiting the functionality of a mechatronics system.

The current upright bicycle, most recently revised by 2019’s team, Pump My Ride, controls the hydraulic circuit with an industrial PLC. The rider provides input with four pushbuttons, that inform the controller which drive mode to actuate. Wiring four independent input signals requires the use of 10 GPIO pins on the PLC, including the high/low signal for each input, reference voltage, and ground. This uses the majority of the GPIO pins on the PLC and requires several feet of cabling to run between the handlebars and the controller. The cabling present on the current upright bicycle is visible below in Figure 2.5.



Figure 2.5 Electrical wiring on the current upright bicycle.

The presence of excessive wiring makes signals more difficult to track. When debugging complex mechatronics systems, it is desirable to keep wiring as simple as possible. Furthermore, more wiring increases the vulnerability of the electronics. Loose connections and splayed wires can result in signal loss or degradation, which can significantly affect the operation of the vehicle. This demonstrates a need to reduce the amount of wiring used onboard.

Pump My Ride achieved a highly effective control system using an ECDR 060A controller. The controller actuates different valves based on which drive mode is selected by the user. The ECDR 0506-A, as shown below in Figure 2.6, is categorized as a Programmable Logic Controller (PLC). PLCs are highly durable because all circuitry is fully encased and protected. PLCs range in functionality and can be easily programmed through a graphical, block-diagram interface.



Figure 2.6 HydraForce ECDR 0506-A Controller

The existing mechatronics system is effective because all its components, including valves and hardware connections were fully designed and supported by HydraForce. All electrical connections are stable and durable, and the system is well-suited for the vehicle since all components were specifically designed for hydraulic control systems. The reliability and durability of the current mechatronics system is consistent with Soulenoid Cycle's goals to achieve a high level of protection for all electrical components from harsh weather conditions.

The current mechatronics system is most lacking in data acquisition from sensors and a graphical user-interface that displays data to the rider. Though sensors can be easily integrated into the current controller, the limitations of the ECDR 060A inhibit the development of a robust, customized interface. Other open-source platforms, such as Arduino or Raspberry Pi, are more effective in these applications; line code and an infinite diversity of external components and modules are advantageous in designing a customizable control system.

Soulenoid Cycle's greatest concern about open-source platforms is durability. Since they are entirely modular, these platforms require soldering, wiring, and coding that are vulnerable to power shorts and software bugs, which can result in a fragile and unreliable system. However, with careful design considerations, these platforms can be used to create highly robust and effective control systems.

A screen capture of part of the programming for the PLC is shown below in Figure 2.7. The block programming below is installed on the ECDR 0506-A onboard the current 2019 upright bicycle. The software used for this controller is HF Impulse, a tool designed by HydraForce to interface with their controllers. In the program below, the accumulator discharge mode, or boost mode, is referred to as "Ludacris Mode." This drive mode corresponds to an integer value of 1; regenerative braking and direct drive correspond to 2 and 3, respectively. Since Variable 4 is initialized with the value of 1, which is visible in the diagram below, the program immediately switches to boost mode on startup. If the accumulator is charged, then the bike will immediately start moving when the battery is plugged in, which presents a safety hazard. Soulenoid Cycle will fix this error and ensure that the vehicle starts in direct drive.

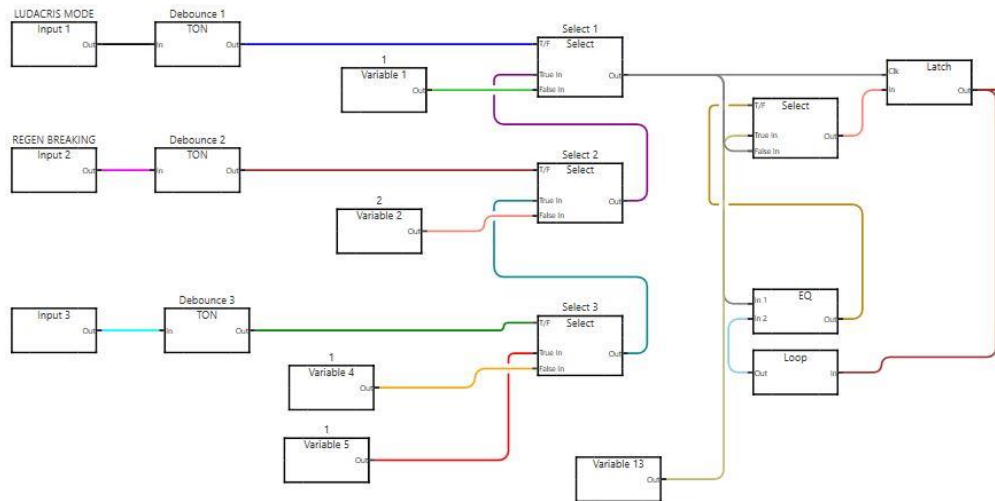


Figure 2.7 Screen capture of existing valve driver software.

2.2.2 Hydraulic Circuit

According to NFPA's rules, three drive modes are required: direct drive, regenerative braking, and accumulator discharge. Additional drive modes such as coasting or a hybrid charge can be included. The hydraulic circuit consists of the hardware that directs the hydraulic fluid from the reservoir to make the different drive modes possible. The main components consist of the pump, motor, accumulator, and valves. Each component is detailed in the following sections. Some consideration is needed for the hydraulic circuit lines. The lines transport the fluid to different parts of the circuit. Excessively long hydraulic lines and sharp bends cause additional pressure losses in the system which decrease the overall efficiency.

2.2.2.1 Fluid Reservoir

The hydraulic circuit requires a neutral pressure reservoir to draw fluid from. Hydraulic fluid is drawn from the reservoir, pumped through the circuit, and returned to the reservoir. The current reservoir, shown below in Figure 2.8, was designed by the Incompressibles in 2018 to fit the geometry of the upright bicycle frame.

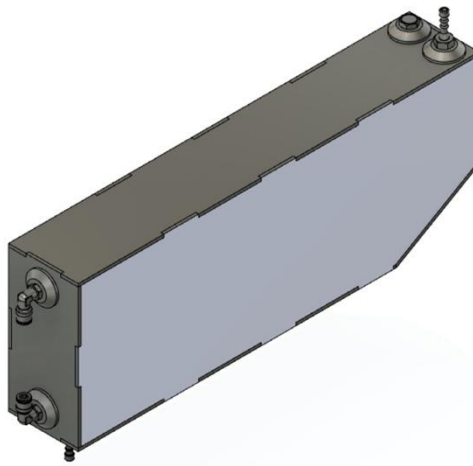


Figure 2.8 1.3-gallon reservoir designed by the Incompressibles in 2018.

The reservoir was manufactured from 1/8" thick aluminum sheet metal. The pieces were cut using a Waterjet and tig welded together. After welding, the exterior of the reservoir was coated in a sealant to prevent leaks. There are five orifices in this reservoir, made from weld-on threaded inserts. The two ports on the far left of the reservoir house a sight tube, which allows the rider to examine the fluid level inside the tank. A drain port on the bottom of the reservoir is connected to the pump, which draws fluid from the reservoir and sends it through the hydraulic circuit. A return port on the top right of the reservoir returns fluid after it flows through the circuit. Lastly, a drain is present in case the reservoir is too full.

While this reservoir design is effective and works well on the current upright bicycle, its long and narrow geometry does not conform well to a recumbent vehicle. A new reservoir will be designed to include the same features and functionality as the current one, while better fitting a new vehicle frame.

2.2.2.2 Pump and Motor

Since the vehicle cannot be driven by traditional sprockets and chains, the most common system for the NFPA competition utilizes a hydraulic pump and motor to move hydraulic fluid in the system. The pump is human powered which creates the pressure in the system that pushes the hydraulic fluid from the reservoir to a hydraulic motor or any other part of the circuit. The motor does the opposite of a pump by converting the fluid energy back to mechanical work in the form of a rotating shaft and by extension, a wheel. A variety of hydraulic motors and pumps exist. Gear motors and pumps use meshed gears and a pressure difference from the flowing hydraulic fluid to rotate a gear with an attached drive shaft. Gear pumps and motors work well in high speeds and pressures but tend to wear out faster due to the friction of the gears.

Vane motors and pumps are similar except they use a single gear-like vane which is off-centered. The varying volume of the vane as it rotates creates a pressure difference in the fluid. They are used for low viscosity fluids and are more complex in design. Piston pumps and motors use pistons that are attached to a cylinder block. The cylinder block fills with hydraulic fluid at one side of its cycle pushing the piston outward in a linear motion. The force of the piston pushes against a stationary swash plate situated at an angle. This causes the piston to slide, rotating the cylinder block and the attached shaft. These pumps and motors can come in either in-line or bent-axis configurations. The radial pump/motor uses cylinders configured perpendicularly around a shaft. Fluid enters and leaves the pistons causing the pistons to actuate back and forward. The pistons are timed at different intervals where their linear motion is transferred to a shaft by a cam. The last piston style pump commonly used is the linear piston. This design is similar to a floor jack where a mechanical input causes a piston to move. The linear piston movement creates pressure in the system as it compresses and expands the volume of the cylinder. The linear piston is used more as a pump since the rider needs to input the mechanical energy to move the piston.

The previous Cal Poly teams have used Bosch piston units in a bent-axis configuration for both the pump and motor because of its good efficiency at wide ranges of flowrate and smooth pressure delivery. Furthermore, the bent-axis configuration allows the piston to expand further in each cycle resulting in greater displacement and torque when compared to the in-line configuration. Other schools like Arizona State University choose to pair a gear pump with a bent-axis piston motor. Although gear pumps/motors are simpler in design and cheaper in price when compared to the piston pumps/motors, their max pressure ratings are typically smaller and are less versatile when flow rates vary.

2.2.2.3 Accumulator

Per the competition rules, all vehicles must have an energy storage device. Since the project is centered around hydraulics, this energy-storage device used by all of the teams is an accumulator. There are two major types of accumulators that have been used in the competition, piston accumulators and bladder

accumulators. While piston accumulators consist of a cylindrical body with a lightweight piston separating the fluids, bladder accumulators contain a flexible bladder in a hard shell. Piston accumulators can be used for higher flow rates and have compression ratios of up to 10:1, compared to bladder accumulator compression ratios of 4:1. The advantages of bladder accumulators are their universal application and light weight. The NFPA specifies a maximum accumulator size of 1 gallon, so the variation for teams to decide on is in the type of accumulator and the amount of pre-charge. Typically, the teams with the largest amount of stored energy perform best in the sprint race, which is one of the reasons there is a maximum accumulator size.

2.2.3 Brakes

There are a few different approaches in regard to bicycle braking method and design. The simplest and most common approach is the cable actuated rim brake. Cable actuated brakes are simple, reliable, inexpensive, and easy to maintain and replace. Their downside lies in their smaller potential for mechanical advantage, resulting in a lower peak braking force than other designs. The other commonly used bicycle brake is the disc brake. Disc brakes can be cable driven; however, they most commonly are driven using hydraulics. The primary advantage of disc brakes is their superior modulation capability, allowing for greater peak braking force while also affording the user far more subtlety in their control. Additionally, disc brakes are self-cleaning and have a longer wear time than their rim brake counterparts. The disadvantage of disc brakes is their increased complexity and cost. Additionally, disc brakes require more precise maintenance in order to function properly.

Due to the nature of the competition and course, exceedingly high braking deceleration is unnecessary and should actually be avoided. Since a regenerative braking cycle is being implemented, it is critical to recapture as much energy as possible during braking, instead of letting it go to waste as heat with traditional friction brakes. For these reasons, the main criterion for the braking method is to be able to lock the rear wheel during full accumulator discharge, and to be able to stop the bike safely in the case of regenerative braking failure. Thus, rim clamping brakes should be sufficient; however, recumbent bikes often implement disc brakes as a result of their geometry.

2.2.4 Pneumatics

Pneumatics were a recent addition to the competition during 2019-2020. Although they were not strictly required as a component on the vehicles, they were a recommended addition which the judging panel looked for when evaluating a team's design. The release of the 2020-2021 competition rules emphasized that the inclusion of pneumatics is mandatory for this year's competition. Each team must implement a pneumatic system that assists the function of the vehicle.

Norgren is the competition's industry sponsor for pneumatic components and will provide each team with up to \$500 worth of pneumatic components. Suggested implementations of pneumatics are brakes, suspension, safety shield, seat height, and pneumatic actuators. Per the competition rules, the pneumatic system must be regulated to a maximum of 100 psi. Each team is allowed to have a 150-psi capacity pressure vessel for air storage.

Prior to its mandatory status, the most common use of pneumatics was in the braking system, which consisted of compressed air applying pressure to the brake pads. The pneumatic shock absorber for the seat is described in the section on Milwaukee School of Engineering's in the background (Section 2.3.4). In addition to researching other pneumatic options, Soulenoid Cycle is committed to implementing a pneumatic system on their vehicle since it seemed to be highly valued in the 2020 virtual competition.

2.2.5 Frame

Soulenoid Cycle's focus this year is on designing and manufacturing a new frame. Relevant research includes the advantages and disadvantages of upright bicycles and recumbent tricycles with respect to hydraulic power.

2.2.5.1 Standard Upright Bicycle

A standard bike is the most common type of frame used for this competition. This bike frame design has been around for about two hundred years and has been innovated and improved upon countless times to be the efficient, lightweight, and familiar standard that is known today. The current frame that was built by The Incompressibles for the 2019 competition is of this form and is pictured in Figure 2.9.



Figure 2.9 Upright bicycle frame, built by The Incompressibles, 2019.

The advantages of standard bike frames include the packaging flexibility and size, and a main disadvantage is aerodynamic design due to the large upright cross-section of the rider. While the standard frame tends to be much lighter than recumbent frames, Soulenoid Cycle was looking towards trying something new, since Cal Poly has competed with a standard frame throughout the school's history in the competition.

2.2.5.2 Recumbent Tricycle

Recumbent vehicles have been around for less than a hundred years and are much less commonly seen on a daily basis. However, they have increased in popularity due to the advantages they provide for riders such as full back support and comfortable seating. In terms of this competition, recumbent vehicles are aerodynamic, stable for mounting hydraulic components, and require less engagement of the upper body. There has been an increase in the use of recumbent vehicles in the FPVC and they have performed extremely well, seeing as the overall winners from 2019 and 2020 used a recumbent frame. Recumbent bikes come in many forms, allowing for the design of the bike for competition to be optimized. Some variations of recumbent vehicles are shown in Figure 2.10.



Figure 2.10 Recumbent tadpole (left), and delta trike (right), recumbent designs.

Tadpole-style tricycles have two wheels in front and one in the back, resembling the shape of a tadpole. It is typical for the front wheels to steer and for the back wheel to be powered. This configuration aligns with the competition purposes because it is ideal for the back wheel to be powered. This is because the back wheel is in the location with the maximum amount of normal force on it, which translates to torque. Front wheel steering is typical of tadpole trikes but requires an additional steering mechanism so that both front wheels can steer. In comparison to delta trikes, tadpole trikes are typically smaller, lighter, faster, and sportier, which bodes well for the purposes of the competition.

Delta tricycles have one wheel in the front and two in the back. It is typical for one of the back wheels to be powered, but this can result in the trike veering to one side when accelerating or climbing. They are usually easier to get into and are taller than tadpole trikes, but they also tend to be larger, heavier, and slower, which does not align with Soulenoid Cycle's goals for the competition. Delta trikes tend to have over seat steering (OSS), which makes maneuvering the vehicle more familiar to the rider.

2.3 System Identification

This year's team will improve upon system modeling by including more feedback from sensors. The inclusion of a more developed mechatronics system will produce more measured values that will be incorporated into modeling. The modeling process will begin by testing and understanding the models created by the previous team. Once Soulenoid Cycle obtains physical access to the vehicle, this year's team will test the models against actual system performance.

Because the control system will be completed simultaneously with the rest of the vehicle, system modeling will be completed in two phases. The first phase will rely solely on improving and testing current models, without implementing measured values from sensors. This phase will be completed prior to Critical Design Review. The second phase will be completed after the completion of the control system, during which each model will be modified to include measured data from sensors. Measured data may include pressures, supplied power, and speed. Three separate Simscape models have been developed over the years. This allowed Soulenoid Cycle to adjust various parameters (i.e., accumulator pre-charge, vehicle weight, hydraulic line length, and solenoid) and how it affected vehicle performances. These models are the Sprint, Accumulator Recharge, and Direct Drive. The Sprint Model (shown in Figure 2.11) predicts the vehicle performance under the accumulator discharge. This gives an estimate of the results of the Sprint Challenge by showing how fast the vehicle completes 600 feet of track. The Sprint Model has been the most accurate for the previous Cal Poly teams when compared to their actual test results being around 15% off. Soulenoid Cycle used the Sprint Model to verify different component selection since it is the most accurate and presents a lot of relevant vehicle performance predictions.

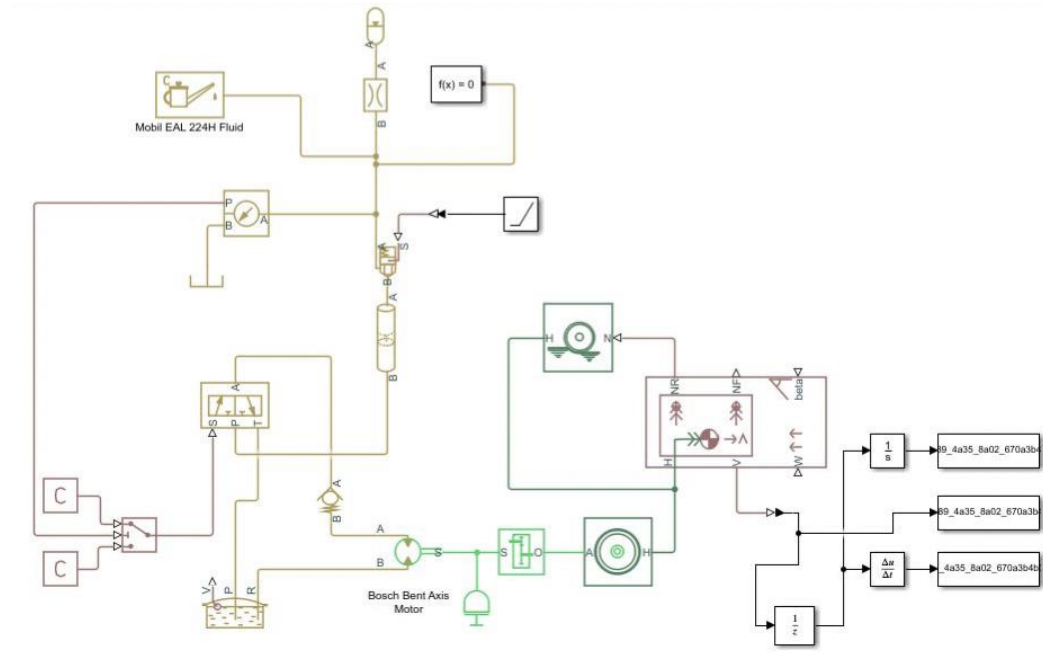


Figure 2.11 Simscape model of sprint challenge.

The Accumulator Recharge Model shown in Figure 2.12 simulates the accumulator conditions as it recharges from regenerative braking. The vehicle body parameters have been removed since the only concern is how fast the accumulator recharges from the motor, which is now being driven by the rear wheel. The valves and line parameters are also adjusted to represent the different lines the fluid flows in Regenerative Braking Mode.

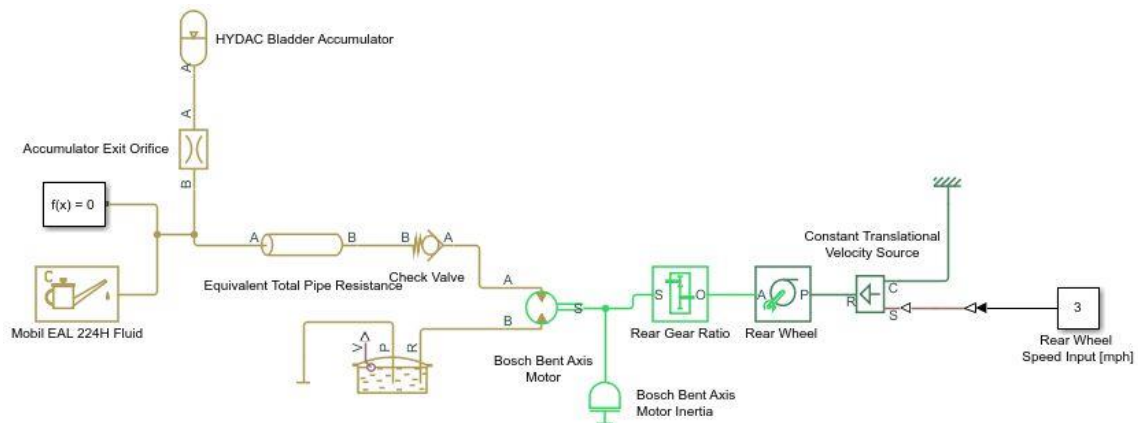


Figure 2.12 Simscape model of accumulator charge.

The last model is the Direct Drive Model which is included in Attachment 5. Its purpose is to predict the vehicle's performance when a driver is powering the pump. The model allows for the input of the rider's power profile. Modeling the rider's input is the biggest drawback to this model since obtaining an exact rider power profile is difficult and susceptible to error. The second part of the model focuses on converting the power input into a tangential force and applying it to a sinusoidal function to best model a pedal crank. It then converts that force input to a torque at the crank before it is transferred through the front gears and

applied to the pump. The remaining Simscape model is similar to the Sprint Model in which the fluid is modeled through a hydraulic circuit and translated to the vehicle body.

Soulenoid Cycle used the Simscape Sprint Model to estimate vehicle performance by changing the frame to a recumbent tadpole design. Various parameters were adjusted in an attempt to best model the new changes which are detailed here and summarized in Table 2.2. Since the rider and components are able to sit lower when compared to a traditional bicycle, the center of gravity was reduced from 33” to 18”. The tire diameter was decreased 26% since recumbent frames also allow for smaller tires. Although this increased the rolling resistance, it decreased the wheel inertia. The rolling resistance force is small and directly proportional to the rolling resistance coefficient. The wheel inertia is a function of the wheel’s diameter squared. Thus, the wheel inertia appears to be a more dominant factor. Soulenoid Cycle still accounted for the extra rolling resistance by increasing the coefficient 25%. To model the decrease in drag typically found in recumbent designs, the frontal area was decreased 5%. An estimated drag coefficient was obtained from a paper published from the Dayananda Sagar College of Engineering’s CFD tests that determined their design to be 0.56. A value of 0.6, about a 32% decrease from the previous bicycle frame, was used in this model. Finally, the weight was increased from 103 pounds to 100, 120, and 140 pounds. All other parameters including a rider weight of 160 pounds were kept constant.

Table 2.2 System parameters that were modified to model a recumbent frame.

Parameter	Bicycle Frame	New Recumbent Frame	% Change
Center Of Gravity Height [in]	33	25	-24%
Frontal Area [in ²]	528.3	501	-5%
Drag Coefficient [-]	0.88	0.6	-32%
Bike Weight [lb _f]	103	100	-3%
		120	17%
		140	36%
Tire Diameter [mm]	686	508	-26%
Rolling Resistance Coefficient [-]	0.004	0.005	25%

The predicted results for the 600’ sprint race are presented in Figure 2.13. As predicted, the performance improved as the vehicle weight decreased with the largest gain being 10% using a new recumbent frame at 100 pounds. However, at the maximum design specification of 120 pound, the model still predicts an 8% improvement. The performance benefits of a recumbent frame began to be less significant when the vehicle weighed 140 pounds with only a 4% increase. This reassured Soulenoid Cycle of the decision to change the frame to a recumbent tadpole design.

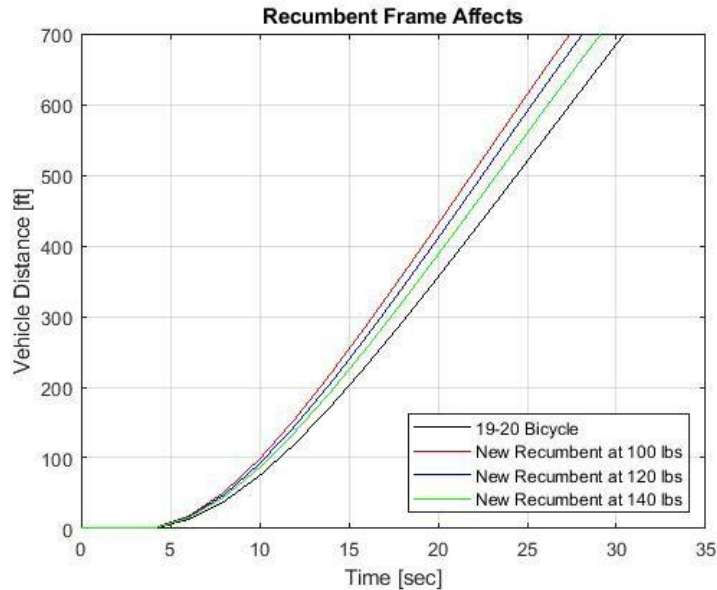


Figure 2.13 Predicted results of the spring challenge with a recumbent frame.

The next result analyzed was that of the vehicle velocity over time shown in Figure 2.14. A similar trend to that of the sprint time is shown for the maximum velocity, with the lightest recumbent frame having the best improvement at 12%. At the maximum specification of 120 pounds, the vehicle's maximum velocity still improved by 10%. Having a higher maximum velocity is not always advantageous. As the trend in the plots shows, the velocity peaks earlier with a recumbent frame and eventually drops after the accumulator has run out of energy. However, with the exception of a recumbent frame at 140 pounds, the velocity decrease reaches a similar velocity of the previous year's bicycle frame at around 30 seconds. This was convenient since the models predict the sprint race to end at around 25 seconds. Thus, the recumbent frame is still faster than the bicycle frame by the end of the race. This verified Soulenoid Cycle that the velocity drop after peak velocity was not detrimental.

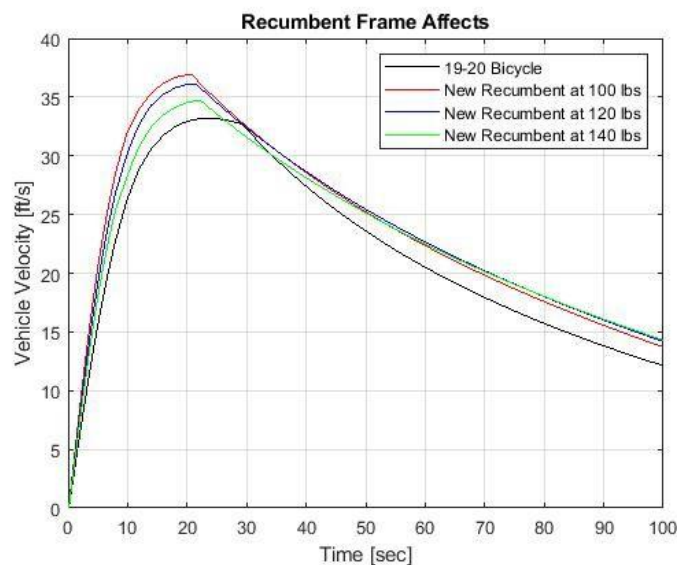


Figure 2.14 Predicted vehicle velocity with respect to time using a recumbent frame.

3 Objectives

Soulenoid Cycle's main objectives are outlined through the problem statement, customer requirements, quality function deployment, and engineering specifications below. After the Preliminary Design Review, this section was updated to better quantify the objective of decreasing vehicle drag. In addition, this section clarifies the requirements of the pneumatic system onboard the vehicle.

3.1 Problem Statement

Cal Poly's current fluid power vehicle needs to be redesigned and improved upon to compete for the title in the 2021 Fluid Power Vehicle Challenge (FPVC). The competition, hosted by the National Fluid Power Association (NFPA), requires teams to design, build, and test a hydraulically powered vehicle that maximizes efficiency, endurance, and sprinting capabilities. This requires teams to combine two types of input/output power cycles, which must include the use of an accumulator for energy storage, an electronic control system, a regenerative system, and other creative features, such as pneumatics. The design must consider safety, efficiency, and ergonomics, and all design choices must be supported with rigorous engineering analysis that demonstrates an understanding of hydraulics and industry knowledge.

This year's team will focus on the addition of a comprehensive mechatronics system that provides an intuitive interface for controlling the vehicle in its various power modes, a data acquisition system with integrated sensors, and weather-proofed electrical components. The frame of the vehicle will also be reconsidered with weight-saving and ergonomics in mind. This includes an evaluation of the type of frame and more importantly, refining the mounting points of the components to the bike. Additionally, an area of interest is the implementation of pneumatics, whose most effective application will be determined through further investigation. This year's team will also look to refine the existing hydraulic system by reducing internal losses, reexamining components to reduce weight, and tuning system parameters to optimize performance.

3.2 Boundary Diagram

Figure 3.1 shows Soulenoid Cycle's system boundary diagram, which is a sketch of the relationships between the subsystems of the vehicle. A single-ended arrow represents a one-way interaction, and a double-ended arrow represents a two-way interaction. The three most prominent sub-systems include the hydraulics, the mechatronics, and the powertrain. The subsystems involve multiple components interacting within the system.

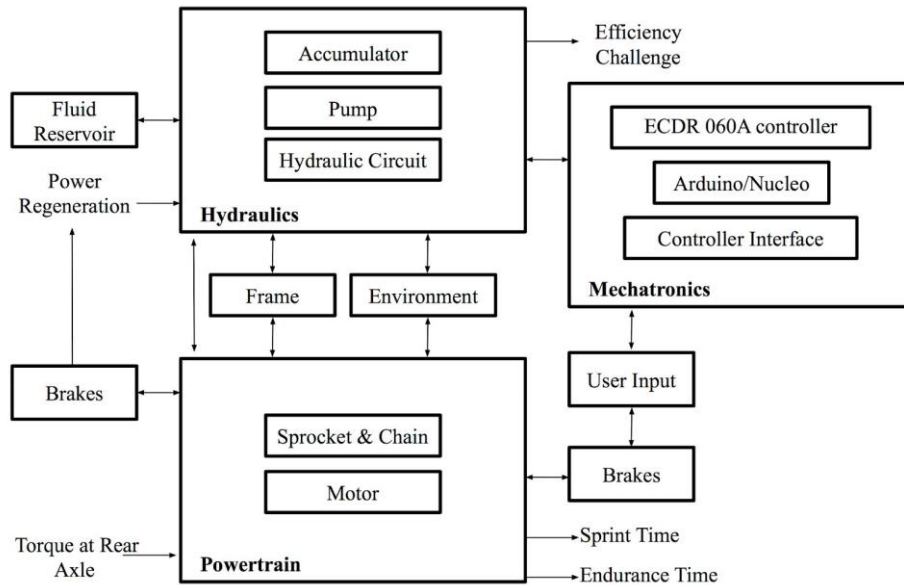


Figure 3.1 Vehicle system boundary diagram.

3.3 Customer Requirements

The primary stakeholders in this project include: the competition judges, team sponsor, industry sponsor, and instructor. The competition challenges engineering students to apply their knowledge toward building and testing a competing vehicle. As a result, many customer requirements are features and modes of operation that satisfy the competition rules, such as the inclusion of an accumulator, control system, regeneration, and at least two different drive modes. However, success is measured on two axes: relative performance reflected by the competition results, and the extent to which the team meets or exceeds customer requirements. Therefore, additional requirements are innovative features, such as unique safety considerations, other renewable energy methods, and electronics and mechatronics. A complete list of customer requirements is located in Appendix A.

3.4 Quality Function Deployment (QFD)

QFD is an important workflow that helps identify appropriate goals that satisfy customer requirements. The “House of Quality” exercise is a comprehensive comparison between customer requirements, how well current competitors meet those requirements, and how well this team will meet those requirements. The relative performance of current competitors provides guidance on which areas of improvement are most critical for this team. For example, the House of Quality spreadsheet, located in Appendix B, reflects that all three current competitors outperform Cal Poly in meeting the sprint time customer requirement. This demonstrates that this area of the competition requires more attention from this year’s team, which helps to create engineering specifications that if met, will improve Cal Poly’s sprint time. The engineering specifications obtained from Soulenoid Cycle’s QFD are located below in Table 3.1.

3.5 Engineering Specifications

Table 3.1 lists Soulenoid Cycle’s engineering specifications along with their target goals, tolerances, the risks associated, and the compliance.

Table 3.1 Tabulated engineering specifications.

Spec. #	Specification Description	Target Goal	Tolerance	Risk	Compliance
1	External Leakage	None	Max	H	I, T
2	Bike Weight	120 lbs	Max	L	A, T, S
3	Efficiency Score	18%	±5%	H	T, S
4	Sprint Time	15 sec	±5 sec	H	T, S
5	Endurance Time	5 min	±1 min	M	T, S
6	Drive Mode Switch Time	2 sec	±1 sec	M	A, T
7	Internal Leakage	0.5 psi/s	Max	H	I, T, S
8	Pneumatics Pressure	100 psi	Max	M	I, T, S
9	Pinching Points	0	Max	M	I
10	Drag: Coast Down Time Increase	10%	Min	M	A, T, S
11	Accumulator Charge Time	10 Min	Max	H	A, T, S
12	Presentation Score	100%	Max	H	T, S
13	NEMA Rating	Type 4	Min	M	I, S
14	Measurement Accuracy	10%	Max	M	A, T
15	Durability: Tipping damage	None	Max	H	A, I, S

Specification #1: External Leakage

One of the NFPA regulations restricts the leakage of any hydraulic component. The smallest leak from a line, valve, or fitting can eliminate Soulenoid Cycle from any competition event. Extra care must be taken in choosing and installing components along with operating the vehicle within its limit.

Specification #2: Bike Weight

Cal Poly's current bike weight is 103 lbs, which is light relative to previous competitors. For example, Purdue Northwest University, Murray State University, and Cleveland State University claim their vehicles to weigh 125, 136, 171 pounds, respectively. The lightest 2020 vehicle was reported by Purdue University at 90 pounds. This year's team will improve on this specification by redesigning the mountings for hydraulic components and investigating other aspects of the bike that unnecessarily increase the total weight.

Specification #3: Efficiency Score

The targeted efficiency score of 18% would improve the current Cal Poly vehicle tested value of 12.17%. Getting competitor's values to compare is especially difficult for this challenge since the scoring was revised after the 2019 competition and the 2020 event was canceled. For the 2020 competition, NFPA intended to use a spreadsheet that included various correction factors that calculated the bike's efficiency from the input values for max system pressure in the accumulator, pre-charge accumulator pressure, accumulator total volume, weight of rider and vehicle, and distance traveled before stopping. The only team besides Pump My Ride that reported an efficiency number was the University of Denver with their simulated 35%. However, they do not present the distance or weight from this calculation, making the number presented questionable. Soulenoid Cycle believes designing and improving on Pump My Ride's tested number is the most effective option. The spreadsheet used to quantify efficiency is located in Attachment 7. Refer to the design verification plan for procedural steps taken by Soulenoid Cycle to calculate vehicle efficiency.

Specification #4: Sprint Time

To be competitive in the sprint challenge, Soulenoid Cycle is targeting to complete 600 feet in 15 seconds. This would be a 31.7% increase in performance when compared to the current Cal Poly vehicle's test sprint time of 22 seconds. The first and second place teams of the sprint challenge from the 2019 event were Cleveland State and Murray State University, respectively. Each resulted in a sprint time in the high 14 seconds, about 7 seconds faster from the third-place finisher. However, both teams used accumulators larger than 1 gallon.

Specification #5: Endurance Time

The goal for Solenoid Cycle is to complete a 1-mile road course in 5 minutes. Each team will start with pedaling (Direct Drive mode). At one point of the challenge, each team is expected to use their Regenerative Braking to activate Boost mode. Similar to the efficiency challenge, rule changes since 2019 with a virtual competition in 2020 makes finding competitive specifications difficult. The only team that reported a simulated endurance result was the University of Denver with 30 mins. A more reasonable specification to look at is Pump My Ride's tested time of 5 mins and 40 seconds. Solenoid Cycle intends to improve upon last year's team 12%

Specification #6: Drive Mode Switch Time

The time it takes from the moment the rider toggles a switch to when the vehicle's drive mode actually changes is called latency. The mechatronics must deliver the signal to the valves and the hydraulic flow needs to be redirected in 2 seconds.

Specification #7: Internal Leakage

Internal leakages are unwanted leaks within the hydraulic system that can be caused by poor tolerance components or build errors. If significant, they can decrease the overall efficiency of the system or damage bigger components, such as a pump or motor. Pump My Ride inherited this issue from The Incompressibles but managed to eliminate the leakage to 0 psi/s. Soulenoid Cycle intends to replicate the previous year's success but keep a 0.5 psi/s maximum.

Specification #8: Pneumatic Pressure

The 2020-2021 competition rules specify the requirement of a pneumatic system that assists in the function of the vehicle. Air can be stored at a maximum of 150 psi, although it must be regulated to a maximum of 100 psi for use. The requirement of a pneumatic system increases the overall weight of the vehicle due to the addition of a pressure vessel for air storage.

Specification #9: Pinching Points

It is difficult to quantify goals for ergonomics, comfort, and safety. Adding more moving components, such as pumps, motors, and chains increases “pinching points”, or locations on the vehicle where the rider can be pinched. This specification attempts to combine a safety and ergonomic goal. Specifically, this goal will influence the placement of the hydraulic system considering the comfort and safety of the rider.

Specification #10: Drag

Each added weight and piece of machinery will increase the drag on the vehicle compared to a regular bicycle. The 2019-2020 University of Cincinnati team estimated the drag force on their vehicle based on frontal surface area, velocity, rider weight, tire diameter, and tire pressure. They estimated a total drag force of 3.46 lbs at a velocity of 15 mph. Without measurement equipment, such as wind force and frontal area measurements, drag force is difficult to quantify. For this specification, Soulenoid Cycle estimates the effects of drag based on coast-down time: the time taken to come to a complete stop after reaching a given velocity. By switching to a recumbent frame and lowering the vehicle, Soulenoid Cycle’s goal is to increase coast-down time by 10% compared to the current upright vehicle frame.

Specification #11: Accumulator Charge Time

The specification for the accumulator charge time is intended to assure the NFPA regulation is met. The rules for the 2020 competition states that teams have a maximum of 10 minutes prior to the sprint and efficiency challenges to charge the accumulator with hydraulic fluid. This year’s vehicle must be able to charge its accumulator to 2800 psi in less than 10 mins in order to compete.

Specification #12: Presentation Score

The NFPA takes into consideration not only the results from the challenges, but also the team’s presentation. Judges score in various categories including visuals, delivery, and responses to questions. A perfect score of 100% for the final presentation will give Soulenoid Cycle a better chance to achieve the main goal of winning 1st place overall.

Specification #13: NEMA Rating

NEMA (National Electrical Manufacturers Association) developed a set of standards for electrical housings that rank relative protection against various environmental conditions. These standards are comparable to IP (Ingress Protection). NEMA ratings are commonly used in the HVAC industry for controller enclosures. IP ratings, though native to Europe, are used as a benchmark in many consumer electronics, including smartphones. They are formed solely considering contamination from abrasive solids and resistance to water. However, NEMA ratings also consider corrosives, rust resistance, and exposure to various environmental conditions.

After the 2019 competition, Cal Poly's vehicle was left outside, which irreparably damaged the mechatronics system from rain and wind exposure. This year's team would like to implement a high degree of protection from environmental conditions that will protect the mechatronics system and its electrical components. The electrical components on the vehicle will be expected to withstand rain, wind, dust, rust, reasonable force impacts (from the bicycle tipping or falling), and oil or hydraulic fluid. These requirements are more consistent with the NEMA rating system, rather than the IP rating system. Specifically, based on the definition NEMA 4 rating (NEMA.org). Soulenoid Cycle's goal is to protect electrical components from the elements. In addition to protecting the vehicle against dust and rain, electrical connections will be designed to provide protection against vibrations and impact.

Specification #14: Efficiency and Measurement Accuracy

Though efficiency is a main judging category in the competition, there is currently some ambiguity in quantifying the overall efficiency of the hydraulic vehicle. Using a spreadsheet provided by NFPA, the efficiency of each competing vehicle is currently calculated based on accumulator pre-charge, its total charge and volume, combined vehicle and rider weight, and distance traveled. Competing teams seldom obtain enough performance data to generate their own efficiency data outside of computer modeling. This year's team will focus more heavily on data acquisition with the goal of better quantifying efficiency metrics. Setting a goal for achieving a degree of measurement accuracy will allow this team to better understand the efficiency of the vehicle. Accuracy measurement data will also positively influence system modeling, which will ultimately improve performance.

Specification #15: Durability

One of the biggest concerns about Cal Poly's current vehicle raised by the judges during the 2020 virtual competition was the placement of the accumulator. The accumulator, encased in a softer composite, is currently mounted to the side of the bicycle, which puts it more at risk for damage if the bicycle tips over. This year's team will measure the durability of the vehicle with a predefined fall or tipping envelope that will ensure undamaged components. This envelope will also include an appropriate factor of safety.

Determining an appropriate target will begin by examining the fragility of each component and their placement on the vehicle. Next, the effects of impact from different drop heights will be considered with simple kinematic models. Testing may include dropping objects with similar masses to the hydraulic components and observing impact forces and damage

4 Concept Design Development

The previous sections described the introduction, background, and objective of Soulenoid Cycle's design. Since defining the scope of work, Soulenoid Cycle has supplemented the background section with reflections on additional meetings and feedback from advisors. In addition, the engineering specifications were modified with more realistic tolerances, and an updated weight goal to reflect a recumbent frame selection.

4.1 Component Selection

This section discusses the component selection process, separated by vehicle subsystem as described in Section 2.2.

4.1.1 Mechatronics

This section discusses the component selection process within the mechatronics subsystem.

4.1.1.1 Existing Solutions

Two existing solutions were considered: an OPUS A3F Wachendorff Display Unit, and a SparkFun Arduino CAN shield. The OPUS display unit is a standalone controller that can communicate with other controllers over a CAN bus. Shown in Figure 4.1, the display has eight configurable button inputs, a pressable rotary knob, and three additional buttons for navigating an interface. It has a 4.3-inch LCD and touchscreen and has a standard DB-9 connector that can be plugged directly into the ECDR 0506-A.



Figure 4.1 OPUS A3F Wachendorff display unit.

The SparkFun CAN shield is designed to add a CAN communication ability to an Arduino Uno. Shown in Figure 4.2, it fits over the footprint of an Arduino Uno, and contains an MCP2515 CAN controller and MCP2551 CAN transceiver circuit. Like the OPUS A3F, it carries a standard DB-9 connector that can be plugged directly into the ECDR 0506-A. The breakout module also has a micro-SD card port, a joystick, and an additional port to connect to a SparkFun GPS breakout module.

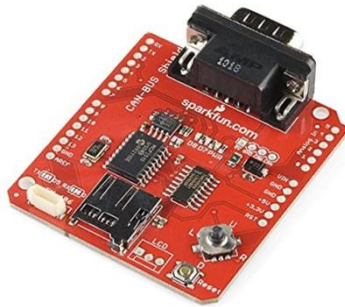


Figure 4.2 SparkFun CAN bus shield for the Arduino Uno.

This product's main advantage is that SparkFun has already written Arduino code for interfacing with it. SparkFun provides clear and open-source documentation that allows for quick software debugging. However, this product limits the system's microcontroller to an Arduino Uno's ATmega328. Discussed further in Section 4.1.1.2, the Arduino Uno may be insufficient for navigating a complex user interface with a Real Time Operating System (RTOS).

4.1.1.2 Microcontroller Selection

This section describes the selection process for the CAN node's microcontroller and its other hardware components. The Arduino framework in C++ was chosen as this project's software basis. The Arduino framework is well-documented, open-source, and can be used to program a variety of microcontrollers and development boards. Two microcontrollers were considered: an ATmega328, and an STM32. ATmega328, produced by Atmel, is an 8-bit AVR microcontroller commonly found on Arduino modules. STM32 is a family of 32-bit ARM microcontrollers produced by STMicroelectronics. Both ATmega328 and STM32 microcontrollers are available on development boards that carry small footprints. Shown in Figure 4.3, the Arduino Nano and Blue Pill development boards are both relatively small and carry many useful software and hardware peripherals.

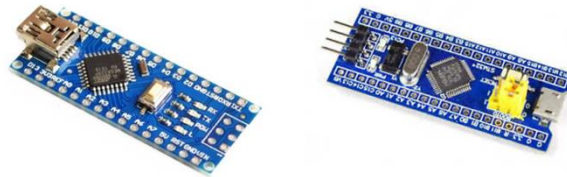


Figure 4.3 Arduino Nano with ATmega328 (left) and STM32 Blue Pill (right).

The biggest advantage of using an Arduino development board, such as the Arduino Nano of Figure 4.3, is that its microcontroller is preloaded with the Arduino bootloader. This allows the programmer to upload C++ code directly to the board, which its bootloader uses to program the microcontroller. Conversely, most STM32 development boards require the use of the ST-Link programmer, which is a dedicated controller produced by STMicroelectronics that programs an STM32 in its machine code. Some development boards, such as the Nucleo L476RG, have a built-in ST-Link circuit, however the Blue Pill of Figure 4.4 carries too small of a footprint to have space for the programmer module.

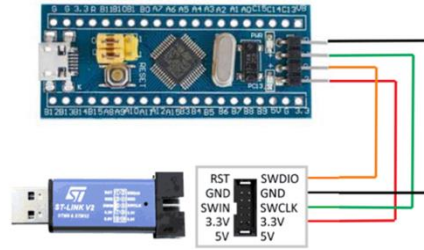


Figure 4.4 ST-Link module used to program the STM32 Blue Pill development board.

The ST-Link programmer is a separate module, shown above in Figure 4.4, that interfaces with an Integrated Development Environment (IDE) on a PC. While the Arduino Nano can simply be programmed from its USB port, the Blue Pill must be programmed using a serial connection to the ST-Link, as it does not have a bootloader. Although the Arduino Nano is easier to program, its ATmega328 carries less processing power than the STM32. As an 8-bit microcontroller, it is not ideal for an RTOS and also has fewer communication peripherals. For example, the Arduino Nano only has one USART port, while the Blue Pill's STM32F103 has three. Furthermore, the Arduino Nano may be clocked up to 16 MHz, while the Blue Pill may be clocked up to 72 MHz. Given the tradeoff of ease of programmability and processing power between the Arduino Nano and Blue Pill development boards, it was prudent to design and prototype with both before choosing a final design.

4.1.1.3 CAN Communication

While the STM32F103 on the Blue Pill has a built-in CAN controller, it cannot be easily accessed with the Arduino framework. To access its CAN peripheral, the microcontroller must be programmed using STM32CubeIDE, which is an IDE produced by STMicroelectronics. To keep the project as open-source as possible, an external CAN controller was chosen, which allows the microcontroller to be programmed in any IDE using the Arduino framework. The MCP2515 CAN controller was chosen because it is well-documented with many different open-source C++ libraries. In order to communicate with a CAN bus, the MCP2515 receives commands from a microcontroller using a Serial Peripheral Interface (SPI), and then transmits a CAN message using a CAN transceiver. Two transceivers were considered: the MCP2551 and TJA1050. Shown in Figure 4.5, the two integrated circuits are housed in slightly different packages and have different pinouts.

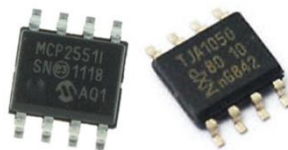


Figure 4.5 MCP2551 (left) and TJA1050 (right) CAN transceivers.

Aside from their physical differences, the transceivers are functionally the same and are both compatible with the MCP2515 CAN controller. The MCP2551 is used on the SparkFun product of Figure 4, while the TJA1050 is used on a standalone CAN breakout module of Figure 4.6.



Figure 4.6 MCP2515 and TJA1050 CAN bus breakout module.

4.1.1.4 Display Selection

In order to design a graphically pleasing interface that can display text to the rider in clear, large fonts, two full-color LCD options were explored: A 2.8-inch Adafruit touch screen with the ILI9341 LCD driver, and a 2.8-inch Nextion touch screen. Both options are significantly smaller than the OPUS A3F display unit and can be easily driven by a microcontroller programmed with the Arduino framework. The LCD breakout module of Figure 4.7 is a low-cost, generic version of an Adafruit Arduino Uno shield. The LCD is driven by the ILI9341 LCD driver, which communicates with a microcontroller over SPI. The breakout module also has a resistive touch screen and SD card slot for displaying bitmap images. This module is easy to use with the Adafruit Graphics Library, which is a suite of Arduino code designed to communicate with several Adafruit display products. Its ease of programmability allows for the quick design of complex shapes and text designs, and the LCD's resolution and brightness are comparable to that of Nextion displays.



Figure 4.7 2.8-inch TFT display with ILI9341 LCD driver.

Since this product is nearly three times as cheap as the Nextion display, it was tested first with an Arduino Nano. A skeleton interface was written in C++ and uploaded to an Arduino Nano using the Arduino IDE. The software uses the Adafruit Graphics Library to write data to the screen. The result, discussed in SECTION XX, was visibly very slow because the Adafruit library uses blocking code to write each shape to the screen. In other words, it was only capable of drawing one independent shape or character at a time without the ability to multitask between communication and pixel-writing.

The Nextion display differs from a standard LCD driver because it has its own microprocessor with an RTOS. This allows it to multitask independent of the system's master microcontroller, which results in fast screen refresh rates. A microcontroller communicates with this screen using a UART connection, which is shown in Figure 4.8 as a 2-wire connection with additional wires for ground and power.



Figure 4.8 Nextion LCD.

Its functions and screen layout are configured in Nextion Editor, which is a free HMI tool developed by Nextion to program their display modules. The software, shown in Figure 4.9, allows the programmer to drag-and-drop buttons, images, and text onto the screen. This is a much simpler process than using line code to write each individual pixel or shape. Furthermore, Nextion displays can be easily communicated with using Arduino code. A programmer can use standard serial communication code in either C++ or Python to send commands to the screen.

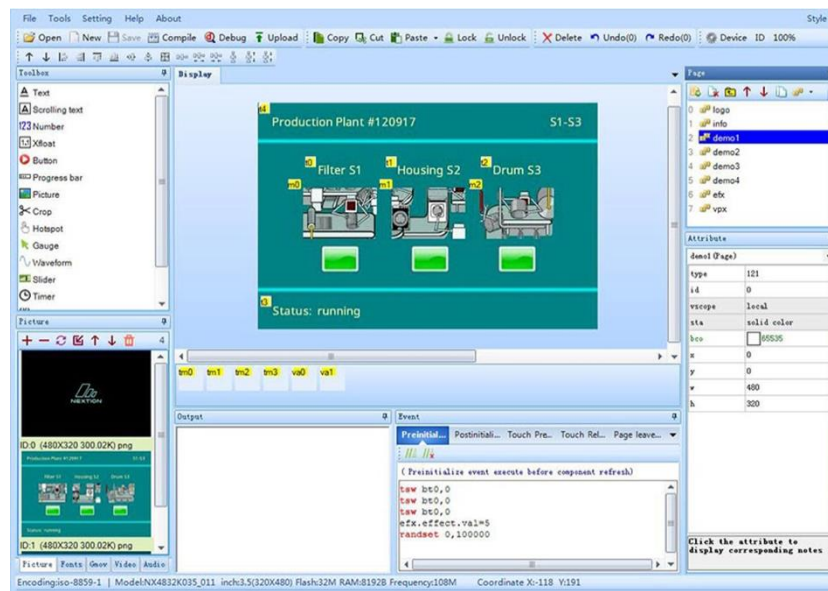


Figure 4.9 Nextion Editor HMI Software.

While its robust configuration tool gives Nextion displays a greater ease of programmability, another required piece of software adds a layer of complexity to the project. The mechatronics system already requires the use of HF Impulse to configure the PLC and a C++ development environment to program the microcontroller. A third programming software would further complicate debugging efforts because it requires the programmer to sift through three different platforms to diagnose problems with a single system.

4.1.2 Hydraulic Circuit

This section discusses the component selection process within the hydraulic circuit subsystem.

4.1.2.1 Hydraulic Hardlines

Two common lines used in the hydraulic industry were considered. Hydraulic hoses, more commonly used in the NFPA Fluid Challenge, are rubber and flexible lines designed to withstand pressures seen in hydraulic systems. They are easy to work with since they can bend to connect different components. However, hoses expand under pressure decreasing efficiency. Hydraulic hardlines are drawn tubing made of either steel or aluminum, so their rigid material does not expand under pressure. Since hardlines cannot bend like hoses, they require more planning to incorporate.

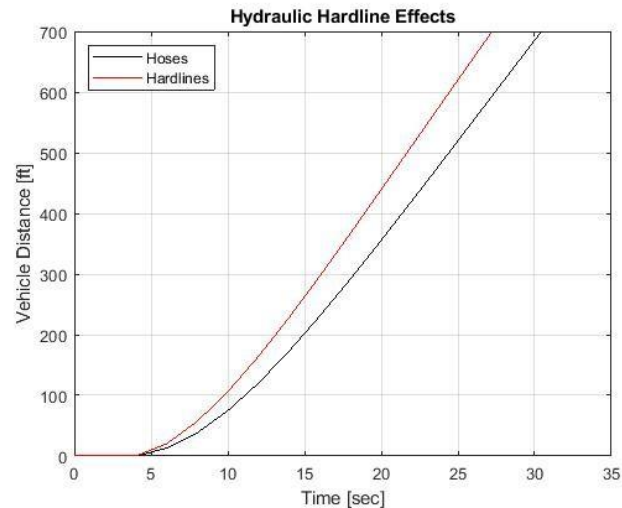


Figure 4.10 Predicted performance in sprint challenge using hydraulic hardlines.

The Sprint Model was used to verify that hydraulic hardlines would improve overall performance. Last year's team did not have enough time to design for hardlines and instead used hydraulic hoses. To simulate their vehicle, the pipe wall type was set to flexible and the tube's surface roughness remained at 3.0×10^{-5} feet. Hardlines were simulated by changing the wall type to rigid and decreasing the surface roughness to match that of drawn tubing, 5.0×10^{-6} feet. All other parameters were kept constant.

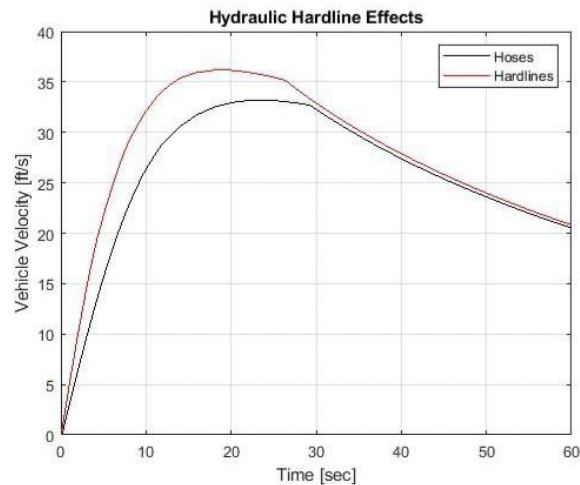


Figure 4.11 Predicted maximum velocity using hydraulic hardlines.

The results are shown in Figure 4.10 and Figure 4.11. The models showed an improvement from last year's parameters of 11% in the sprint competition and of 9% in the vehicle's max velocity. Soulenoid Cycle determined the benefits of hardlines to be substantial and worthy of the time to include them.

4.1.2.2 Accumulators

The NFPA competition rules specify a maximum accumulator size of 1 gallon, so the component selection process was limited to accumulator type and material. In terms of selecting a type, it came down to the weight of bladder versus piston accumulators. As seen in Figure 4.12, the graphic produced by Steelhead Composites shows that piston accumulators are generally heavier than bladder accumulators no matter the material.

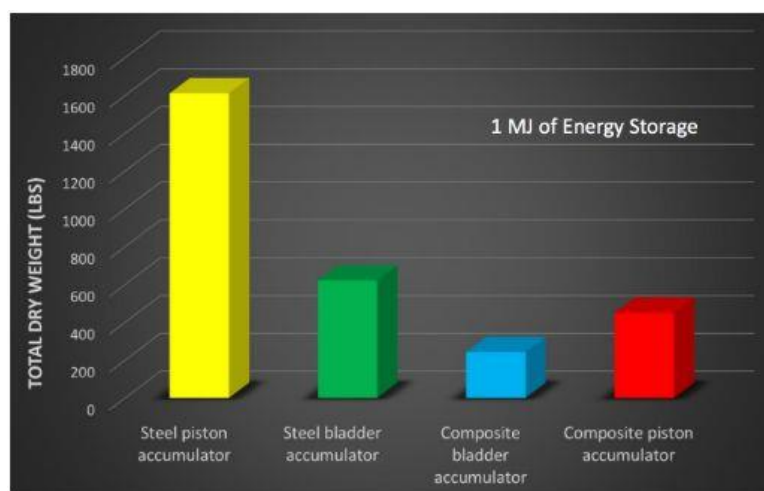


Figure 4.12 Comparison of accumulator weights (lbs), varied by material.

Since weight reduction was one of Soulenoid Cycle's main goals, the decision to continue with a bladder accumulator was made. The previous year's team, Pump My Ride used a composite bladder accumulator on their vehicle, along with about half of the teams in the competition. Upon more research, a 1-gallon bladder accumulator lighter than the one that was already purchased could not be found. Based on the above information, the decision matrix in Table 4.1 was created.

Table 4.1 Accumulator decision matrix.

Criteria	Weight (1-9)	Accumulator Type		
		Current Accumulator	New Bladder Accumulator	Piston Accumulator
Safety	6	Datum	0	0
Cost	1		-1	-1
Durability/Reliability	4		0	0
Weight	5		-5	-5
Creative/New Features	2		2	2
Pressure	3		0	3
Total			-4	-1

From research and the decision matrix, Soulenoid Cycle again used the Steelhead Composites MicroMax Series 1 Gallon Accumulator. The specifications for this accumulator are given in Attachment 2.

4.1.2.3 Pumps & Motors

The pump and motor used last year was a Bosch Series 6. It is an axial piston configured as a bent axis. Soulenoid Cycle considered replacing the type of pump for a gear pump or a linear pump. The criteria chosen to evaluate the best pump is shown on a decision matrix in Table 4.2. Pump weight along with pump performance like flowrate and pressure were more heavily weighted.

Table 4.2 Decision matrix to compare the current pump type (axial piston) to linear and gear pumps.

Criteria	Weight (1-9)	Pump Type		
		Current Pump	Linear Pump	Gear Pump
Safety	6	Datum	0	0
Cost	1		-1	-1
Durability/Reliability	2		0	0
Weight	9		9	-9
Size	3		0	3
Creative/New Features	4		4	0
Flowrate	7		-7	-7
Pressure	8		-8	-8
Displacement to Weight Ratio	5		5	0
Total			2	-22

The decision matrix found that the linear pumps hold a small advantage over the axial-piston pumps while gear pumps are drastically less practical. The drawback to linear pumps that could not be quantified on a decision matrix is that they required the design of a cam system to transfer rotation movement from a crank to linear movement. Additionally, to optimize linear pumps, two are needed to work in opposing strokes to assure hydraulic fluid is constantly flowing through the system. This meant mechanical timing was critical and the weight advantage they provided for one unit was less of a factor. The advantages to linear pumps were small, thus the necessary changes to the drive system were not worth the change.

Additional consideration was spent on determining how much more performance axial-pumps provide over gear pumps. The decision matrix clearly showed axial pumps were better. However, the performance and weight advantages of the axial-piston pump were small. Furthermore, the conditions the pumps and motors were exposed to on previous vehicles were nowhere near their rated performances. Thus, judging their performance solely based on specification documents made it difficult. Controlled experiments comparing the two pumps at the expected conditions would have provided more definitive numbers. But because of COVID-19 pandemic, that option was quickly eliminated. In the end, Soulenoid Cycle concluded that gear and axial-piston pumps were too similar to determine a definitive better performing pump. Since the current 0.3 CIR (5 CCR) Bosch Series 6 pump, whose specification sheet is provided in Attachment 1, still weighs less than similar displacement gear pumps by about 1.5 pounds, it was determined to be the best option for both the pump and motor.

The expected operating range of the pump is expected to be around 800-rpm and 1-gpm. However, the 800 rpm speed is slower than the ideal range. As shown in Figure 4.13, the ideal operating speed to maximize efficiency is greater than 3500 rpm. This speed is consistent with other bent axis pumps. However, the

Bosch pump is still rated to have an efficiency of around 95% at the 800 rpm. Other pumps like Parker's do not provide a rating at lower speed range.

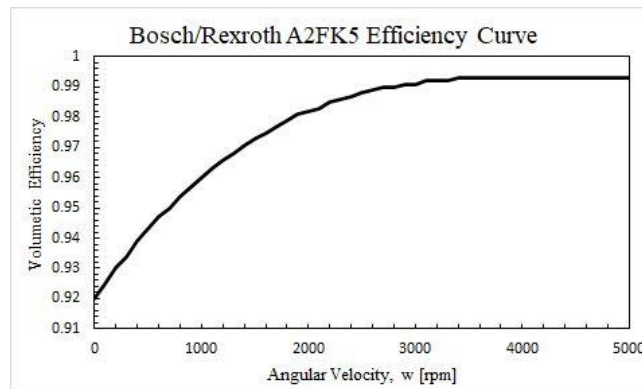


Figure 4.13 Volumetric efficiency curve for Bosch pump/motor.

To help achieve the operating speed at the pump, an Apex Dynamics hypoid 4:1 gearbox is attached to it. The attached gearbox makes the overall gear ratio from crank to pump 10:1. Thus, the operator's pedaling speed will be multiplied by 10 to help achieve better pump speed. The rear motor is still connected to the rear wheel with a gear ratio of 4:1 from the rear gear cog to the motor.

4.1.2.4 Manifold

Hydraulic manifolds are the central hub of a fluid powered system where fluid enters, gets redirected (usually with solenoid valves), and delivered to another component. They decrease pressure losses in the system by shortening the length of the lines and reducing the number of connections and bends. The reduced lines and fitting may also reduce weight. Additionally, manifolds can help transfer heat from the fluid further improving the overall system efficiency. Pump My Ride designed a custom manifold from HydraForce (CAD model shown in Figure 4.14 and drawing in Attachment 3) for the 2020 competition, but they were unfortunately never able to use it in competition. The improvement in overall system efficiency from the manifold aids in optimizing the competition efficiency score, sprint time, and endurance time. It also made the accumulator charge more efficient assuring the maximum charge time of 10 minutes is met. By centralizing the fluid direction flow, the time to change between drive modes is reduced. Reducing the number of fittings and connections meant the internal leakage is minimized and the possibility of any external leakage is reduced. Finally, many teams from last year did not implement a manifold in their system. The manifold presented a unique component for the judges ultimately improving the presentation score. Soulenoid Cycle viewed not using Pump My Ride's manifold as a disservice to their team and agreed with their decision of using a manifold to regulate the fluid flow through the circuit.



Figure 4.14 CAD render of the HydraForce manifold, installed on the 2019 vehicle.

The hydraulic manifold consists of different valves to control the direction of flow. However, these valves have pressure losses which are unique to each type and a function of flow rate. An estimate of the pressure losses for each drive mode is presented in Table 4.3. These losses are for a fast flow rate for the system of 1.3 gpm.

Table 4.3 Estimated pressure loss for each drive mode at 1.3-gpm.

	Pressure Drop Across Each Valve [PSI]						TOTAL
	SV08-28	SV08-22	SV08-21	SVC08-21	CV08-21	CV10-24	
Direct Drive	0	0	5.94	0	0	8.30	14.2
Boost	56.1	27.2	5.94	0	0	0.00	89.2
Regen Braking	0	27.2	0	0	17.2	8.30	52.7
Pedal Charge	56.1	27.2	0	0	0	8.30	91.6

4.1.2.5 Gearing and Drive System

To deliver power from the driver to the pump and the motor to the drive wheel, driving systems needed to be designed. Belt and chain drive systems were first compared with a decision matrix shown in Table 4.4. The biggest advantage of belt drive is the low maintenance. However, the pulley and belt needed is generally heavier when compared to a chain drive. Due to belts being more elastic than chains, they lose a small amount of efficiency. Solenoid Cycle decided to stay with the traditional chain and sprocket drive system for both the front and rear gearing. Pump My Ride produced various models to determine the ideal gear ratios for both the sprint and endurance races and then decided on a compromise between the two. Solenoid Cycle plans to manually test different gear ratios on their vehicle to find the peak efficiency for both the sprint and endurance challenges.

Table 4.4 Decision matrix comparing belt and gear drive methods.

Criteria	Weight (1-9)	Drive Type	
		Chain	Belt
Efficiency	3	3	0
Weight	4	4	0
Complexity	1	1	0
Maintenance	2	0	2
Total		8	2

4.1.3 Frame Selection

In addition to evaluating each type of frame in the decision matrix workflow, small scale models of the delta and tadpole tricycles were 3D printed in order to get a better understanding of where each hydraulic component could be placed on the vehicle.

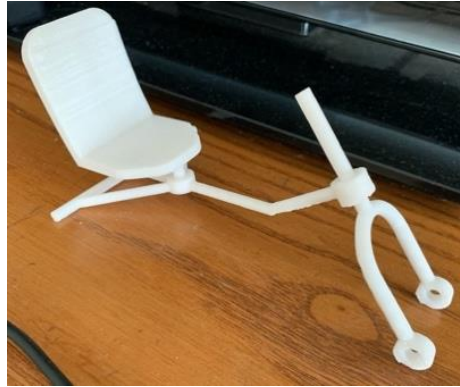


Figure 4.15 Delta tricycle 3D printed model.

Each prototype was modeled in Fusion 360 with an overall length of 12 cm. The biggest result of prototyping this design option was a better understanding of a possible steering mechanism. Having a single wheel at the front of the vehicle is advantageous because there only needs to be a single pivot point that handles all steering. However, the two rear wheels were difficult to model without rigidly attaching both to a single axle. This difficulty indicates the need for a differential that would allow the rear wheels to turn with the vehicle without skidding. Another possibility is to only drive one rear wheel and allow the other to float freely, which could destabilize the vehicle and prompt weight distribution to offset any dynamic loading.



Figure 4.16 Tadpole tricycle 3D printed model.

Prototyping the tadpole design, shown above in Figure 4.16, presented similar difficulties to the delta design. What was immediately noticed was that the delta tricycle design generally allowed for more space on the vehicle to mount hydraulic components. In addition, though having a single rear wheel to drive makes power transmission significantly less complicated, it introduced the need for a steering linkage to turn both front wheels. Unlike a differential, a simple linkage was able to be printed to scale and placed on the vehicle. Shown below, the “handlebars” can turn both wheels about a single pivot point with a small amount of drag. Though modeled to fit on the scale model, the linkage itself was not modeled to scale; its

dimensions were driven by the abilities of the 3D printer used to print the parts. These prototyping efforts provided valuable insight into which tricycle design to pursue. Even at a 3D printing level, it was clear that a functioning delta tricycle prototype would be more difficult to manufacture than a functioning tadpole tricycle. Soulenoid Cycle determined that the tadpole design would ultimately be more effective and easier to build, even with the addition of a steering linkage and reduced room for mounting components.

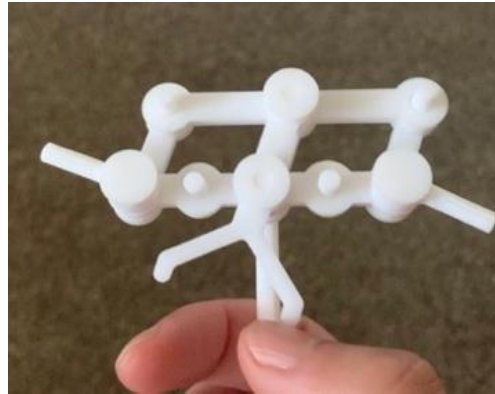


Figure 4.17 3D printed steering linkage model.

Soulenoid Cycle settled on designing a tadpole-style recumbent for use in the 2021 challenge. Tadpoles are built better for speed, and the steering and drive power methods align more closely with the needs for the competition. The decision to manufacture a completely different type of frame is a large undertaking, considering that it has never been done at Cal Poly. The selection of this frame requires more research into the specific design aspects of tadpole tricycles so that Soulenoid Cycle is able to design the frame to meet all of their goals.

4.2 Preliminary Hydraulic Circuit Design

Previous Cal Poly teams designed thorough drive modes that met the competition rules and aided in some vehicle functions. Since Soulenoid Cycle reused Pump My Ride's manifold, drastic changes to the drive modes were not necessary.

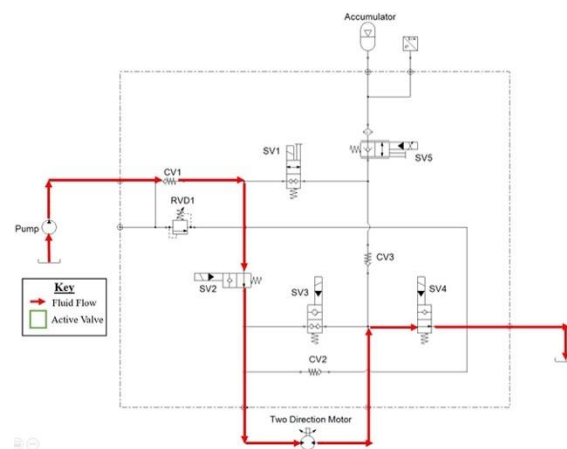


Figure 4.18 Hydraulic circuit in Direct Drive mode, concept design.

Direct Drive mode as shown in Figure 4.18 is a required competition mode used in the endurance challenge. This mode is most similar to traditional cycling wherein the driver of the vehicle pedals a crank to propel the vehicle forward. Instead of the crank being connected to a drive gear, it rotates the pump. The pump draws fluid from the hydraulic tank. The fluid then flows through a check valve (CV1) and a solenoid valve (SV2) before reaching the driving motor. To recirculate the circuit, the fluid flows from the motor through another solenoid valve (SV4) and back to the hydraulic tank.

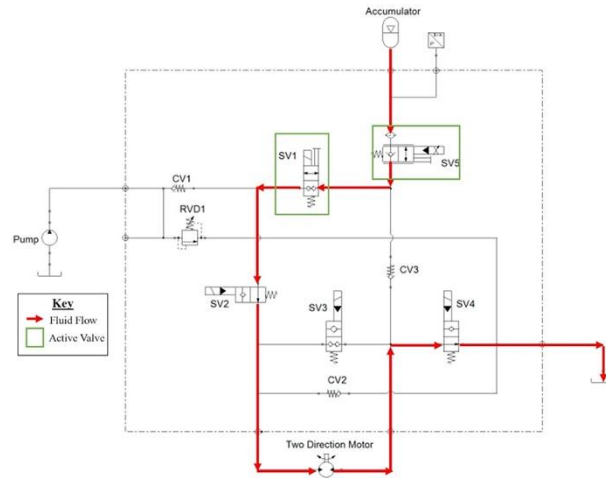


Figure 4.19 Hydraulic circuit in Accumulator Discharge mode, concept design.

Boost mode uses only the accumulator discharge to rotate the drive motor. It is used primarily in the sprint challenge and is modulated in the efficiency challenge. A varying poppet valve (labeled as SV5 in Figure 4.19) is activated along with a solenoid valve (SV1). The hydraulic fluid flows through the normally open solenoid valve (SV2) before reaching the motor. The fluid continues through the last solenoid valve, SV4, as it flows into the hydraulic tank.

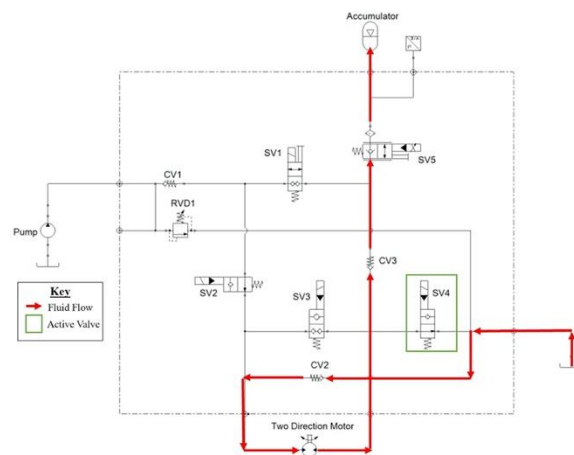


Figure 4.20 Hydraulic circuit in Regenerative Braking mode, concept design.

The final required drive mode is Regenerative Braking as presented in Figure 4.20. It is demonstrated in the endurance challenge and its purpose is to convert the vehicle's kinetic energy into stored energy in the accumulator. To accomplish this, a solenoid valve, SV4, is activated to prevent output flow of the motor to go back into the tank. As the motor rotates due to the rolling vehicle, it draws hydraulic fluid from the tank

through a check valve (CV2). The fluid then continues to flow past a second check valve (CV3) and the varying poppet valve, SV5, to charge the accumulator.

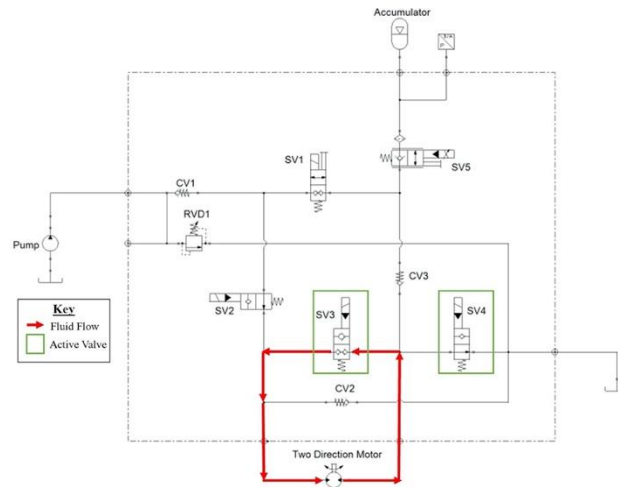


Figure 4.21 Hydraulic circuit in Coast mode, concept design.

Coasting allows the vehicle to freely circulate hydraulic fluid as the motor rotates. The key difference in this mode is that no component is driving the motor. This mode behaves similarly to a clutch in traditional vehicles since all driving components are disengaged when the vehicle is moving. The resistance of the motor is also reduced as the fluid is able to freely flow in a closed circuit. Figure 4.21 shows the simple coasting mode. Two solenoid valves, SV3 and SV4, are activated. SV3 allows the flow from the motor to circulate back to the motor. SV4 blocks the fluid flow back to the tank.

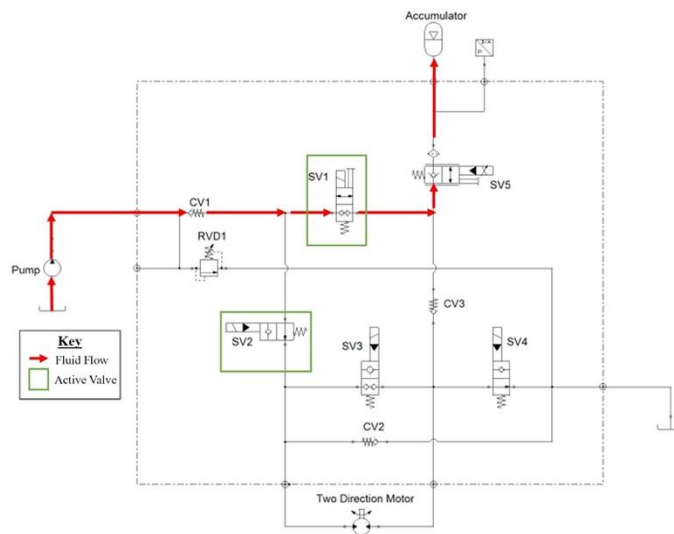


Figure 4.22 Hydraulic circuit in Pedal Charge mode, concept design.

Soulens Cycle incorporated a new drive mode shown in Figure 4.22. Pedal Charge allows the driver to pedal and use the pump to recharge the accumulator. Previous Cal Poly teams have used the Regenerative Braking mode and pushed the vehicle around to charge the accumulator in between competition events.

Although functional and still a viable option, Solenoid Cycle wanted to incorporate Pedal Charge as a practical and alternative method to charge the accumulator. Additional space to push the vehicle is no longer needed. The driver can now stay on the vehicle and pedal to charge the accumulator instead of standing up and pushing. Similar to Direct Drive, fluid flows from the pump to a check valve (CV1). Instead of flowing towards the motor, a normally open solenoid valve is activated to prevent it. A normally closed valve, SV1, is also activated to allow the hydraulic fluid to flow towards the accumulator. A check valve (CV3) prevents fluid to flow towards the other side of the motor and tank.

4.3 Preliminary Frame Design

An added benefit of switching to a recumbent design is the increased flexibility for mounting and arranging components on the vehicle. To get a better understanding of where the larger hydraulic components could be placed on a recumbent tadpole design, 3D models of each component were arranged on a preliminary CAD model of a possible frame design. The design, shown below in Figure 4.23, is based on a single-bar frame design, that runs from the crank set to the rear drive wheel.

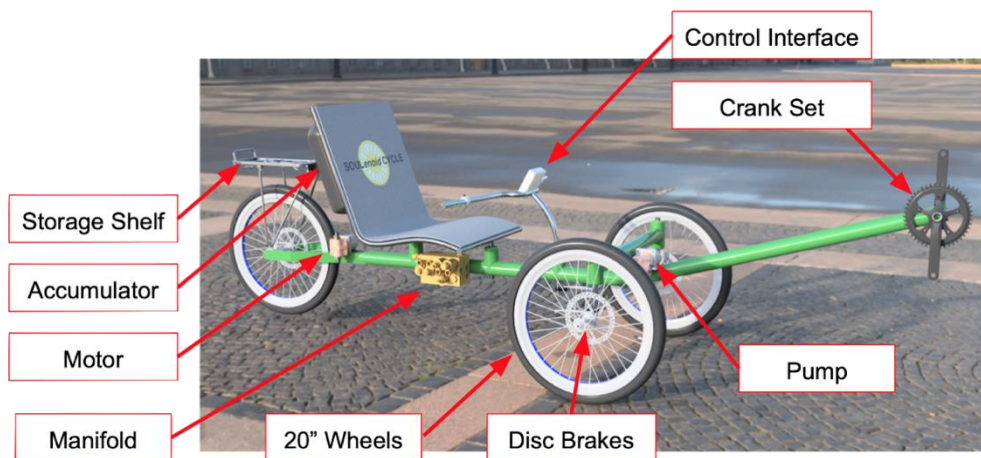


Figure 4.23 Preliminary recumbent frame design.

What is most notable about this tentative layout is the placement of the accumulator. Last year's team, Pump My Ride, mounted their accumulator to the side of the bicycle, making the vehicle vulnerable to tipping and damaging the vessel. On this recumbent design, the accumulator can be mounted behind the seat at the center of the vehicle, a much safer location.

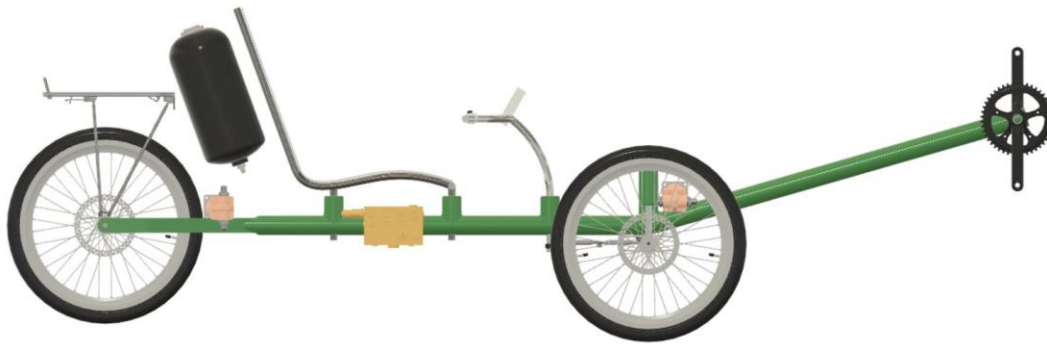


Figure 4.24 Orthographic profile of preliminary frame design.

Pump My Ride's primary motive for mounting the accumulator on the side of their frame was its vertical orientation. For bladder accumulators, a vertical orientation with the output valve at the bottom is optimal for energy storage. Though the accumulator in Figure 4.24 is oriented at an angle of 70 degrees from horizontal, there is still sufficient room to mount the accumulator vertically behind the seat. The 20-inch diameter wheel size in this preliminary model was chosen based on the results of a Simscape model discussed in section 4.1.4. In addition, the seat is centered between the front and rear wheels, with 55 inches between the front and rear wheels. The crankset is oriented at a 16-degree incline, extending 40 inches. These dimensions are subject to change with additional ergonomic research.

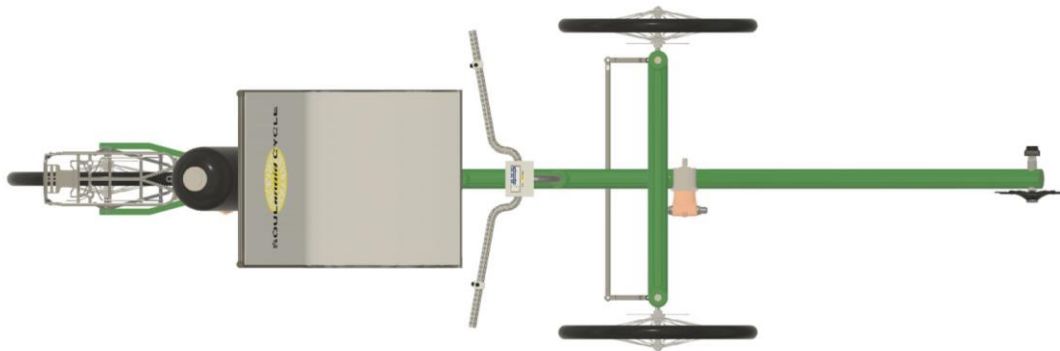


Figure 4.25 Orthographic top view of preliminary frame design.

The steering system shown in the preliminary designs is symbolic with regard to component placement. Though a functioning steering linkage was successfully prototyped, a parallel steering linkage is not advisable for a recumbent frame. The standard steering method on recumbent vehicles is a trapezoidal linkage that causes the inner wheel to rotate more than the outer wheel to eliminate drag.



Figure 4.26 Preliminary mechatronics interface layout.

The placement of the control interface, as shown above in Figure 4.26, reflects the similar layout used by The Incompressibles in 2019. A center-mounted screen maximizes visibility to the rider, and buttons located on the handlebars allow the rider to switch drive modes while steering. Lastly, the shelf attached to the rear drive wheel is useful for mounting additional components, such as the fluid reservoir and electrical components.

4.3.1.1 Structural Loading

A benefit of an aluminum frame over steel is the reduction in weight. Though more difficult to weld, using aluminum would significantly reduce the overall weight of the vehicle. However, aluminum is more vulnerable to fatigue than steel; the structural design of the frame must account for static and dynamic loading. Furthermore, aluminum is weakened by welding and requires heat treatment. If Soulenoid Cycle were to continue to pursue an aluminum frame, heat treating would need to be outsourced to a local company, which will increase the frame's overall manufacturing costs. In concept design, static loading considerations include the weight of the rider, and the bending moment applied by pushing on the crank set.



Figure 4.27 Predicted static loading on preliminary frame design.

To investigate the general effects of these static loading considerations on a single-bar aluminum frame, static loads were applied at the locations shown above in Figure 4.27. The two vertical forces represent the weight of the rider (150 lbs) applied at the seat connections, and the angled force represents the static force applied to the crankset while pedaling (30 lbs). The two front wheel connections were fixed, and the rear wheel connection was modeled as a pin joint. The aluminum tubing modeled in this design has an outer

diameter of 1.5" with a 1/8" wall thickness. For FEA, the material properties of Aluminum 6061-T6 were applied.

The results of the static loading simulation, conducted in Fusion 360, calculated a factor of safety of 3.07, and a maximum displacement of 0.08 inches at the crankset. The magnified displacement distribution is shown below in Figure 4.28.

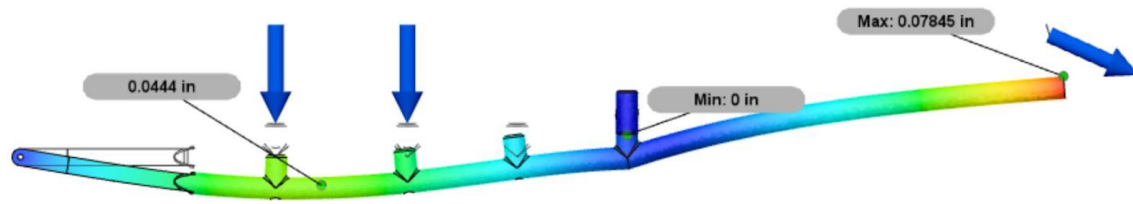


Figure 4.28 Predicted frame displacement due to static loading.

This simulation neglects the placement and weights of the hydraulic system, which apply additional static loads to the vehicle. Given the added weight of the hydraulic components, Soulenoid Cycle has chosen a target factor of safety of 3.0. This static factor of safety is low enough to make reasonable reductions in tube thickness while still accounting for unexpected additions of loading.

4.3.1.2 Preliminary Motor Mount Design

The motor mount is designed to be cut from 0.08" thick aluminum sheet metal. The motor mount, pictured below in Figure 4.29, the motor mount includes locating slots to account for chain tensioning. It spans the width of the vehicle and is mounted between the rear crossbars. Triangular folds alleviate some cantilever stress that the motor will apply. The mount will be tig-welded along the seams after folding.

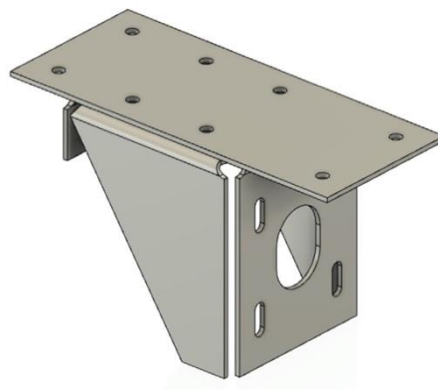


Figure 4.29 Preliminary motor mount design.

This motor mount is designed to be manufactured from the same material as the motor mount used by the Incompressibles in 2018. The same slot and hole dimensions and sheet metal thickness were used as well. To simulate the loading effects that the hydraulic motor could apply to the mount, FEA was conducted on a simplified model, shown below in Figure 4.30.

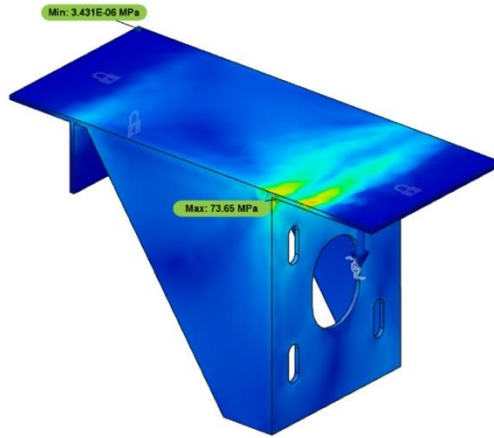


Figure 4.30 Results of FEA of preliminary motor mount design.

In this analysis, the ends that are to be bolted to the frame were constrained as fixed. A shear force and bending moment were applied to the inside of the slotted face that the motor bolts to. Given that the hydraulic motor weighs 5 lbs, conservative loads of 30 lbs of shearing force and a bending moment of 20 ft-lbf were applied. These loading considerations yield a factor of safety of 3.05, which is suitable for this application. Manufacturing and detail drawings for this design are located in Appendix L.

4.4 Preliminary Reservoir Design

The hydraulic fluid reservoir is a critical component of the hydraulic circuit. It is the source of hydraulic fluid that is drawn by the pump and must be at atmospheric pressure. Given the complex geometry of bicycle and recumbent tricycle frames, the reservoir design must be tailored to a specific vehicle frame. Soulenoid Cycle's reservoir design, pictured below in Figure 4.31, is designed to be waterjet from 1/8" aluminum sheet metal. Locating ears are included to aid with assembly and welding.



Figure 4.31 Preliminary reservoir design.

The triangular shape of this reservoir, angled at 36 degrees, is designed to fit underneath the seat. In addition to closely fitting the frame geometry, the placement underneath the seat provides structural support. There are 6 orifices in the reservoir. They are accessed through weld-on, threaded fittings. The outlet of the reservoir, which is drawn from the pump and circulates through the hydraulic circuit, must be located at the lowest possible point of the reservoir. This is done to decrease the power needed by the pump to draw the fluid. At the return port, shown in the upper right corner of the reservoir, hydraulic fluid is returned to the reservoir after flowing through the hydraulic circuit. A vent valve, located opposite the return valve, consists of a brass screw, that can be taken out if the reservoir is too full and needs to be drained. A fill port, located to the left of the vent, is used to fill the tank prior to use. Having the ability to fill the tank from a separate port will allow the tank to be emptied between uses and decreases the vehicle weight during shipping. A dedicated fill port is a new addition compared to the 2018 and 2019 vehicles. Lastly, a sight tube informs the rider of how much fluid is in the reservoir. Sight tubes eliminate the need for internal measurement devices or electronics that measure the volume of fluid in the reservoir. Manufacturing and detail drawings for this design are located in Appendix L.

4.5 Preliminary Circuit Board Design

Throughout prototyping with both Arduino Nano and Blue Pill development boards, two viable Printed Circuit Boards (PCBs) were designed. One PCB includes an Arduino Nano with the MCP2515 CAN controller and MCP2551 transceiver, and the other PCB includes a Blue Pill with the MCP2515 CAN controller and TJA1050 transceiver. After considering both options, the Blue Pill was chosen. The first PCB implements most of the components on the SparkFun CAN shield of Figure 1.3.2. SparkFun publishes open-source schematics of their products. The PCB, shown in Figure 4.32, contains a CAN communication circuit with the MCP2515 and MCP22551 integrated circuits. In addition, the PCB has a serial port to connect to a Nextion display and JST snap-fit connectors to connect to the pushbuttons. The pairs of pushbuttons are isolated on independent ground planes, separated by milled slots. This allows both pairs of switches to be detached from the main board and placed in a more convenient location for the vehicle's rider. To preserve space, this PCB was designed to fit directly beneath a Nextion display, so both components could be stacked on top of each other.

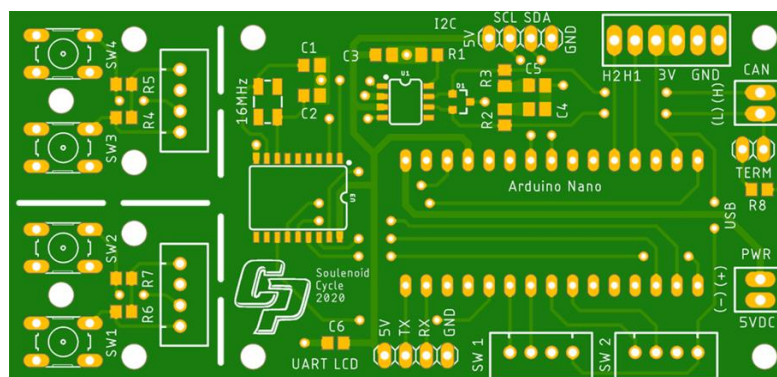


Figure 4.32 PCB design with Arduino Nano.

Indicated by vertical and horizontal slots traced onto the circuit board, this board is designed to be separated into three components. The two left sections house the tactile push buttons that the rider will use to switch drive modes. Each pair of buttons is mounted on either handlebar, allowing the rider to easily switch drive modes with their thumbs. Shown by the white rectangles, the three boards connect to each other with JST-XH snap-fit connectors. Below in Figure 4.33, JST connectors are versatile and rugged.



Figure 4.33 JST-XH snap-fit wire connectors, 4-pin.

In low-powered electrical systems, JST connectors are preferable because they support solid-core wires. Stranded core wires are more prone to tearing and damage, and screw-pin terminals can sometimes expose wires to dirt and dust, which impedes signal strength. On the far right next to the “UART LCD” silkscreen label, four male pin-headers output data and power to the Nextion display. Male pin headers were selected for the display and for the hall effect sensors because female pin headers often accompany both components. For added clarification, Figure 4.33 shows the wire connections that ship with the Nextion display, which connect to the microcontroller through four female pin headers. Lastly, screw-pin terminals were chosen for the CAN bus and power supply ports. The PLC uses similarly sized screw pin terminals, so any shared signals between the two controllers should use the same wire connections. Overall, the inclusion of a printed circuit board helps achieve the NEMA 4 rating goal. With screw pin terminals and snap-fit connectors, the printed circuit board reduces the total amount of loose wire connections and allows more electronic components to be housed in a single casing.

4.6 Preliminary Graphical User Interface Design

The on-board display provides feedback to the rider about the operation of the vehicle. Such feedback includes displaying the current drive mode, raw sensor data, plotting recorded data, and managing errors, data storage, and telemetry. The rider can interface with the display by either touching on-screen buttons or with buttons mounted on the handlebars. Each physical button on the handlebar activates a different drive mode. The on-screen touch buttons are used to display data and manage errors. Ideally, physical buttons are easiest to operate on a moving vehicle because they don’t require the user to locate a virtual button on the screen, which is distracting when riding. However, since each button requires a dedicated input/output pin, using too many buttons could inhibit the use of additional sensors. Therefore, it makes sense to use a combination of physical and virtual buttons, with virtual buttons reserved for actions not needed while riding.

Given the requirements of the interface, a five-page operating system was developed to be compatible with an SPI TFT screen--the same display used by The Incompressibles. The home screen continuously updates two output metrics to the user: accumulator pressure and bike velocity. On the right side of the home screen, as shown below in Figure 4.34, the selected drive mode is indicated to the rider with a red circle. The letters: D, B, C, and R represent the Direct Drive, Boost, Coast, and Regeneration modes, respectively. The home screen also includes four virtual buttons: Check, Pressures, Flowrates, and Data.

The “Check” button switches to a page for managing and displaying errors and testing the functionality of different input transducers. This page is shown in Figure 4.35.

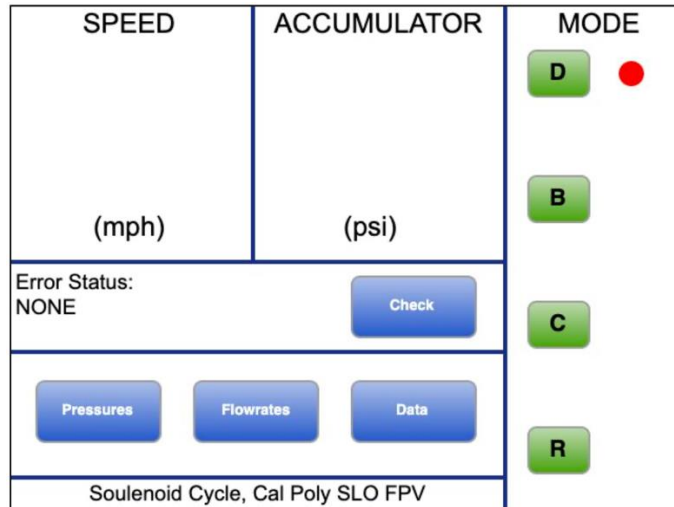


Figure 4.34 Preliminary home screen page.

The interface pages were designed using Pencil Project, a free, open-source computer software for prototyping display interfaces. After each page was designed, the interface was replicated in line code, using C++ in the Arduino IDE.

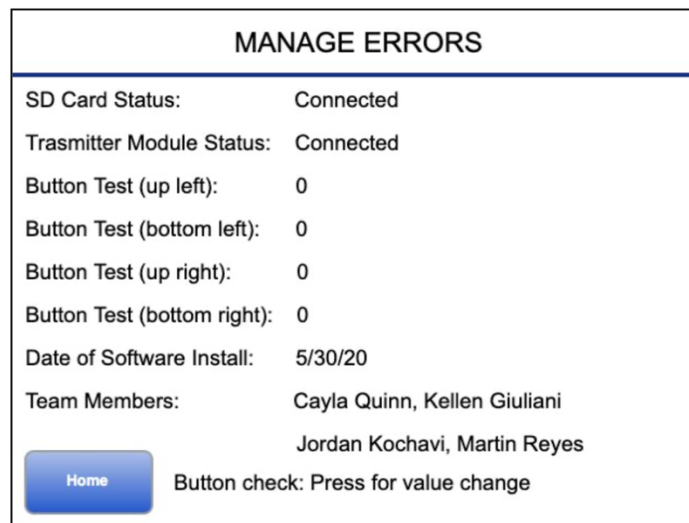







Figure 4.35 Preliminary error diagnosis page.

The “Manage Errors” page is valuable to the on-board display system because it allows the rider to diagnose wiring errors. Momentary push buttons are notoriously easy to burn out, especially without professional soldering. In this page, the value displayed next to each push button represents the binary voltage read from the microcontroller: when a button is pressed, the component completes a circuit, resulting in a voltage differential that is interpreted by the microcontroller as either high (binary 1), or low (binary 0). Pressing each button toggles its value to a 1, which indicates to the rider that it is operating correctly.

A third page, shown below in Figure 4.36, displays current pressure sensor readings. Each sensor has the option to display recorded data in the form of a time graph, which can be viewed by the user with the green buttons on the right side of the screen. All buttons on the “Pressure Monitoring” screen are virtual and

cannot be accessed with the physical buttons on the handlebars. In addition to a “Home” button that returns the user to the “Home” screen, a “Start” and “Stop” button toggle data acquisition.

PRESSURE MONITORING		
Location	Value (psi)	Graph
Accumulator		
Before pump		
After pump		
Before motor		
After motor		









Figure 4.36 Preliminary pressure monitoring page.

Though this screen continuously displays current pressure sensor readings, the “Start” button creates a new spreadsheet that logs each sensor reading in time increments determined by software timer interrupts. The “Stop” button ends the data collection. Each graph button displays a time graph for the most recent data collection. Though any data processing is much more efficient on a computer, a primitive display of sensor values allows the rider to quickly look for trends and problems in the hydraulic systems without having to dismount and examine the data on a computer. A fourth page, as shown below in Figure 4.37, has the same functionality as the “Pressure Monitoring” page, except that it displays all data from flow sensors. On either page, the “Start” and “Stop” buttons enable and disable logged sensor data for both pressure and flow sensors.

FLOWRATE MONITORING		
Location	Value (psi)	Graph
Accumulator		
Before pump		
Before motor		






Figure 4.37 Preliminary flowrate monitoring page.

The last screen, shown below in Figure 4.38, manages data logging and displays the status of any storage and telemetry components. Though slightly redundant to the “Manage Errors” screen, a separate page for managing data logging is useful when adding additional data logging components. Lastly, shown below in Figure 4.45, a simple “Graph” screen plots the selected data. For efficiency and memory conservation, a single graph screen is used to plot every output metric, rather than creating a unique graph screen for each location and units. The word, “Location” in the graph screen title is simply substituted with the specified location.

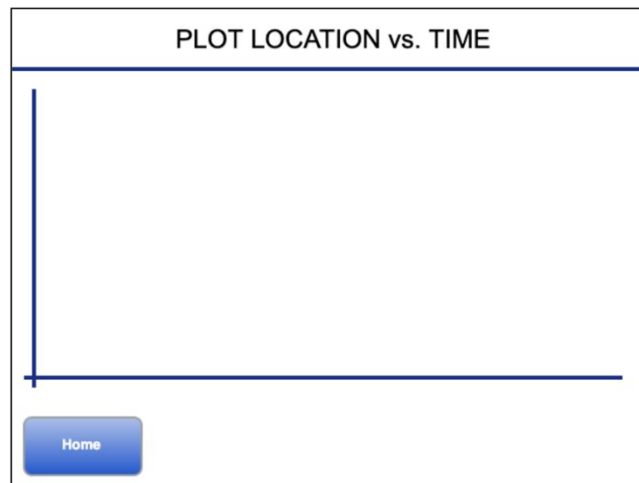


Figure 4.38 Preliminary data plotting page.

Even though sensors, physical buttons, and other external modules were not yet installed, the preliminary display interface was installed on an Arduino Nano, connected to an ILI9341 2.8” SPI TFT display, as shown in Figure 4.39. As noted in the Interface Selection section, these displays require a large number of input pins and have relatively poor visibility compared to other display options. In addition, the possibility of slow refresh rates is concerning when the system must continuously update values to the rider. C++ code for the preliminary interface is located in Attachment 4.

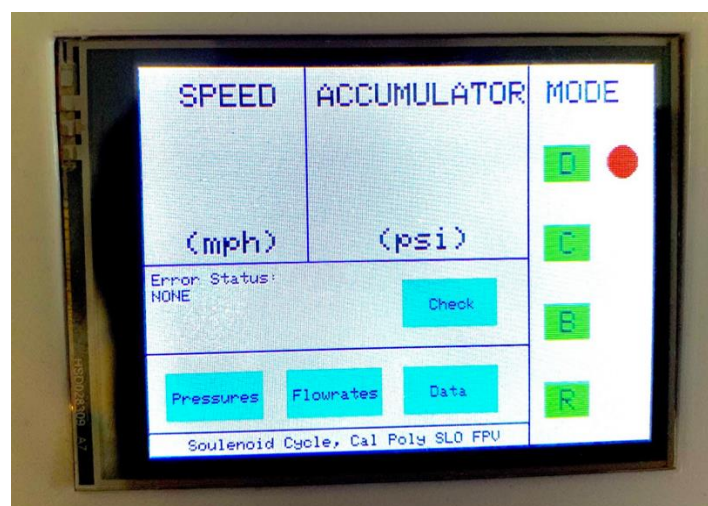


Figure 4.39 Testing with preliminary touch screen interface.

The loading speed of each screen was measured using the microcontroller's internal clock. Before writing each word, shape, or line to the screen, the internal C++ function, `millis()`, is called to return the milliseconds elapsed since the controller was powered on. After each element is written to the screen, the function is called again. The difference in elapsed time readings represents the time taken to write each element to the display. The table below compares the writing speeds of each element on the display. The Arduino Nano internal clock, which uses a relatively crude ceramic resonator, carries an uncertainty of 0.05% when using the `millis()` function. The values below were calculated from an average of three trials; a raw data sheet for these measurements is located in Appendix C. In addition to measuring display times, the screen visibility was tested under sunlight exposure, compared to indoor use. Though direct sunlight makes the display harder to read, the interface's white background improves contrast.

Table 4.5 Results of speed testing conducted on ILI9341 TFT display.

Screen Element	Writing Time [seconds]
Fill entire screen with a solid color	3.09
A single green drive mode icon	0.038
A single blue virtual button	0.095
Large font text	0.149
Small font text	0.044
Thin line	0.012
Total home screen initialization time	4.073

As shown above, the time taken to initialize all of the elements on the display takes over four seconds. Not including the time taken to clear the display by filling it with a solid, white color, it takes almost one second to write all elements of the home screen to the display. These numbers are likely slightly inflated because they do not account for the time taken to output the elapsed times to the serial interface in the Arduino IDE, which is not measurable. Nonetheless, a total initialization time of four seconds for a single, 2.8" display is excessively slow. However, for nearly all normal operation of the vehicle, the interface will mostly remain on the home screen, and viewing the other pages is needed infrequently. Since the time needed to write text was measured to be relatively quick, it may still be useful to continue to use this interface, as it indicates that updating measured values can be achieved with fast refresh rates. In addition, the processor of the Arduino Nano may also contribute to screen-writing times. The Arduino Nano is based on the ATmega328p microchip with 32 kB of flash memory and 2 kB of dynamic memory. Compared to other Arduino modules, the nano is compact, slower, and has a lower memory capacity. The Arduino Mega, a larger and more powerful board, is based on the ATmega2560 microchip, has 256 kB of flash memory and 8 kB of dynamic memory. Switching to a board with a significantly larger memory capacity would likely improve refresh rates.

The preliminary software in Attachment 4 programs Soulenoid Cycle's user interface, designed for the ILI9341 LCD module used by the Incompressibles in 2018. This code requires minor modifications to be made compatible with the Nextion LCD Module. The preliminary software receives rider input from virtual

buttons on the touch screen. While the Nextion display has touch screen capabilities, rider input to switch drive modes comes from the pushbuttons on the handlebars. When pressed, each of the four buttons trigger a hardware interrupt, after which the microcontroller will communicate the selected drive mode to the ECDR 0506-A. Communication between the ECDR 0506-A and the Arduino is clocked by timer or software interrupts. Every 10 ms, the ECDR 0506-A will send a CAN packet to the Arduino containing pressure measurements and valve statuses. After receiving the CAN packet, the Arduino will proceed to display the data to the Nextion display. The Arduino also receives input from up to two hall effect sensors used to calculate rotational speeds. It calculates each speed and displays them on the screen. For added clarification, the task-state diagram below documents the tasks carried out by the Arduino.

4.7 Preliminary Electronics Schematic

The mechatronics system onboard Soulenoid Cycle's recumbent vehicle consists of two independent controllers. Shown in Figure 4.40, the ECDR 0506-A controls the hydraulic circuit by actuating four solenoid valves and receives feedback from three pressure sensors. The custom controller interfaces with the rider by receiving button signals and writing data to an LCD screen. The two controllers communicate over Controller Area Network (CAN). CAN is an efficient and fast communication protocol, commonly used in industrial and automotive devices. For example, in a personal car, all onboard processors, including its main computer, HVAC controls, light sensors, and lubrication systems communicate over CAN. CAN is an advantageous communication protocol because it only requires two signals, as opposed to SPI, which requires at least four. Also, CAN protocol can support several devices at once in a communication bus.

Nearly all industrial controllers, such as the ECDR 0506-A, have hardware peripherals that support CAN communication. Most microcontrollers, such as STM32 and Arduino development boards, have the software capabilities needed to communicate over CAN, yet sometimes require extra hardware to connect to a CAN bus. Figure 4.40 presents a general, simplified schematic of how the different devices in the mechatronics system communicate.

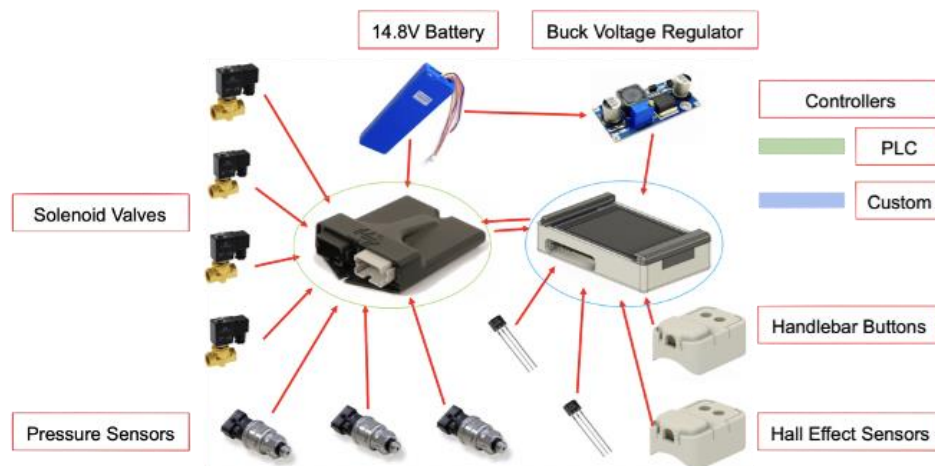


Figure 4.40 Preliminary schematic of vehicle electronics.

The mechatronics system is powered by a 14.8V lithium polymer battery due to the power requirements of the solenoid valves and the ECDR 0506-A. In order to power the Arduino, the battery supply is regulated to 5V through a Buck Voltage Regulator.

The Arduino receives input from four tactile pushbuttons. The buttons operate on 3.3V logic and output a logic “high” when pressed. The Arduino is also configured to receive input from two hall effect sensors.

Hall effect sensors output an analog voltage when they contact a magnetic field and are typically used to calculate angular speeds. A hall effect sensor is held stationary at the edge of a wheel or rotating shaft, and a magnet, or pattern of magnets, is glued around the rotating component. Angular speed is directly proportional to the frequency of the sensor's contact with the magnets. One hall effect sensor is placed on the rear wheel to measure the speed of the vehicle. The second sensor is placed on the pump to measure human power input.

The Arduino is configured to receive input from the hall effect sensors and buttons because it has more GPIO pins than the ECDR 0506-A. The ECDR 0506-A only has 6 input pins and 6 output pins, while the Arduino Nano has 20 General Purpose Input/Output (GPIO) pins. By moving all low-voltage signals to the Arduino, the ECDR 0506-A is more available to control and read higher-voltage signals.

The custom controller displays information to the rider with a 2.8" Nextion HMI display. In addition to a full color touch screen, Nextion displays are particularly effective because they possess their own microprocessor that refreshes the display. Most displays need to be programmed by a microcontroller using custom documentation that is written to interface with a specific display. For example, the ILI9341 LCD module, used by The Incompressibles in 2018, is driven directly by an Arduino. In order to draw a green rectangle on the screen, C++ code could include,

```
ILI9341.drawRect(x1, x2, y1, y2, GREEN);
```

which means that Arduino must tell the screen to draw a shape at a specific point in time. When the Arduino has other tasks to complete, such as reading sensor data and communicating with the ECDR 0506-A, drawing a simple shape is an alarmingly slow process. For small ASCII screens, speed is not an issue—it takes only microseconds to display a single ASCII character. However, for large, full-color displays, using an Arduino to print complex shapes, animations, and text is too slow to be a practical user interface. Appendix C contains tabulated measurements of time required to display differently sized elements on an ILI9341 LCD module.

Nextion displays eliminate the speed challenges of normal LCD modules because they are not directly programmed by the Arduino. Instead, they are configured in a Human Machine Interface (HMI), which is a visual-based computer program similar to Adobe Illustrator. The display layout, including different shapes, text, animations, and virtual buttons are all pre-configured, which results in much higher refresh rates. In other words, the Arduino does not need to tell the display when to draw a shape because it already knows how and can refresh itself without being told to. Thus, the Arduino only needs to output numerical values and text to the screen, without needing to worry about where they are displayed, and their size, shape, color, etc.

4.8 Preliminary Electronics Enclosure Design

Each component, aside from the PCB and Nextion display, are designed to be 3D printed on a Bibo 2-Touch 3D printer, owned by a team member. Loose and sliding fit parts are designed with 0.6mm clearance, and tight-fit parts are designed with 0.4mm clearance. Permanent press-fit are designed with 0.25mm clearance. The sliding top for the screen is only intended to cover the screen while the vehicle is not in use. Before using the vehicle, the screen can be slid off entirely, and then stored by sliding it onto the four press-fit nubs on the bottom of the display case, shown in gray on Figure 4.41. Rounded slots in the case allow for cables to connect to the microcontroller board. Lastly, the case includes two protrusions to be bolted onto either the left or right handlebar. The tight and press-fit parts are designed to be fixed together with superglue after assembling. Visible in Figure 4.41, both the screen and the microcontroller board have mounting holes to be fixed to the casing. The case is designed to allow for threaded metal inserts. The metal

inserts contain 3mm threads and are installed in the casing with a soldering iron. The soldering iron heats the 3D printed enclosure, allowing the metal insert to sink into the part.

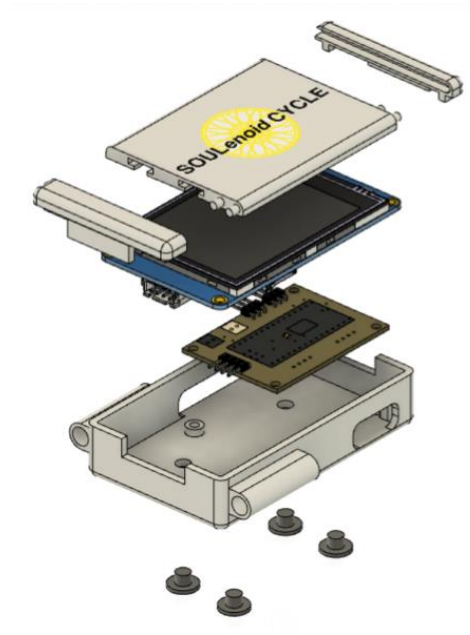


Figure 4.41 Preliminary enclosure design, exploded view.

In addition to the screen enclosure, similar cases are designed for the drive mode select buttons. Shown below in Figure 4.42, the button enclosure is just two pieces. A small extrusion, along with an arched hole, allow enough room for the JST connectors. Two holes allow the buttons to stick through the 3D printed top. The bottom of the case is rounded to conform to the radius of the rounded handlebars. Similar to the interface enclosure, these parts are designed to be tightly fit and glued together.

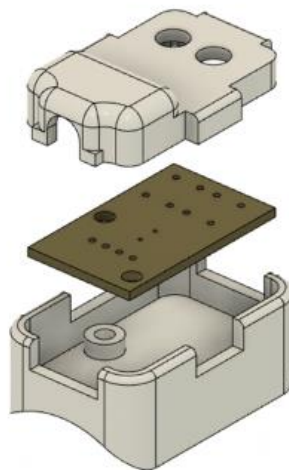


Figure 4.42 Preliminary button module enclosure, exploded view.

Described above, the interface is designed to be mounted on the handlebars. In a recumbent position, the rider will not be able to look between their legs, and the screen would be too far away to read easily. Placing

the components on the handlebars will bring the screen close enough to the rider to view the screen and manipulate the drive-mode buttons with their thumbs. Below, Figure 4.43 presents a render of the controller interface layout on the vehicle.



Figure 4.43 Preliminary component placement of electronics.

4.9 Steering Linkage

Much like the vehicle frame, the steering linkage design process was guided by the principles of recumbent tricycle manufacturers, both professional and amateur alike. The following section details the final linkage design process.

There are a few different design principles that must be taken into consideration when designing a recumbent tadpole steering linkage: direct or indirect, Ackermann's steering geometry, center-point steering, and caster angle.

There are two types of recumbent tricycle steering linkages: direct and indirect. Direct steering linkages connect the handlebars directly to the headset of each wheel, while indirect linkages connect the handlebars to a pivot point on the vehicle frame which then connects to the wheels via some sort of additional linkage. Direct linkages usually create a more twitchy and reactive experience for the rider, while indirect linkages are smoother yet sacrifice some fine control as well as turning radius. For Team Soulenoid Cycle though, the critical difference between these two linkage types is a marked difference in complexity, both in operation and fabrication. Shown in Figure 4.44 are examples of both linkage types.



Figure 4.44 Direct vs. indirect steering linkages.

Ackermann's steering geometry is an arrangement of linkages designed to solve the problem of a vehicle's two front wheels needing to rotate to different angles when making a turn. This linkage geometry, as shown

in Figure 4.45, eliminates the sideways tire slip that would otherwise occur by making the center-point of all wheel turning circles coincident. A tie rod, capped on each end with a ball joint rod end, connects the two front wheels and completes the linkage, ensuring that the wheels pivot together.

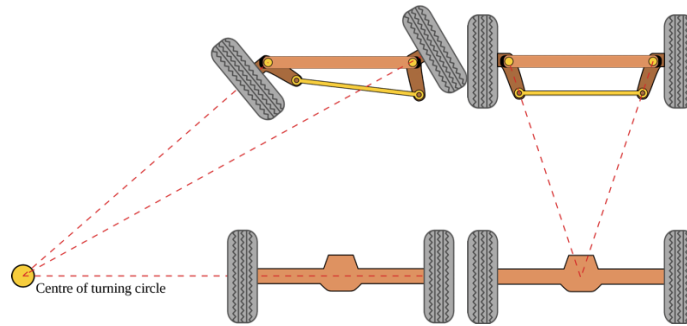


Figure 4.45 Diagram of Ackermann steering linkage geometry.

Center-point steering is a technique utilized by recumbent tricycle manufacturers where the rotational axis of the kingpin intersects the road contact patch of the tire, as shown in Figure 4.46. This allows the wheels to rotate about a point beneath them instead of one that is offset, drastically reducing the effort required to turn the wheels at low speed while simultaneously improving vehicle handling and higher speeds. Furthermore, forces acting upon the wheels, like bumps in the road or uneven braking, are directed along the axis of the kingpin, so no torque can be exerted which might jerk the steering.



Figure 4.46 Preliminary steering design that implements center-point steering.

Lastly, caster angle is a technique utilized by tricycles in which the kingpin is canted at an angle such that its rotational axis leads the contact patch of the tire, as seen in Figure 4.47. Set at around 10-15 degrees of inclination for tadpole recumbents, the axis passes through the point towards which the wheels will naturally steer, allowing for self-centering steering, a necessity for vehicle stability and safety at low and high speeds alike.



Figure 4.47 Preliminary steering design that implements a caster angle of 10 degrees.

The mechanical simplicity and therefore ease of fabrication that the direct steering linkage offers is more desirable for Soulenoid Cycle. The preliminary steering linkage selection is a further iteration of the direct linkage, where the circular crossbar tubing is replaced with the same square tubing as the rest of the vehicle frame as seen in Figure 4.48. Additionally, this change makes fabrication simpler in that the vehicle frame from the seat to crank set is already canted at a 15 degree angle, so the caster angle of the steering linkage is built into the frame. This results in a far simpler fabrication process for connecting the crossbar and kingpins.



Figure 4.48 Orthographic view of preliminary steering design.

4.10 Simulated Performance of Concept Design

After completing the conceptual design for the frame and hydraulics, Solenoid Cycle wanted to get an estimate of how the new design would perform. Similar to how it was done to verify component selection, the Simscape Models were again used. Since some models like the Direct Drive and Efficiency still have a large percent error, the models were mainly used to compare the performances of last year's vehicle to Soulenoid Cycle's new design. This was most practical since last year's parameters were easily attainable.

Table 4.6 Comparison of model parameters used in the 2019 and 2020 vehicles.

Parameter	Vehicle		
	19-20	20-21	% Change
Tube internal Diameter [in]	0.37	0.60	62.2%
Tube Length [in]	120	70.0	-41.7%
Tube Roughness [ft]	3.0E-05	0.000005	-83.3%
Bike Weight [lbf]	103	100	-2.9%
CG Height [in]	33.0	14.7	-55.5%
Rolling Resistance Coefficient	0.004	0.005	25.0%

Most of the Simscape parameters remained the same from last year's since most of the hydraulic components would be reused. One of the minor changes to the parameters where the hydraulic fluid itself. NFPA changed the rules allowing teams to choose their hydraulic fluid. Instead, they have assigned each team 5 gallons of Lubrizol. This meant that fluid properties like density and viscosity of the previous Mobile hydraulic fluid were changed to model the Lubrizol's. Other parameters were altered and are presented in Table 4.6. The tube diameter and roughness model the change to hydraulic hardlines. The line type in the actual Simscape model was also changed to rigid instead of flexible. The other parameters presented are the results from changing to a recumbent tricycle. This includes a center of gravity reduction of 55.5%.

The sprint Simscape model is currently the most accurate. Pump My Ride calculated the percent error to be around 5%. This model uses only the accumulator to discharge 2800 psi of hydraulic fluid to the motor. A solenoid with a linear function is used at the accumulator discharge to prevent all 2800 psi to directly discharge to the motor and prevent potential damage. The model results are present in Figure 4.49.

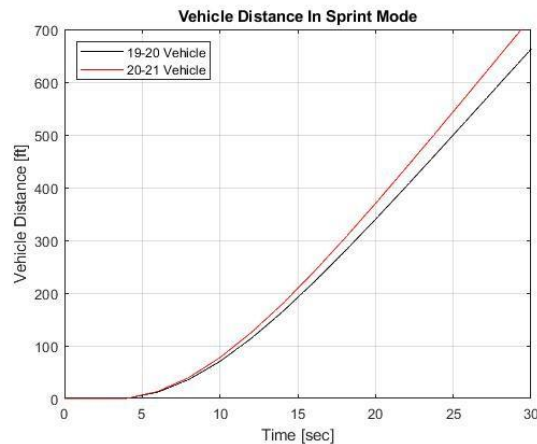


Figure 4.49 Predicted performance of concept design in the sprint challenge.

With the assumption of the sprint race being 600 feet, the models predict Solenoid Cycle's sprint time to be around 2.5 seconds faster, or a 5% improvement. It is a small advantage, however, previous Cal Poly teams have done well in the sprint competition, so any improvement is good.

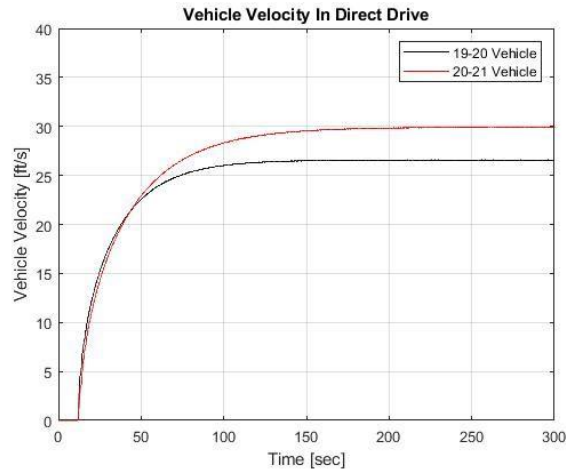


Figure 4.50 Predicted performance of concept design in the endurance challenge.

The endurance challenge is difficult to model. First, the direct drive model is dependent on the rider input. Having a physical person consistently pedal for a mile is almost impossible. Additionally, the models don't take account for the part of the Endurance Challenge that requires teams to test their regenerative braking. These factors largely contribute to the 15% error in the Direct Drive model. So, to get an estimate, the max vehicle velocity is taken and assumed to be constant for an entire mile, a method used by the previous teams. The Simscape results (Figure 4.50) shows that Solenoid Cycle's max velocity peaks at 30 ft/s. This is a 15% improvement, which is significant when considered that the Endurance Challenge is a mile long.

The third challenge tests how efficiently the vehicle uses its stored energy. The goal is to travel as far as possible with minimal stored energy. Previous teams have found that pulsating the accumulator discharge as shown in the accumulator's pressure in Figure 4.51 has yielded the furthest distances. Solenoid Cycle turned to the newest Simscape model originally designed by Pump My Ride to get an estimate of how far the vehicle will travel before coming to a stop. The distance predicted is then used in an Excel spreadsheet provided by NFPA (Attachment 7) that accounts for the accumulator pressure, pre-charge pressure, accumulator volume, and total rider and vehicle weight to calculate the predicted efficiency score.

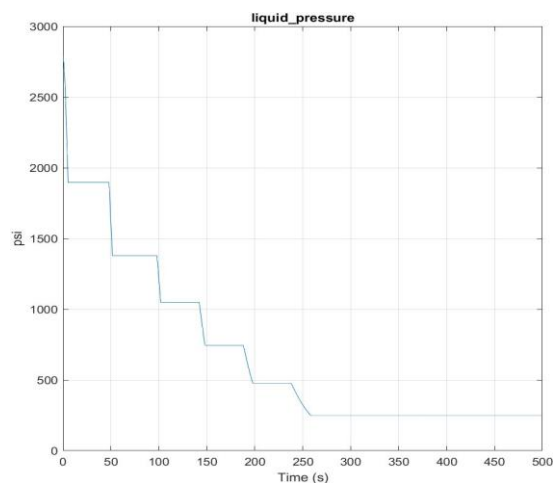


Figure 4.51 Predicted ability of the accumulator to meter its discharge.

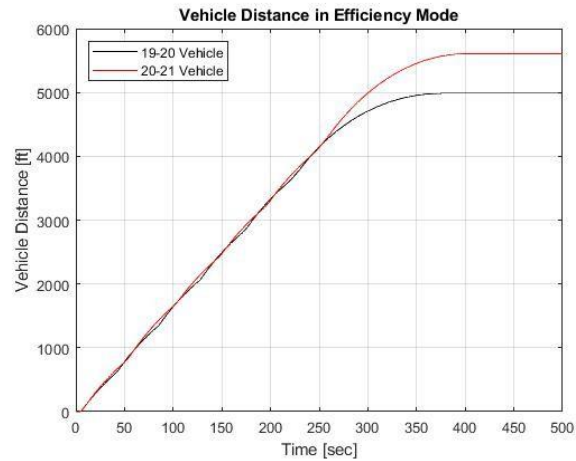


Figure 4.52 Predicted performance of concept design in the efficiency challenge.

The model predicts the Soulenoid Cycle’s vehicle to travel 600 feet further when compared to Pump My Ride’s. The 12% increase is similarly reflected in the final efficiency calculation with a gain of 13%. Even though we expect the efficiency number to be much lower because of the errors still in the model, the improvement gained when directly comparing the two vehicles is still promising.

4.10.1 Weight Approximations

Excluding the hydraulic system, the following weight estimations were obtained from the material properties of each component in the preliminary frame CAD.

Table 4.7 Weight estimates of preliminary frame design.

Component	Material	Quantity	Weight [lbs]
Frame	Aluminum	1	19
Wheels	Steel	3	2.9
Steering	Steel	1	3
Handles	Aluminum	1	2
Seat	Aluminum	1	2.3
Total Weight [lbs]			35

Using these weight approximations, in order to achieve a total vehicle weight of less than 120 lbs, the hydraulic components must weigh less than 85 lbs. The weight of each hydraulic component is measured using a standard balance.

4.11 Risks, Challenges, and Unknowns.

There are two major challenges in designing a safe and effective frame: structural design and manufacturing. Previous Cal Poly teams designed upright bicycle frames using the Patterson Model, which supplemented a structural analysis on the frame body. Soulenoid Cycle must use a similar model to design an effective recumbent frame, while considering static and dynamic loadings. Furthermore, manufacturing, specifically welding with aluminum, presents its own risks and challenges.

For hydraulic components, there is a significant risk in leaking hydraulic fluid. When operating at high pressure, a small leak could cause an explosive jet stream that could endanger the rider and surrounding people. An implementation of a fail-safe method to discharge the accumulator would mitigate this risk.

Lastly, though no electrical components operate at high voltage, exposed wiring and circuitry could damage electrical components. To better quantify these design hazards, refer to the Design Hazard Checklist, located in Appendix E. Based on the applicable hazards, a corrective action plan is presented in Table 4.8.

Table 4.8 Design hazard corrective action plan.

Description of Hazard	Planned Corrective Action	Planned Date	Actual Date
Revolving of rotating parts such as chains and sprockets.	Implement chain guards and covers to isolate moving parts.	December 2020	-
At high acceleration, the vehicle could become unstable and risk the safety of the rider.	Use models to assess the vehicle stability and rideability.	September 2020	-
The vehicle is considered a large moving object and therefore could deliver a dangerous force on impact.	Implement both front and rear brakes in order for the rider to stop as desired.	October 2020	-
The accumulator stores highly pressurized fluid (≤ 3000 psi) in the system. Discharge is only possible through “boost mode”.	Add a cover over the “boost mode” activation key and code the mechatronics system to default to “direct drive mode” or “coast mode”.	December 2020	-
The hydraulic fluid used in the system is flammable.	Identify and fix all system leaks.	September 2020	-
The user will be required to pedal the bicycle in a recumbent position.	The user manual will instruct all riders to warm up and stretch before using the vehicle to reduce the likelihood of injury.	October 2020	-
Hydraulic fluid is hazardous to humans (e.g. injected into the bloodstream, pierced skin, etc.).	Identify and fix all system leaks. Perform hydraulic system checks on a regular basis.	Continuous Course of Action	N/A
The vehicle may be operated in an unsafe manner.	The vehicle will only be operated with at least one team member present, since they are knowledgeable on bike features and operating procedures.	Continuous Course of Action	N/A

5 Final Design

Cal Poly's 2020-2021 fluid powered vehicle includes the core hydraulic system from the 2019-2020 vehicle, upgraded with relocated components for improved hydraulic efficiency, a newly fabricated fluid storage tank, and newly designed component mounting brackets. The vehicle frame has undergone a complete redesign, from a standard two-wheeled upright frame, to a three-wheeled recumbent tadpole frame. The vehicle has four operating modes — boost, direct drive, regenerative braking, and pedal charge — triggered via buttons located on the handlebars. An ECDR hydraulic controller activates the solenoid valves in the hydraulic manifold and collects data from pressure sensors. Operating alongside the ECDR is a microcontroller that pushes data to an LCD touchscreen, measures the speed of the vehicle, and takes input signals from the drive-mode selection buttons. The hydraulic pump and motor deliver power from the crankset pedaled by the rider, or via energy stored in the vehicle accumulator. Pictured in Figures 5.1 is a CAD render of the overall vehicle design. Not shown are hydraulic hoses, electrical connections, sensors, pedals, or chains.



Figure 5.1 Complete render of final vehicle design.

5.1 Final Circuit Board Design

After prototyping with the Arduino Nano, as discussed in Section 4, the STM32 development board was selected due to its increased processing power. The final PCB design uses the CAN circuit on the breakout module in Figure 4.6, which contains the MCP2515 and TJA1050 integrated circuits. While its overall size is slightly larger than the PCB described in Section 4.5, it still fits underneath a Nextion display. This PCB, shown in Figure 5.2, features a similar push-button layout and screw pin terminals for power input and CAN transmission. A polarized capacitor is also placed closed to the power terminals to act as a high frequency noise filter, which reduces noise in the CAN signals. The full circuit board schematic, as designed in Autodesk Eagle, is located in Appendix I.

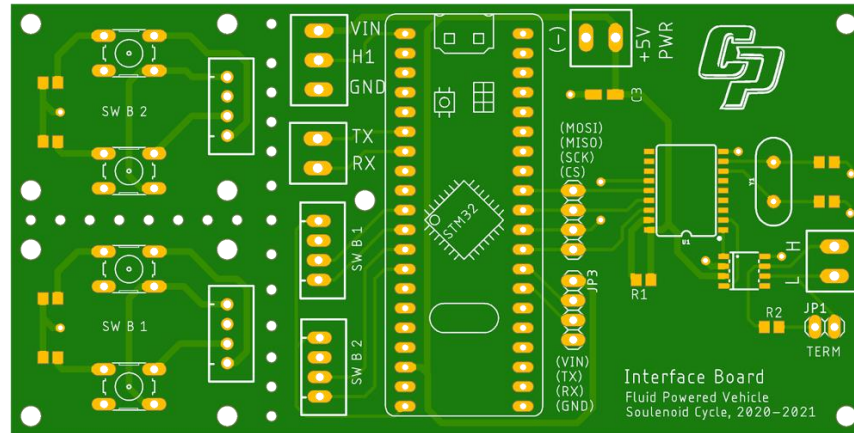


Figure 5.2 Final PCB design that uses an STM32 development board.

Aside from the difference in microcontrollers and CAN transceivers, this circuit boards is functionally identical to the preliminary design discussed in Section 4. After prototyping with the Arduino Nano, this board was ultimately selected because of the STM32's increased performance abilities. Another advantage of selecting an STM32 over an ATmega328 is its abundance of serial peripherals. Shown in Figure 5.2, the RX/TX port is configured in software to print debugging information to a serial monitor. If the user encounters a problem with the interface, they can simply connect to the PCB's serial port to monitor its software and communication.

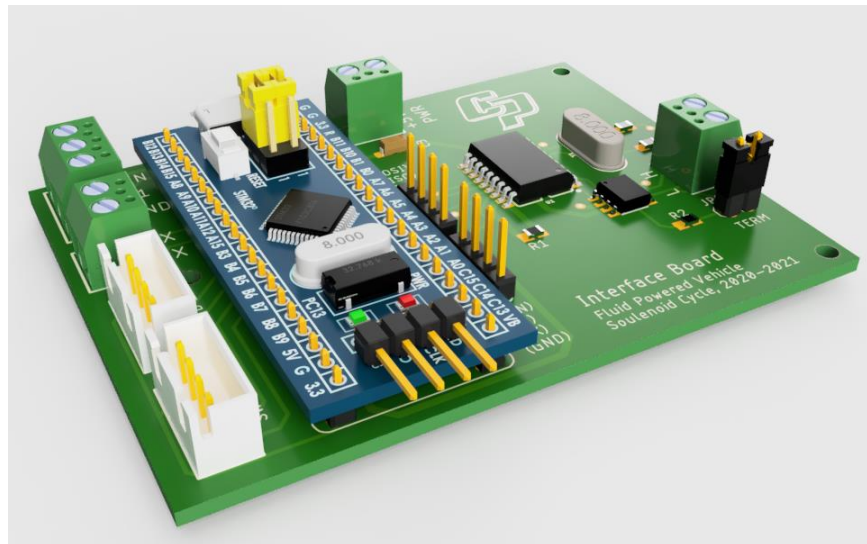


Figure 5.3 Render of final PCB design, populated with 3D models of electrical components.

After designing the circuit board layout in Autodesk Eagle, a 3D model was created in Autodesk Fusion 360 in order to accurately dimension a 3D printed enclosure. A render of the circuit board is shown in Figure 5.3. Populating the circuit board with 3D models, which were obtained from GrabCAD, allowed for more accurate enclosure modeling. The PCB interfaces with its peripherals using a combination of screw pin terminals and JST snap-fit connectors. Screw pin terminals are effective for tightly securing power connections and long-distance signals. JST snap-fit connectors were chosen for the button modules to allow for quick disconnecting. The circuit board was designed after constructing a fully-functional breadboard prototype, which is shown in Figure 5.4.

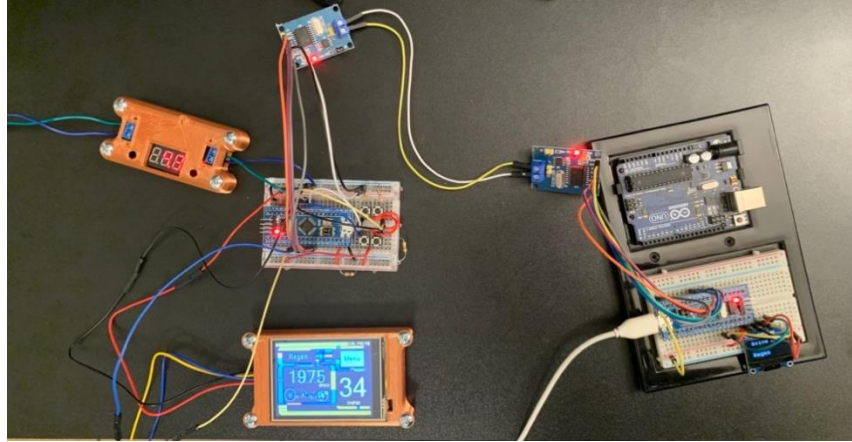


Figure 5.4 Breadboard prototype of CAN interface.

The left half of Figure 5.4 represents all of the components that interact with or are mounted on the printed circuit board. The top module is an MCP2515 and TJA1050 breakout module, and the breadboard contains an STM32 development board and four buttons. The screen is also connected to the STM32 development board. The right half of Figure 5.4 represents the expected response of the ECDR 0506-A (the Arduino Uno is not used here). Due to COVID restrictions, the actual ECDR 0506-A was inaccessible when this prototype was built, which necessitated a “simulated” controller for prototyping. In Figure 5.4, the yellow and white wires are the CAN lines. The software installed on the main STM32 is the same software discussed in Section 5.2. The simulated ECDR 0506-A on the right half of Figure 5.4 consists of another STM32 development board, an MCP2515 and TJA1050 breakout module, and a small OLED. The simulated ECDR 0506-A receives messages from the main interface and displays them on the OLED to demonstrate that the CAN bus is functioning normally. Visible in Figure 5.4, both screens display the word “Regen,” which indicates that both controllers are aware that the vehicle should be in regenerative braking mode. Shown in Figure 5.5, the PCB works as expected. A Dremel rotary tool with a cutting wheel attachment was used to separate the button modules from the main board, and sand paper was used to clean up its edges. The single mounting hole directly next to the white JST connectors was difficult to access after assembly; in a future iteration, it is recommended to extend the board to provide sufficient space for more mounting holes.

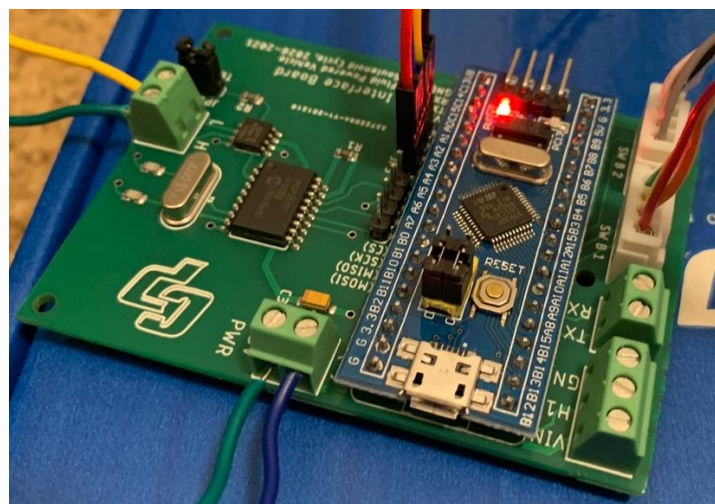


Figure 5.5 Photograph of final circuit board after assembly.

The screw pin terminals effectively secure the CAN and power lines, however it would be more convenient if their terminals were located closer together. This PCB requires wires to leave the board from three of its sides, which makes it more difficult to band wires together in cable strips. The PCB also has a significant amount of free space. Finally, it is recommended to switch to smaller connectors. The screw pin terminals, Dupont connectors, and JST connectors significantly raise the overall height of the PCB assembly, which contribute to the thickness of its enclosure. Connectors that carry smaller footprints would reduce the overall size of the interface module.

5.2 Software Design

This section describes the software design for the STM32 that communicates with the Nextion display and the ECDR 0506-A. The STM32 relays button presses to the ECDR 0506-A over a CAN bus, and receives a pressure measurement from the ECDR 0506-A. The STM32 relays the button presses, pressure measurements, and the vehicle speed to the display. A schematic of inter-controller interactions is shown in Figure 5.6.

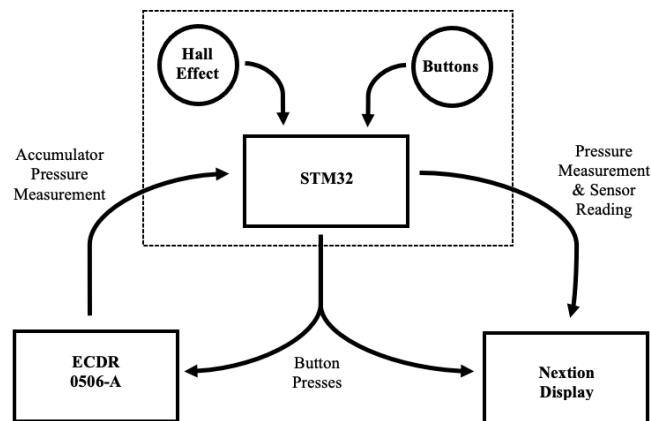


Figure 5.6 Inter-controller system boundary diagram.

The dashed outline in Figure 5.6 represents the system boundary of the STM32's software. The circled components are passive and are read using hardware interrupts and polling. For detailed software documentation, visit the GitHub repository at the following link: <https://jkochavi.github.io>. Software for the STM32 uses FreeRTOS, which is an open-source RTOS that works well with STM32 microcontrollers and the Arduino framework. The code is structured into three high-level tasks: display communication, CAN communication, and sensor measurement. In addition, each button is tied to a hardware interrupt.

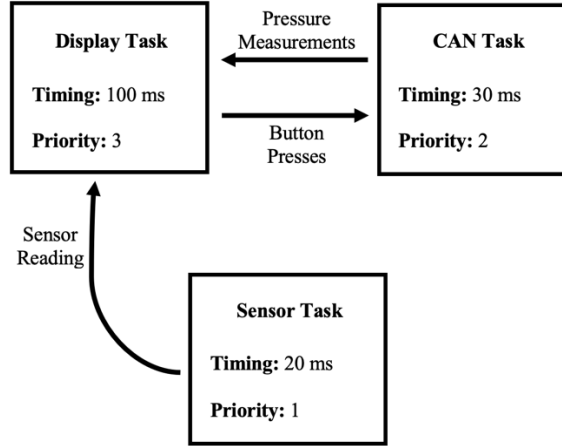


Figure 5.7 High-level task diagram.

Shown in Figure 5.7, the display task receives information from the CAN and sensor tasks, which is subsequently relayed to the Nextion display. The display task runs every 15 ms, the CAN task runs every 30 ms, and the sensor task runs every 20 ms. Timing is most critical for the sensor task. The sensor task periodically checks the status of a GPIO pin attached to a hall effect sensor, which is used to measure the speed of a 26-inch bicycle wheel. The task must check the sensor frequently enough such that it doesn't miss a trigger. The maximum timing period for the sensor task is calculated using the equation,

$$T_{Sensor,max} = \frac{\pi D}{V},$$

Where D is the wheel diameter and V is the vehicle's translational velocity. Using a conservative maximum speed of 45 mph for the human-powered vehicle and a wheel diameter of 26 inches,

$$T_{Sensor,max} = \frac{26\pi \text{ in}}{45 \frac{\text{mi}}{\text{hr}} \times 63360 \frac{\text{in}}{\text{mi}} \times \frac{\text{hr}}{3600 \text{ sec}} \times \frac{\text{sec}}{1000 \text{ ms}}} = 103 \text{ ms}.$$

In order to ensure that the sensor task will catch the sensor trigger without fail, it is best practice to poll 5 times faster than the maximum period or settling time. Therefore, a 20 ms timing period was selected. The sensor task reads the state of the hall effect sensor using a Finite State Machine (FSM). As shown in Figure 5.8, the FSM switches states based on the high/low status of the hall effect signal.

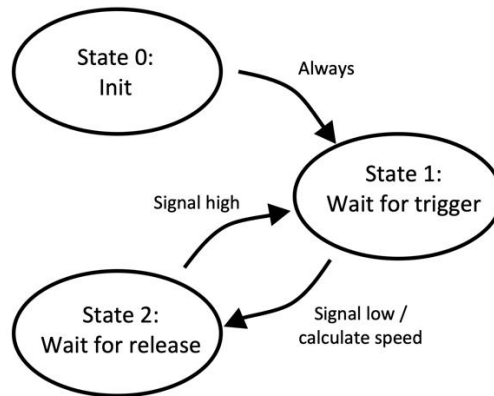


Figure 5.8 State transition diagram for hall effect sensor task.

In State 1, the task continuously waits for a hall effect trigger. Since the sensor is active-low, the task uses the function `debounce()` to identify when the signal transitions from high to low. When this change is identified, the task calculates the speed of the vehicle and stores it in two inter-task variables: `bikeSpeed` and `floatSpeed`. See variable descriptions for more information. After the speed is calculated, the task transitions to State 2 to wait until the signal transitions back to high. When the signal returns from low to high, the task transitions back to State 1 to wait for the next pulse.

The STM32 transmits and receives packets of data from the ECDR 0506-A using the MCP2515 library written by GitHub user, *autowp* [1]. Messages to and from the ECDR 0506-A are transmitted in bytes. Each CAN frame has an 11 bit message ID. The STM32 first identifies the ECDR 0506-A with the message ID, and then constructs and sends a message. The code below sends a button press in 1 byte of data. The function, `sendMessage()`, transmits the message through the MCP2515 controller.

```

if (buttonState != previousButtonState_CAN)
{
    struct can_frame canMSG;                                // Create a CAN message structure

    canMSG.can_id = 0x181;                                    // COB-ID for transmitting a PDO message

    canMSG.can_dlc = 1;                                       // Define the message length as 1 byte

    if (buttonState == 1) {canMSG.data[0] = 0x01;}           // If buttonState is 1... then send a 1
    else if (buttonState == 2) {canMSG.data[0] = 0x02;}       // Else if buttonState is 2... then send a 2
    else if (buttonState == 3) {canMSG.data[0] = 0x03;}       // Else if buttonState is 3... then send a 3
    else if (buttonState == 4) {canMSG.data[0] = 0x04;}       // Else if buttonState is 4... then send a 4
    else if (buttonState == 5) {canMSG.data[0] = 0x05;}       // Else if buttonState is 5... then send a 5

    node.sendMessage(&canMSG);                                // Send the message

    previousButtonState_CAN = buttonState;                    // Reset to prevent continuous transmitting
}

```

The accumulator pressure is measured from a digital pressure transducer that is installed in the hydraulic manifold. The pressure transducer that is connected to the ECDR 0506-A is configured to output an analog voltage, ranging from 0.5 - 4.5 Vdc. When the controller receives input from this sensor, it interprets the sensor's reading as an integer ranging from 0 - 5000, which represents 0 - 5 Volts. Therefore, the output of `CAN_readPressure()` will always be an integer ranging from 500 - 4500. When the pressure outputs its maximum voltage, which is 4.5 Volts, it reads its maximum pressure of 5000 psi. When it outputs its minimum voltage, which is 0.5 Volts, it reads its minimum pressure, which is 0 psi.

The sensor was calibrated by incrementally charging the accumulator in Regenerative Braking mode. The raw sensor voltage was recorded along with the accumulator pressure. The accumulator pressure was read from an Ashcroft analog pressure gauge, which carries an accuracy of $\pm 1.5\%$. In other words, at 3000 psi, this gauge is accurate to ± 45 psi. A linear curve fit was applied to the data to determine a relationship between the accumulator pressure and sensor voltage, which is shown in Figure 5.9.

After applying an experimentally determined curve fit to convert the raw sensor reading into a pressure measurement, this function saturates the calculation between 0 and 5000 psi. A plot of the pressure transducer calibration curve is shown in the graph below. Given the accuracy of the analog pressure gauge, the pressure transducer can reasonably measure the accumulator pressure to an accuracy of ± 50 psi.

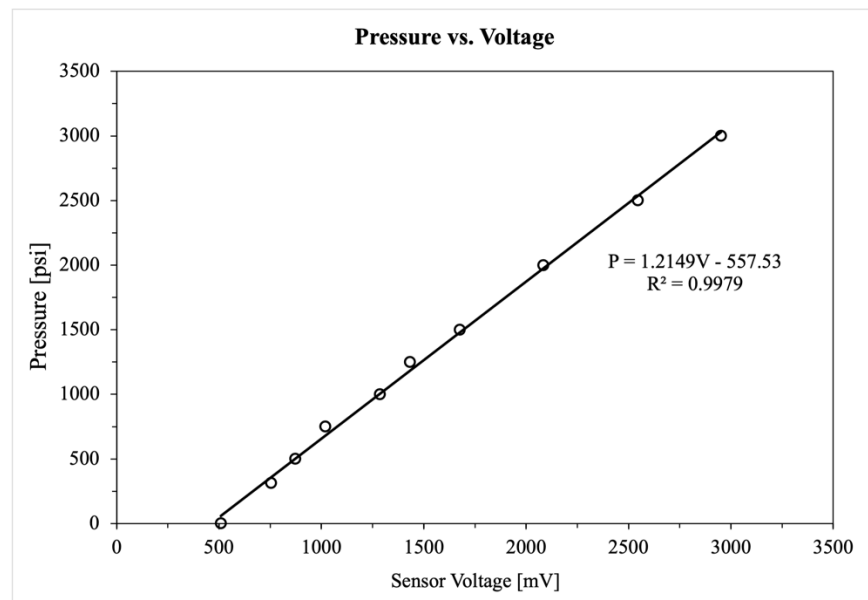


Figure 5.9 Pressure transducer calibration curve.

The Nextion display's RTOS assigns an ID to each item on the screen. A text box may have the ID, *t0*, and a button may have the ID, *b0*. Each element on the screen is an instance of a class object: *t0* is an instance of the text box class and *b0* is an instance of the button class. The STM32 interacts with the display by modifying the attributes of its elements. For example, to change the value of *n0* on the screen, the STM32 would send a command like, *n0.val = 10*. This command modifies the "value" attribute of the number object, which is subsequently updated on the display.

Communication between the STM32 and the Nextion display is achieved over a UART connection with the Easy Nextion Library, written by GitHub user, *Seithan* [2]. The code below sends two numbers to be printed on the display.


```
myNextion.writeNum("n0.val",localVar_bikeSpeed);           // Write the speed to the display
myNextion.writeNum("n1.val",localVar_accumulatorPressure); // Write the pressure to the display
```

The display's Graphical User Interface was designed in Nextion Editor. It consists of a home page that displays all relevant data to the user, which includes the speed of the vehicle, and pressure measurements from the ECDR 0506-A. The user can press several buttons on the touch screen that access different pages. Shown in Figure 5.10, a second pages allows the user to select a drive mode from one of five switches. Since there are only four physical buttons, the Pedal Charge mode is only accessible using the touch screen. The Circuit page displays the hydraulic circuit schematic, which labels the five controllable valves installed on the hydraulic manifold. The dashed outline is the system boundary of the manifold. The pump, accumulator, and reservoir are also shown on the circuit page. Depending on which drive mode is active, the valves on the circuit will turn green when energized. The Plot page charts the vehicle speed against time in a scrolling, fixed-scale format. The distance traveled is calculated by multiplying the velocity by change in time. Shown in the plot, the variable that stores the distance traveled is displayed with a resolution of 4 decimal places. This is solely because the Nextion is incapable of working with floating point numbers, so converting speed from miles per hour to feet per second, and then multiplying by a time interval in milliseconds, requires a tedious process that results in a calculated value that displays to four decimal places. Finally, the Help page displays a QR code that links to the documentation wiki.

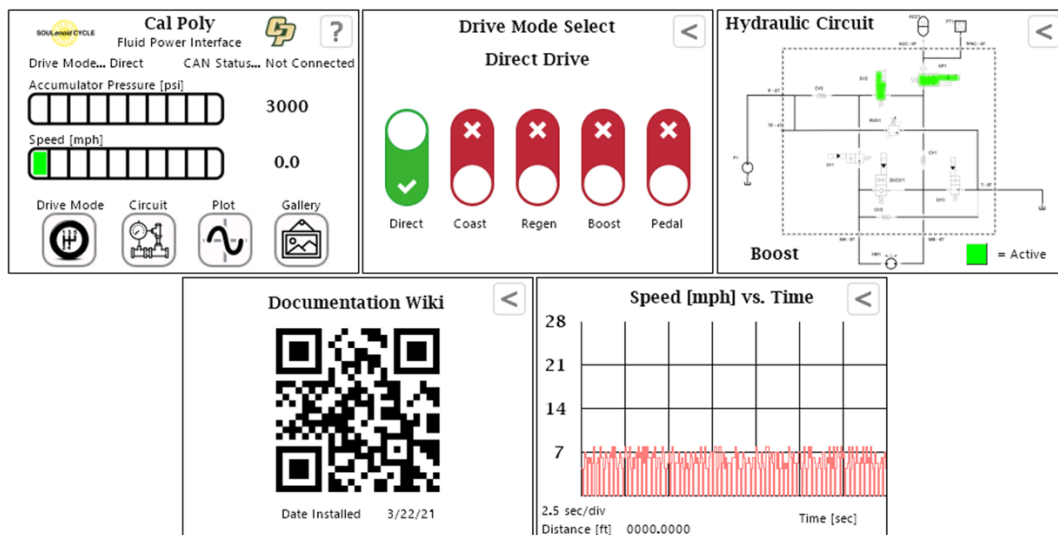


Figure 5.10 Screen captures of five pages from the interface's GUI.

The Nextion display has a single, two-wire UART port, which is used to program the display and communicate with the STM32 PCB. The Nextion connects to Nextion Editor with a USB to Serial converter, which is shown in Figure 1 below.



Figure 5.11 USB to serial converter that is used to program the Nextion display.

As shown in Figure 5.11, this particular USB to Serial converter, which ships with the Nextion display has three switches. This allows the module to be used to convert USB to other forms of two-wire communication, such as RS-485 and TTL. To successfully connect to the Nextion, the switches on the USB to Serial converter must be toggled to the states shown in Figure 5.8: Switch 1 on, Switch 2 off, and the third switch directed away from the TTL label. The table below describes the different variables and software objects used in the Nextion configuration file. Each object belongs to the page that it was created on. Global variables can be accessed on any page and local variables can only be accessed on the page that it was defined on.

Table 5.1 Table of variables defined in the Nextion's software with descriptions of their usage.

Object Name	Type	Scope	Description
page0.va0	Variable	Global	Stores the current drive mode. Identical to buttonState in Interface.cpp, 1->Direct, 2->Coast, 3->Regen, 4->Boost, 5->Pedal.
page0.va1	Variable	Global	Vehicle speed, in miles per hour, <i>integer form</i> . This value is used by the Plot page to chart speed vs. time.
page0.tm0	Timer	Local	This timer object has a period of 50 ms. Every 50 ms, the green bars for the speed and accumulator pressure are updated based on the current speed and pressure.
page0.n0	Number	Global	Accumulator pressure, in psi.
page0.x0	Float	Global	Vehicle speed, in miles per hour, <i>float form</i> . This value is only used on the home page to add resolution to the speed measurement.
page4.tm0	Timer	Local	This timer object has a period of 50 ms. It is used to update the waveform. Every 50 ms, the plot is updated with the current vehicle speed and the distance traveled is calculated.
page4.va0	Variable	Local	Stores the current vehicle speed <i>in integer form</i> , pulled from the value of page0.va1. This value must be reassigned to a local variable in order to correctly calculate distance traveled.
page4.va1	Variable	Local	Stores the intermediary calculation for change in distance traveled (see bullet point at the bottom of the page).
page4.x0	Float	Global	Distance traveled, in feet. As discussed in task_HALL1() this value is displayed to four decimal places solely as a result of calculating distance traveled, as the Nextion is incapable of floating point math.

For more information about the design of the software, as well as its raw code, please refer to the public documentation wiki at: <https://jkochavi.github.io> . In addition, the software for the ECDR 0506-A, along with comments describing its features and usage, is located in Appendix J.

5.3 Final Electronics Enclosure Design

The main interface houses the Nextion display and custom PCB. Shown in Figure 5.12, the enclosure is hinged to provide access to the circuit board. To connect to the PCB's screw pin terminals, the user must unhinge the display to expose its circuitry. Hiding the PCB terminals and connections improves its weather resistance.



Figure 5.12 Render of 3D printed enclosure for the printed circuit board.

Narrow, rectangular slots allow for wires to leave the enclosure. A removable cap with three round holes is attached to the bottom of the enclosure with M2 screws. This cap allows for the user to conveniently snap the JST button connections into place without having to unhinge the display. Shown in Figure 5.13, the enclosure is secured by M2 screws and heat-set brass inserts. The inserts allow for machine screws to be threaded directly into 3D printed parts and are installed with a soldering iron.

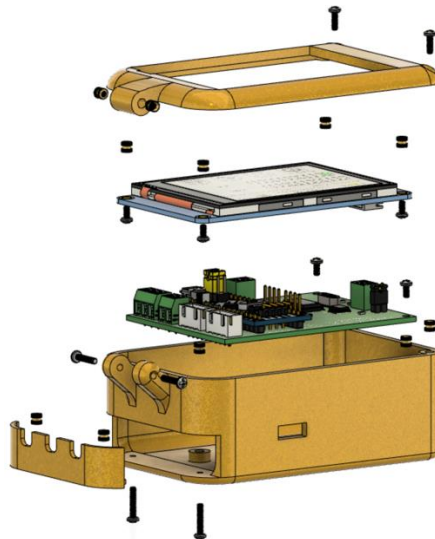


Figure 5.13 Exploded view of 3D printed interface enclosure.

The button modules are placed in ergonomic locations on the vehicle to allow the operator to easily press a button while driving. Shown in Figure 5.14, the button enclosure has a single hole for its signal wires to leave. The rest of the enclosure completely hides its circuit board.



Figure 5.14 Render of 3D printed button module enclosure.

Like the interface enclosure, the button enclosure is secured by M2 screws and threaded brass inserts. Shown in Figure 5.15, the rectangular button covers are held captive inside the enclosure by a slot that prevents them from slipping out.

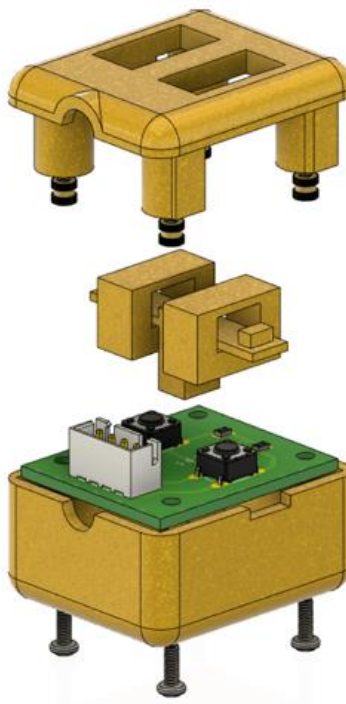


Figure 5.15 Exploded view of 3D printed button module enclosure.

To mount the screen module to the handlebar, a stand was designed to fit over the top of the handlebar tube. Shown in Figure 5.16, the stand is angled upwards at 10 degrees to direct the screen toward the rider's eyes. It fits over the 38 mm aluminum tubing and is fixed to the handlebar using a single #6-32 screw. Visible in the wireframe profile, the stand has an internal feature that allows a pair of 18 AWG wires to snake through and reach the screen module. This feature neatly conceals the power lines inside the handlebars. The screen stand also has deep channels to glue strips of Velcro. The combination of Velcro and the power terminals rigidly fix the screen module to the stand.

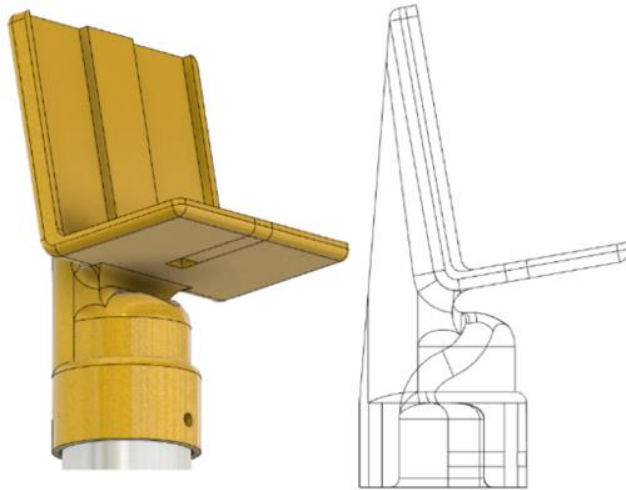


Figure 5.16 3D printed screen stand.

Shown in Figure 5.17, the JST connectors are easily accessible through the enclosure's bottom hatch, and allow the cables to rest in the round notches. In addition, the STM32's programming ports are easily accessible through a narrow slot in the enclosure, which allows it to be programmed without disassembling. Accessing the PCB through a hinge allows the enclosure to remain in one piece, which alleviates the concern of damaging wire connections and losing screws. In order to access the PCB, the user must remove two screws located in the corners of the display, which are visible in Figure 5.13. In a future design iteration, it is recommended to design snap-fit connections between the enclosure's top and bottom so the user could unhinge the display without removing any screws.

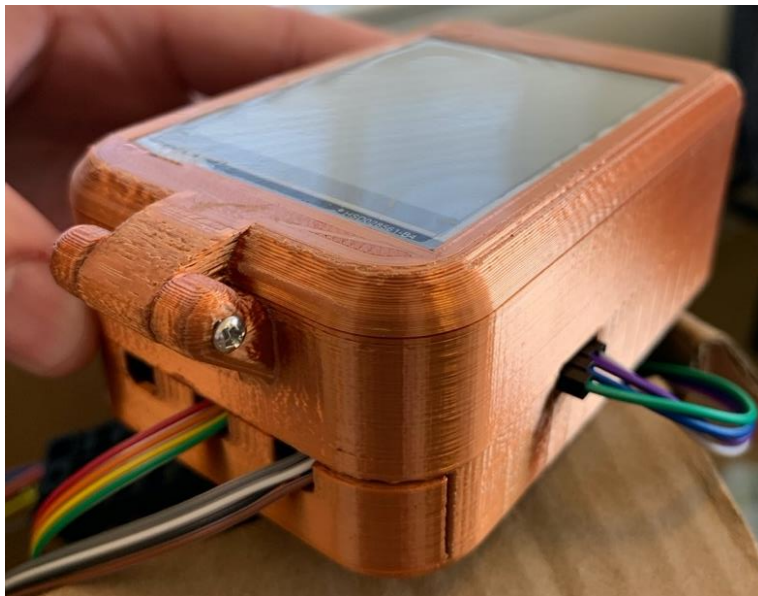


Figure 5.17 Photograph of the 3D printed interface enclosure.

The enclosures were printed with a layer height of 0.15 mm and a print speed of 50 mm/s. These settings are effective for rapid prototyping, however the increased speed and layer height results in layer imperfections and print defects. Shown in Figure 5.17, the hinge had to be sanded to remove some defects,

which also removed some of the PLA's shiny finish. Furthermore, these parts were not printed on a high-end 3D printer, which also contributed to their overall quality. It is recommended to print these parts on a precision 3D printer at a decreased speed and layer height to maximize their surface finish and durability.

The mounting of the screen and buttons are shown in Figure 18. The location of the power terminals on the PCB ended up being ideally placed for proper concealment on the vehicle. An angled stand was designed with an internal hole that allowed the two power wires to snake through the handlebars. Since the handlebars were welded from two aluminum tubes at a right angle, it was difficult to pull more than a few wires through the handlebars. Thus, the wires for the speed sensor and buttons had to be routed along the outside of the handlebars. In addition, the location of the CAN terminals on the PCB required another hole in the handlebars, which is also visible in Figure 5.18. In a future iteration, it is recommended to concentrate all terminals and wire connections in a single location on the PCB. It would significantly improve the aesthetics of the screen mount to construct a single cable ribbon that is completely concealed within the handlebar.

The buttons are attached to the handlebars with Velcro strips, which were surprisingly resilient. The buttons and screen are intended to be as modular to allow the rider to customize their desired layout. The screen module itself is also attached to the handlebar mount with strips of Velcro. For durability, the power supply to the board and the CAN wires should remain thick (18 AWG wire is currently used). However, the wires that only relay 5V signals can be reduced to 24 or 26 AWG to reduce the volume and weight of the wiring.



Figure 5.18 Photograph of the interface mounted on the right handlebar.

An advantage of using a recumbent tricycle frame is the abundance of space for storing electrical components. Shown in Figure 5.19, the cushioned seat is attached to the frame with Velcro strips. Underneath the seat are the ECDR 0506-A and battery, which are therefore more protected from the elements. The ECDR 0506-A is angled toward the manifold, which improved cable management among the valve connections. In order to turn the electronics on, the rider must lift part of the seat and plug the battery in. While this encourages the rider to not leave the vehicle turned on, it would be easier if the battery can be powered on using an easily accessible switch. Also, neither the ECDR 0506-A nor the custom interface are capable of measuring battery level. Each of the five valves requires a current supply of 2 A to full actuate, and the custom interface requires at least 500 mA to function normally. It is recommended to design a power management system that can alert the rider when the battery is unable to supply the current needed to energize the valves and power the screen. This could be accomplished with an additional CAN node that can facilitate the charging of the battery and monitoring its status. Finally, the battery life of the vehicle ranges from 45 minutes to an hour. It is recommended to increase the size of the battery to better accommodate the power requirements of the system.



Figure 5.19 Photograph of the location of the ECDR 0506-A and battery underneath the seat.

5.4 Hydraulic Circuit Design

The hydraulic circuit remained mostly the same since the preliminary design. The biggest difference is the discovery that the SVCV1 was changed late in the design by Pump My Ride. The latest schematics showed a normally closed valve as oppose to the normally open that was on the manifold. The normally open valve allowed the coast mode to be integrated into the direct drive mode by allowing making a dedicated coast mode redundant. The updated hydraulic schematic is shown in Figure 5.20.

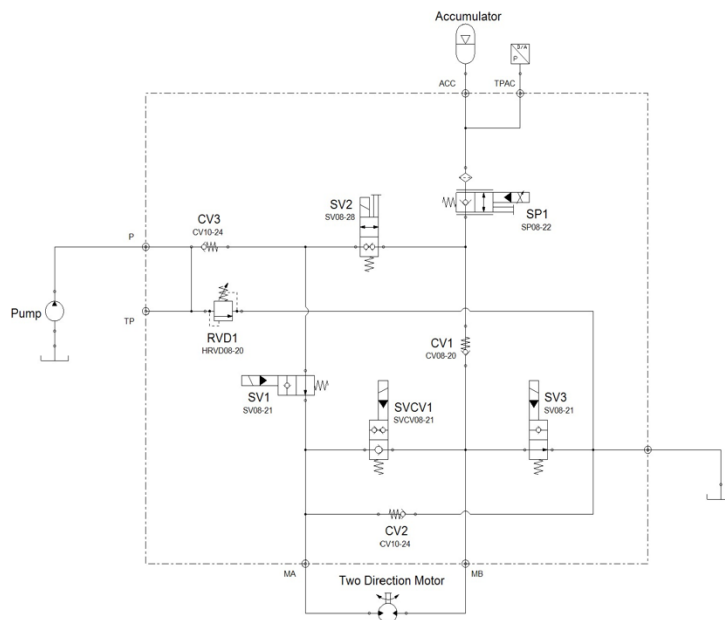


Figure 5.20 Updated schematic showing the hydraulic circuit.

Additionally, it was discovered that, despite criticisms from the judges during the Midway Review event, it was not possible to implement the recommended function of discharging the accumulator directly to the reservoir. Time constraints, missing components, and lack of mounting space on the reservoir required Soulenoid Cycle to forgo implementing the recommended addition.

5.5 Reservoir Design

The final design for the reservoir refined the small details like fittings. The size of the aluminum weld on fittings were increased from the 1/8" NPT to a 1/4" NPT (Figure 5.21) because of concerns that the 1/8" fitting was too small and would restrict fluid flow. The NPT thread is an industry standard for most pipes, especially in pneumatic systems. However, hydraulic fittings usually use the JIC standard. Fortunately, JIC 6 Male to 1/4" NPT Male adapters like in Figure 5.22 are sold in most hardware stores and were used to connect the reservoir to the rest of the circuit.

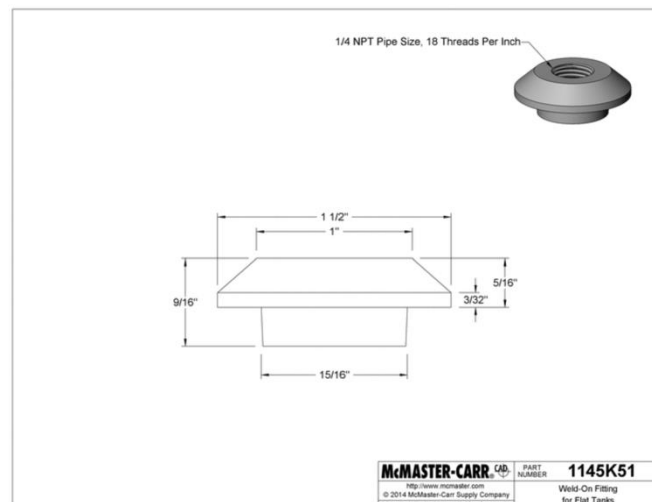


Figure 5.20 1/4" NPT aluminum weld-on fitting.

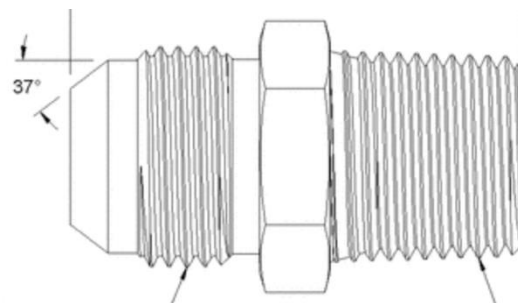


Figure 5.21 JIC male to NPT male straight adapter.

After manufacturing the reservoir, some ports on the were altered to better fit the vehicle design. The fill port that doubled as a vent was switched with the case drain since the case drain port on the pump faced in that direction. The other modification was the discovery that having the return line high in reservoir did not work. The return line for the regenerative braking mode is used as a suction line from the motor. Unless the reservoir was filled to the top, then the regenerative braking mode could work to partially fill the

accumulator. To solve the issue, union tee was placed at the pump inlet port which the motor return line was also connected to (Figure 5.23).



Figure 5.22 Modified pump inlet port to join the pump return.

5.6 Steering Linkage

The final steering linkage design implemented significant changes from the initial concept design, primarily via simplification. Due to time restrictions, the more complex features discussed earlier in Section 4.9 of center-point steering and caster angle were abandoned. Although they would have theoretically improved the steering performance of the vehicle, in practice they proved to be unnecessary once vehicle testing was conducted. The rider never reached speeds above 20 mph and never needed to let go of the handlebars, so caster angle was not necessary, and all operation took place on smooth driving surfaces, so the stability imparted via center-point steering was not necessary either. The final version of this linkage without center-point and caster angle can be seen below in Figures 5.23 and 5.24.

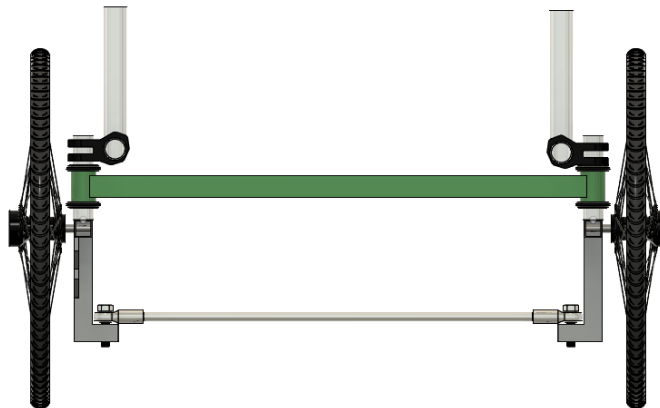


Figure 5.23 Front view of final steering linkage render.



Figure 5.24 Side view of final steering linkage render.

Due to the location of the pump mounting and the path that the chain had to track between the crankset and the pump, the left and right links needed to be significantly modified from their original design in order to allow for the tie rod to connect between the two as seen in Figure 5.25.



Figure 5.25 The lowered tie rod avoids interference with the pump and chain.

These custom fabricated links, the left of which is shown in Figure 5.26 were fabricated from 16 gauge, 1 inch square tubing. Holes were drilled for both the axle and tie rod bolt. On the top of each of the links is welded the steerer tube, a 1-1/8 inch OD round steel tube.

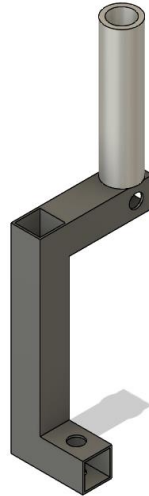


Figure 5.26 Steering link with Ackerman geometry.

Shown below in Figure 5.27, the steerer tube passes up through the headtube, which has a set of FSA The Pig Headset Bearings press fit into either side. On the bottom side, between the square tubing and bottom bearing, a 3/4 inch Sumid Carbon Fiber Headset Spacer. The handlebars are then attached to the steerer tube with a WAKE Mountain Bike Handlebar Stem. The handlebars are made from 1-1/2 inch OD, 6061 T6 aluminum tubing, cut at a 45 degree angle then tig welded together to form the 90 degree bend. The handlebars were mounted in the upwards direction due to their height relative to the rider, allowing for the greatest ease of use.



Figure 5.27 CAD render that demonstrates how the steering link connects to the frame.

The tie rod, as seen above in Figure 5.25 and below in 5.28, was cut to around 25 inches in length from a solid rod of 1/2 inch diameter 6061 aluminum. Threads were cut into each end with a 1/2-20 die so that the 1/2 inch rod ends could be threaded on. These rod ends were then attached to the left and right links using 1/2 by 2-1/2 inch bolts.



Figure 5.28 Aluminum tie rod with threaded ends.

Additionally, as seen in Figure 5.29, a triangular piece of 1/4 inch thick steel plate was welded onto the right steering link in order to mount the caliper for the RUJOI Bike Disk Brakes. This was not repeated on the left steering link seen in Figure 5.30 because the purchased set of disk brakes were meant for a standard bicycle, where the disks are both mounted on the same side of the frame, meaning that each caliper is a physical copy of the other, not a mirrored copy. This meant that the same mounting location would not work for our frame design. In order to rectify this issue, it would have been necessary to purchase specialty brake calipers from a recumbent trike part supplier, a step which was not taken due to time constraints.



Figure 5.29 Steering link with mounted brake caliper.



Figure 5.30 Left steering link without a mounted brake caliper.

Lastly, seen in Figures 5.29 and 5.30 are the 20 inch ICE Recumbent Front Wheels with Disk Hubs and ICE Standard Steel Front Axle, both of which were selected due to the need for a larger 1/2 inch diameter specialty axle in order to withstand the forces of mounting on just one side of the axle without bending or deforming.

5.7 Pneumatics

The required pneumatic system for Soulenoid Cycle was used to actuate a parking brake. The design used a standard bicycle rim brake. Instead of the rider pulling on a wire to actuate the brake, a pneumatic cylinder

was positioned so that its actuation pulled the wire. A manual toggle switch was chosen to open the circuit so that it can be used even if the vehicle was powered off. A pneumatic circuit along with the concept of how it pulls a rim brake is shown in Figure 5.31.

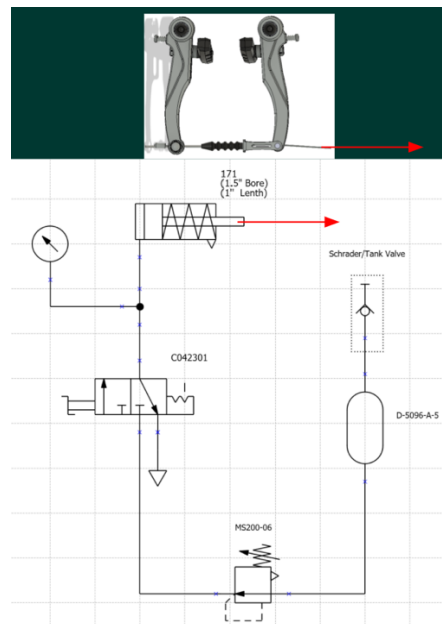


Figure 5.31 Pneumatic circuit to actuate a parking brake.

This concept also solved the requirement for a braking system to hold the vehicle at a full accumulator discharge. By knowing the torque output of the motor at 3000 psi is around 12 ft-lbs, the ratio from the motor to the wheel to be 13:35, and the radius to the rim where the brake pad is to be applied being 12", the braking force of 32.3 lbs was calculated and shown in Appendix U.

After figuring out that 32.3 lbs of is easily achievable with 100 psi, it was decided to over-design the bore diameter to ensure the braking brake can be actuated more than 5 times. Using 20 psi as the minimum pressure for the system to work, a bore diameter of 1.5" was chosen (Figure 5.32) A pressure gauge was placed near the cylinder to verify the pressure is sufficient. A 3-way, 2-position toggle switch is used open the circuit. In one position, the circuit opens and allows air to flow from the tank to the cylinder. Since the cylinder was single acting, the other position blocked the flow to the cylinder from the stored tank while opening the cylinder to atmosphere so that it can release the brake. The next component is a pressure regulator. This was placed so that the pressure in the system does not exceed a pressure set by the pressure regulator. A stored separate tank known as a non-repairable reservoir (Figure 5.33) was used to hold and fill the system with pneumatic pressure. On one end, the reservoir was attached to the circuit. To allow for easy filling and release, a Schrader valve was added to the other end. More commonly seen in bicycle tires, a Schrader valve can be used with a tire pump to introduce air to a system while a needle inside can be pressed to release the pressure from the system.



Figure 5.32 Bimba 171 single-acting air cylinder with a 1.5" bore diameter.



Figure 5.33 Bimba D-5096-A-5 with an attached Schrader valve.

5.8 Frame Design

The purpose of the vehicle frame is to provide ample space for the hydraulic circuit and allow a rider to assume a recumbent position to operate the crankset. Given these design requirements, the frame was designed around two dimensional constraints: component room and seat angle. A profile view of the frame design, along with component placement, is shown below in Figure 5.34.



Figure 5.34 Profile view of final frame design, in CAD.

With the exception of the pump, the hydraulic components are mounted between the seat and the rear wheel. Thus, component room is quantified as the distance between the bottom of the seat and the rear axle. To determine an appropriate dimension for component room, the following dimensions were considered: the radius of the rear wheel, the diameters of the accumulator and motor, the width of the manifold, and an estimated reservoir room. The measured values of these dimensions are tabulated below.

Table 5.2 Measured component dimensions to determine the driving frame dimension.

Component	Dimension [inches]
Rear wheel radius	13
Hydraulic motor diameter	3
Accumulator diameter	8
Manifold width	4
Estimated reservoir space	12
Total space required	40

Adding an extra 6 inches for measurement uncertainty and additional components, the dimension of 46 inches was chosen as the distance between the rear wheel and the bottom of the seat. The second driving dimension is the orientation of the seat. An optimal seat angle was found using a recliner chair. The angle of the seat was adjusted until the user found a comfortable recumbent position that allowed them to see directly in front of them without straining their neck. This process is discussed further in Appendix K. This experiment determined a seat angle of 40 degrees with the ground. To maintain the 46-inch dimension for component room, the rear beam was angled toward the ground, as shown in the sketch in Figure 5.35.

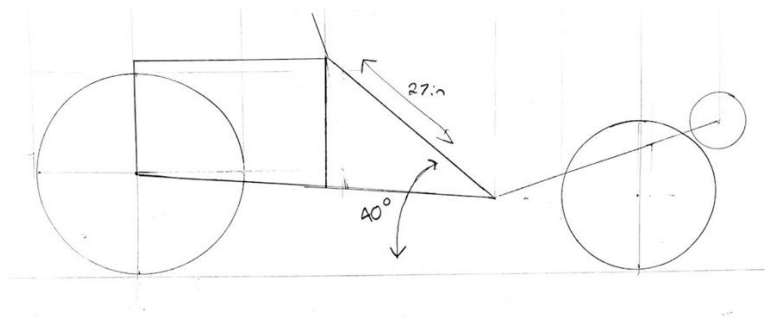


Figure 5.35 Hand-drawn sketch of seat angle and component room.

After determining these two dimensions, a human model was inserted into the CAD workspace to determine an appropriate crankset distance. Shown in Figure 5.36, the crankset distance was determined by observing the rider model's knee at its maximum leg extension. When pedaling a crankset, the rider's leg should never be fully extended because their knee could lock, which risks injury. Hence, the best practice for adjusting the seat on an upright bicycle is to adjust the seat until a slight knee bend is maintained at maximum leg extension. As shown in Figure 5.36, the position of the crankset was adjusted until the rider model achieved a slightly knee bend.

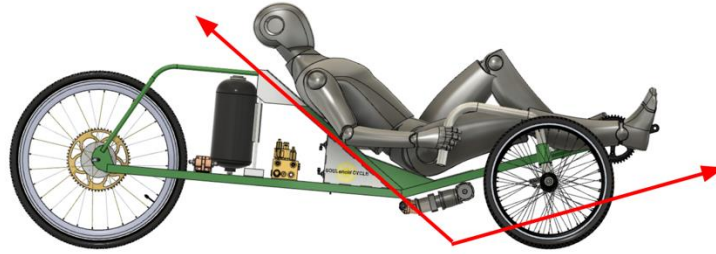


Figure 5.36 Profile of final frame design, in CAD with rider.

The rest of the frame was designed around these two driving factors. Square steel tubing was chosen as the primary material for the frame. Square tubing is easier to cut and machine, while steel is easier to weld given the expertise and prior experience of the team. To determine an appropriate size and thickness for the tubing, an FEA was conducted in Fusion 360. Shown in Figure 5.37, the structural loading in the FEA was over-estimated in an assumed safety factor. A distributed load of 120 lbs represents the weight of the hydraulic components, which is more than the total weight of the 2019 competing vehicle. In addition, the 200-lb load represents the weight of the rider, and the 50-lb load represents their static force on the crankset. Due to COVID restrictions, this FEA was performed without physical access to the 2019 competing vehicle. Therefore these loads were inspired from various analysis performed by teams in the 2020 virtual competition.

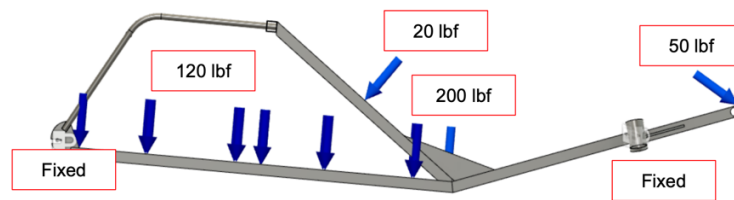


Figure 5.37 Estimated structural loading on final frame design.

Experimenting with an FEA determined that selecting a thickness above 18 gauge would significantly lower the static factor of safety. In addition, thinner tubing increases the difficulty of welding, especially for the less experienced. Therefore, a tube thickness of 16 gauge was chosen out of an abundance of safety. This produced a safety factor of 3.0 in FEA.

Visible in Figure 18, the rear axle is connected to the top of the seat via bent round tubing. An FEA determined that the vertex above the rear wheel is relatively unloaded and does not possess any significant stress concentrations. In addition, switching to 1-inch, 16 gauge tubing for this section of the frame predicted a 2.5-lb reduction in overall vehicle weight. This reduction was found by observing the mass properties of the two structures shown in Figure 5.38.

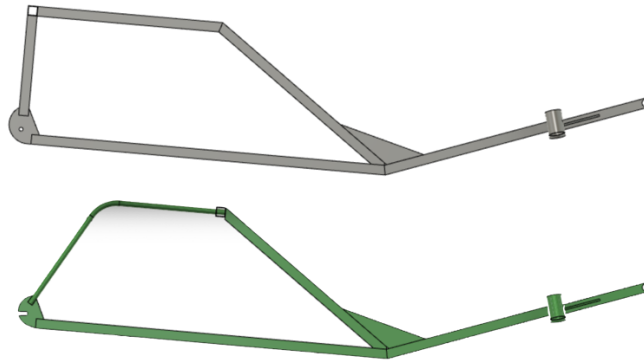


Figure 5.38 Benefits of switching some of the frame's square tubing to round tubing.

The upper design in Figure 5.38 was developed directly from the hand sketch of Figure 5.19 and uses entirely square, 16 gauge tubing. The bottom design removes the square tubing that forms a right angle above the rear wheel and replaces it with bent round tubing. While round tubing poses greater difficulties in manufacturing, this design choice reduced vehicle weight without compromising the frame structure. It reduces the number of welds required on the frame, as well as the number of cuts, as bending eliminates the need for two separate pieces. The two triangles underneath the seat, as shown in the designs above, were found to provide significant structural support to the frame in direct response to the weight of the rider. FEA also identified a high stress concentration at the top of the seat at the intersection of the round tubing. Therefore, the frame was further triangulated behind the seat with 0.5-inch steel tubing, which is visible in Figure 5.18. This triangulation also provides a convenient mounting space for the accumulator, while the triangles underneath the seat provide space for electronic components.

6 Manufacturing

A wide variety of manufacturing processes were used in the fabrication of Soulenoid Cycle's vehicle. The section below describes these processes, which all took place in the Cal Poly Machine Shops.

6.1 Frame Manufacturing

The frame manufacturing process began with the procurement of square steel tubing, round steel tubing, and 1/4 inch steel plate from Metals Depot.

Table 6.1 Stock material used for the vehicle frame.

Name	Specifications	Size
A513 Square Steel Tube	1-1/4 X 1-1/4 X 16GA (.065 wall)	8ft stock
A513 HREW Round Steel Tube	3/4 OD x 16 GA (.065 wall)	8ft stock
A513 HREW Round Steel Tube	1 OD x 16 GA (.065 wall)	8ft stock
A36 Steel Plate	1/4 inch thickness	1ft x 1ft

The round steel tubing was ordered in two sizes, 3/4" and 1" outer diameter, since the team was unaware of what size tubing the available machines on campus could handle at the time. The square tubing was used for a majority of the frame, the round tubing was used for the supporting bars behind the vehicle seat, and the steel plate was used to fix the frame to the back wheel axle and as triangular supports at the base of the seat, as seen in the render below.

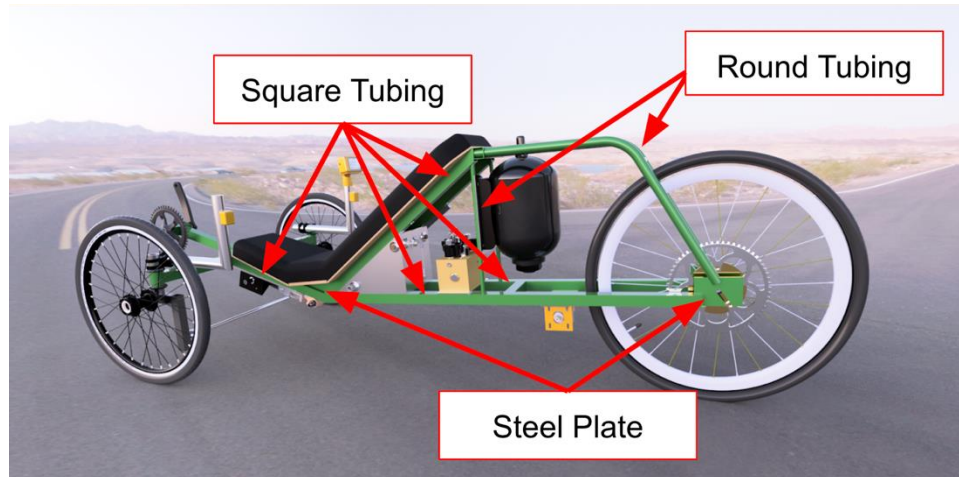


Figure 6.1 Annotated CAD render indicating material types on the frame.

All the square tubing with 90-degree edges were cut to length using the chop saw, as pictured below. Angled cuts were made with the band saw so that the appropriate angle could be set with greater accuracy.



Figure 6.2 Using a chop saw to cut steel tubing stock.

The first focus was on completing the parallel sides of the frame so that these could be used to build off of. The pieces were cut and laid out as shown in Figure 6.3 before being MIG welded together, shown in Figure 6.4.



Figure 6.3 The two planes of the frame were welded separately.

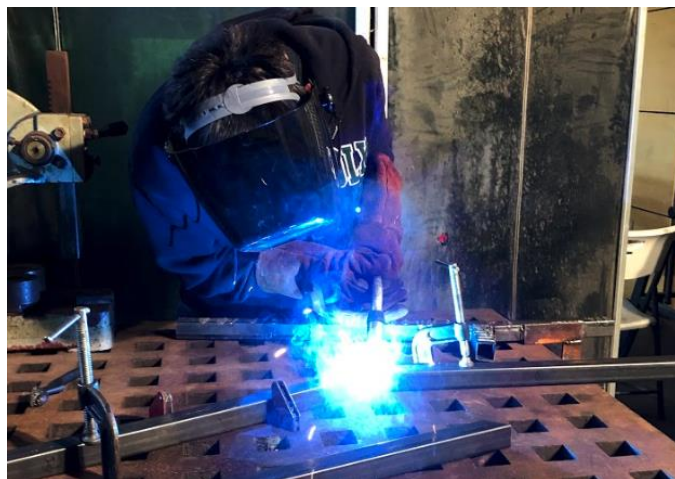


Figure 6.4 MIG welding was used to weld all steel components on the frame.

Based on the angle of the welded assemblies, the round steel tubing was bent using a hydraulic tube bender. The 1" tubing was used since the machine shop had a matching die for 1" outer diameter tubing. This was a time-consuming process, but it was important that the angles of both bent tubes matched as closely as possible so that the frame was symmetrical. The tubes were bent and then cut to length to ensure that the tubes would fit on the existing assembly. The team decided to use the $\frac{3}{4}$ " tubing for the vertical supports behind the vehicle seat for weight purposes. The chop saw was used to cut these sections to length before using a grinding wheel to ensure a tight fit on the frame. The round crossbar at the top of the frame was cut to length and notched on both ends using a mill, as shown below.



Figure 6.5 A hole saw on a mill was used to notch the ends of the round tubing.

The steel plate was cut into triangular supports matching the angle of the welded assembly using the vertical band saw. Rectangular steel pieces were also cut and notched using the vertical band saw. All components were then welded together to form the frame shown below. An angle grinder was used to clean up weld lines along the frame.



Figure 6.6 Completed frame welding, without the steering linkage.

6.2 Steering Manufacturing

Due to the unusual nature of recumbent tricycle steering, many components were ordered that are specifically designed for recumbents. These parts, along with the remainder of the square steel tubing used for the frame and the stock metal for the handlebars, are listed in the table below.

Name	Specifications	Quantity	Supplier
A513 Square Steel Tube	1 X 1 X 16GA (.065 wall), 2ft stock	1	Metals Depot
A513 Square Steel Tube	1.25 X 1.25 X 16GA (.065 wall), 8ft stock	1	Metals Depot
A513 HREW Round Steel Tube	1 OD x 16 GA (.065 wall), 8 ft stock	1	Metals Depot
A36 Steel Plate	¼" thickness, 1ft x 1ft	1	Metals Depot
R312, 6061-T6511 Aluminum Round	1/2 inch diameter, 4ft stock	1	Metals Depot
ICE 20" Front Wheel with Disc Hubs (Pair)	-	1	The Recumbent Trike Store
ICE Standard Steel Front Axles Disc (Pair)	-	1	The Recumbent Trike Store
FSA Orbit MX 1-1/8Inches Threadless MTB Road Headset	Top Cap, Black, NO.20, XTE1504	2	Amazon
SCK 2 Pack 20 Inch Bike Tubes Plus 2 Tire Levers	20x1.75/1.95/2.10/2.125 Schrader Valve MTB Bike Inner Tubes, Black	1	Amazon
JIANKUN Bike Crank Arm Set 170mm 104 BCD	Bottom Bracket Kit and Chainring Bolts for MTB BMX Road Bicycle	1	Amazon
Female Rod End	1/2"-20 Right Hand Thread	3	Grainger

While the main portion of the frame manufacturing was detailed in the previous section, the front portion of the frame that connects to the steering system itself had yet to be manufactured. In order to do so, the 1¼" square steel tubing was cut using the chop saw in order to prepare the following three pieces: the crossbar connecting the wheels, the extension bar that locates the crankset, and the short tube that houses the crankset bearing. To connect the crossbar to the frame, vertical sections of the 1" steel tubing were cut to length on the chop saw to be welded onto the ends of the crossbar. In order to make this possible, the crossbar ends were notched using a belt grinder with a 1" diameter. The remainder of the ¼" steel plate was cut into the triangular supports between the crossbar and the extension bar using the vertical band saw. The assembly was then welded together before being welded to the existing frame. The product is shown below, propped up on all three wheels with the seat resting on top.



Figure 6.7 Vehicle stands on front wheels, without steering linkage.

The 1" square steel tubing was cut to length for each of the pieces in the steering linkage before being MIG welded together. A drill press was then used to create holes to attach the tie rod and the front wheel axle. The completed linkage is shown below.



Figure 6.8 Manufactured steering linkage with adjustable tie rod.

In addition to the manufacturing of the linkages, the custom handlebars also needed to be manufactured. In order to do so, the portable band saw was used to make 45 degree cuts on the aluminum round tubing. Eric Pulse, the machine shop professor, graciously TIG welded the handlebar pieces together for the team. The ordered parts were then assembled and fastened to the manufactured parts, producing the steering system shown below.



Figure 6.9 Photograph of completed steering linkage.

6.3 Hydraulic Reservoir Manufacturing

The triangular hydraulic reservoir was manufactured out of aluminum for weight purposes. The specifications for the stock that was ordered and the fittings used for the reservoir are shown in the table below.

Table 6.2 Stock components used to manufacture the reservoir.

Name	Size/Quantity	Supplier
6061-T6 Aluminum Sheet, .125 (1/8)" thick	2 x 4ft stock	Metals Depot
Breather Vent	2	McMaster Carr
Aluminum Barbed Hose Fitting	4	McMaster Carr
Low-Pressure Aluminum Threaded Adapter	12	McMaster Carr
High-Pressure Push to Connect Tube Fitting	3	McMaster Carr

Soulencoid Cycle chose to use Cal Poly's waterjet in order to cut out the pieces for the reservoir. A DXF file was created based off of the Fusion360 reservoir model. With the help of the Mustang60 machine shop technicians, the file was uploaded to the machine and the program was run. The figure below was taken while the machine was in progress.

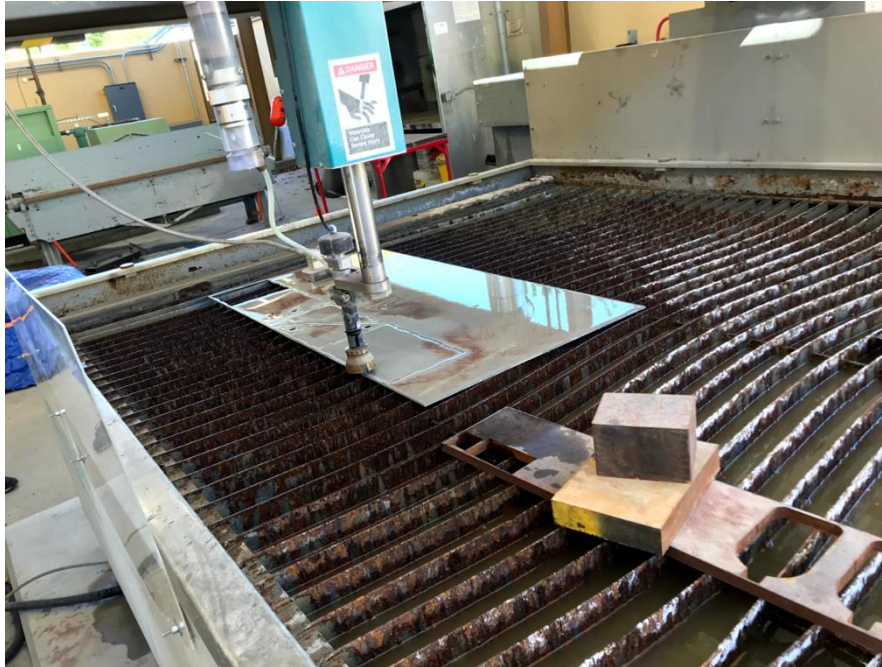


Figure 6.10 Waterjet cutting of the reservoir pieces.

After the pieces were cut, the edges were manually files to ensure a tight fit of the assembly prior to welding. While none of the 2020-2021 Soulenoid Cycle team members were well-versed in TIG welding, the team was fortunate enough for a peer, Junnior Rodriguez, and Cal Poly professor, Eric Pulse, assist in all of the team's TIG welding needs. After the reservoir was welded, the low-pressure aluminum threaded adapters were welded on and the remainder of the fittings were screwed in. The assembled reservoir is shown below.



Figure 6.11 Fully assembled reservoir after welding.

6.4 Component Mounts Manufacturing

The pump, motor, accumulator, and manifold mounts were all constructed out of aluminum in order to reduce weight. The motor, accumulator, and manifold mounts were cut using the waterjet. Additional holes were drilled using the drill press to increase the adjustability of the component locations. A hand drill was used to drill holes in the frame itself in order to securely fasten the mounts to the frame. The accumulator

mounting plate that was cut attached to a fire extinguisher holder that in turn secured the accumulator. The accumulator, fire extinguisher holder, and mounting plate were all then secured to the vertical frame bars using stainless steel hose clamps. The motor, manifold, and accumulator mounts can be seen in use below.



Figure 6.12 Accumulator mounted vertically behind the seat.

Due to the weight and position of the pump, the pump mount was made by stacking two identical pieces of the aluminum plate together for stability, which were cut by hand with a plasma torch. Slots were machined for adjustability using a mill and holes were drilled using a drill press. Soulenoid Cycle did encounter a problem with the front chain clipping the steering crossbar, since the chain connects the pump gear to the crankset. In order to temporarily fix this issue, spacers were added between the mount and the frame to lower the placement of the pump gear, as seen in the image below.

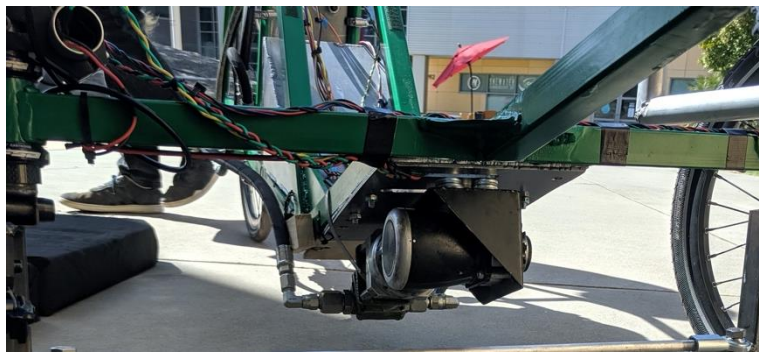


Figure 6.13 Pump mounted underneath the seat.

For additional photographs of the completed vehicle, refer to Appendix O.

7 Design Verification

This section documents the test methods carried out to validate Soulenoid Cycle's design choices and satisfaction of project requirements.

7.1 External Leakage

Soulenoid Cycle has the goal of zero external leaks. This is a requirement to be eligible for the competition. Leaking hydraulic fluid at either low or high pressure poses a serious safety risk to the rider and other contestants, and is grounds for disqualification. In addition to visually observing the vehicle during operation, the following steps will be taken to ensure that there are no external leaks:

1. Inspect all valves prior to operating the vehicle
2. Inspect tubing and junctions for leaks prior to operating the vehicle
3. Inspect all components for damage and leaks after operating the vehicle

7.2 Bike Weight

The weight specification accounts for the estimated weights of hydraulic components, mountings, and frame materials. These estimates will be verified using an industrial scale provided by the Cal Poly machine shops. Due to the ongoing pandemic, the size and resolution of a scale available for use is unknown. If its size permits, the frame will be weighed as a single piece after welding. However, if the scale is too small to fit the volume of the frame, each piece of tubing will be weighed individually. Hydraulic components will be weighed individually as they are removed from the current upright bicycle to be transferred to the new frame.

Results:

To weight the vehicle, the reservoir was filled to its normal operating capacity, and all hydraulic and electronic components were installed on the vehicle. A digital scale was placed underneath each wheel, and the three readings were added together. The scales underneath each of the front wheels measured 33 pounds, and the scale underneath the rear wheel measured 66 pounds. Summing all three readings yielded a total vehicle weight of 129 pounds.

7.3 Sprint Time

The sprint time specification is intended to replicate one of the NFPA challenges. The goal is to complete a 400-600 foot straight course in the fastest time using the accumulator discharge in Boost Mode starting from a stop. Soulenoid Cycle will use Sports Complex Road located next to the soccer fields on the northern side of campus shown in Figure 7.1. This road is ideal because it is relatively straight, only a 1 meter elevation change, not very busy, and almost no parking lot pullouts. There's also plenty of extra road to bring the vehicle to a stop if there was some failure.

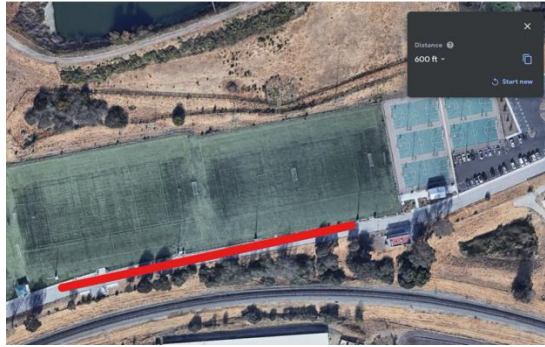


Figure 7.1 Google Earth aerial view of the 500-ft test course.

Equipment Required:

- Stopwatch
- Measuring Wheel

Procedure:

Solenoid Cycle will charge the accumulator to 2800 psi and a pre-charge of 500-psi. However, these pressures will be varied and verified to ensure they produce the fastest time. The vehicle will then be placed at one of the starting points with the lightest person driving. Another person will be at the end point with a stopwatch. As soon as the driver engages boost mode and the vehicle starts rolling, the stopwatch will begin. The stopwatch will continue until the vehicle crosses the end point.

Results:

At the time that this verification test was designed, the Cal Poly track was closed due to COVID restrictions. This test was completed at the virtual competition at the Cal Poly track. For more information, refer to the Competition Results section.

7.4 Efficiency Score

The efficiency requirement is chosen to meet or exceed Pump My Ride's overall efficiency score. Although unable to compete in the 2020 competition, Pump My Ride was able to perform their own tests to calculate an efficiency score of 12.17%. Soulenoid Cycle's efficiency requirement carries an allowance of +/- 5%, such that at minimum performance it meets Pump My Ride's score. To remain consistent with Pump My Ride's testing methods, Soulenoid Cycle will verify its efficiency score under similar conditions.

Equipment Required:

- Measuring Wheel

Procedure:

The test is to take place on the same road used for the sprint test. However, to accommodate the expected longer distance covered, the vehicle will begin on most eastern end of the road. The rider is not allowed to pedal for this challenge and will rely only on the Boost mode. To get the furthest distance out of the

accumulator, the Boost mode will be modulated on and off. Since the road is estimated to be around 2500 feet long, a safety point will be implemented to indicate to the rider that they must engage the brakes and end the test if needed (see Figure 7.2 for drawn out details). Another person will follow behind with the measuring wheel to measure how far the vehicle traveled to be inputted into the Efficiency spreadsheet for an efficiency value. The pre-charge pressure and rider are variables that will be tested and determined.



Figure 7.2 Google Earth aerial view of the efficiency challenge test course.

Results:

At the time that this verification test was designed, the Cal Poly track was closed due to COVID restrictions. This test was completed at the virtual competition at the Cal Poly track. For more information, refer to the Competition Results section.

7.5 Endurance Time

To test the endurance challenge performance of the vehicle, Soulenoid Cycle will measure the time it takes to complete the 1 mile course.



Figure 7.3 Google Earth aerial view of the endurance challenge test course.

Equipment Required:

- Stopwatch
- Access to basketball courts

Procedure:

The strongest or most enduring rider would be selected for this challenge since most of it will be completed in the Direct Drive mode. The accumulator pre-charge would have to be confirmed, but will be varied around the 500 psi value determined from previous years teams. The driver will have to engage the Regenerative Braking mode at one point to start charging the accumulator. They will then have to come to a complete stop and engage Boost mode. Since the loop is 560', the driver will have to complete 9.8 laps to complete the 1 mile challenge. The time to complete the 9.8 laps will be recorded to simulate the Endurance Challenge. An additional stopwatch will be used to measure how much time it takes to charge the accumulator, stop, and initiate Boost mode.

Results:

At the time that this verification test was designed, the Cal Poly track was closed due to COVID restrictions. This test was completed at the virtual competition at the Cal Poly track. For more information, refer to the Competition Results section.

7.6 Drive Mode Switch Time

This specification sets a requirement for the time taken for the hydraulic system to respond to user input. This requirement can be verified by both visual observation and with software. By visual observation, the following test procedure will be used:

Equipment required:

- 1.0 Stopwatch
- 2.0 Fluid powered vehicle

Procedure:

For each drive mode, conduct three measurements of drive mode switch time. Elevate the bike such that the rear wheel is in the air, and will not contact the ground while spinning. One team member, standing next to the vehicle, will press the drive mode buttons. A second team member will stand nearby with a stopwatch. Time will be recorded the instant a drive mode button is pressed. Recording will end the instant the rear wheel is observed to move. In each trial, begin at neutral drive mode.

By software recording, the following test procedure will be used:

Equipment required:

- Fluid powered vehicle

Procedure:

Position the vehicle in the same orientation as the previous procedure: elevate the rear wheel. On the touch screen interface, select the option called “Switch Time”. One team member, standing next to the vehicle, will press each drive mode button. The drive mode switch time will be displayed on the screen; record it after completion.

Software measurement will work by sending a CAN packet between both controllers. When a drive mode button is selected, the Arduino will log a timestamp and proceed to send the button press to the ECDR 0506-A. The ECDR 0506-A will receive the button press and actuate the necessary valve combination. When the valves are fully open, the ECDR 0506-A will send a single bit Boolean to the Arduino as a note of completion. Upon receiving the Boolean, the Arduino will record a second timestamp and calculate the drive mode switch time as the difference between both timestamps. The switch time will be displayed on the screen for the team member to record. This measurement requires calibration, as there will be some visible latency between opening the valves and wheel movement. Although sending multiple transmissions between the controllers appears to be slow, CAN communication operates at 33 kbits/second; the time taken to send a single bit Boolean will take 0.03 ms, or 30 μ s. Since this is virtually unobservable, software measurement should provide an acceptable accuracy.

Results:

As discussed in the software design section, the most time-sensitive software task is polling the status of the hall-effect sensor. This sensor is polled every 20 milliseconds. In an RTOS, each software task needs an appropriate amount of time and memory to “block,” which refers to an interval where the microcontroller is solely occupied with a single task. In order to prioritize the acquisition of data from the hall effect sensor, the update period for the screen had to be relegated to 100 milliseconds. Any faster refresh rate compromised the normal functioning of the software. To test the drive mode switch time, the amount of time elapsed between selecting a drive mode on the touch screen, and receiving confirmation from the ECDR 0506-A was measured. This time period was determined to be 160 milliseconds. While this switch time is significantly slower than expected, the rider is unable to detect this latency.

7.7 Internal Leakage

Internal leaks will be characterized as pressure drops throughout the hydraulic circuit. To test for internal leaks, the accumulator pressure and pressure drop across the manifold will be measured before and after storage. If there are no internal leaks, the circuit should retain the entirety of its pressurization.

Procedure:

Record the time between pressure measurements. Calculate leakage as the difference between pressure measurements. Divide by the time between measurements, in seconds, to compute a leakage rate in psi/s.

7.8 Pneumatics Pressure

In order to satisfy NFPA regulations, the air pressure in the pneumatic system must be regulated to a maximum of 100 psi. This pressure will be verified with an analog pressure sensor placed at the outlet of the pressure vessel provided by the NFPA. If the measured pressure is above 100 psi, the tank will be vented.

7.9 Pinching Points

Pinching points refer to any location on the vehicle where the rider can be pinched by rotating components. Because they can injure the rider, it is a requirement to eliminate any potential pinching points. This requirement will be verified by visual observation while the vehicle is in operation or stationary. No teammate should touch any rotating machinery while it is in use.

7.10 Drag: Coast Down Time

The goal of this test is to measure the coast-down time of the vehicle. Coast-down time is the time taken to completely stop after reaching a given velocity. This test serves as a comparison between the 2019 and 2020 vehicles. Each vehicle will be pedaled and ridden in direct-drive mode to reach a velocity of 20 mph, and then allowed to come to a complete stop on flat ground. Since hydraulic components are to be removed from the 2019 vehicle, this experiment will take place in two parts. First, the 2019 vehicle will be tested, followed by the 2020 vehicle upon completion. This test is to take place on N Perimeter Rd, San Luis Obispo, eastbound after the bus stop, shown below in Figure 7.4. This location is chosen because it provides a long stretch of relatively flat road, and will allow each vehicle the distance needed to reach 10 mph and to come to a complete stop.



Figure 7.4 Google Earth aerial view of coast-down test location.

Do not complete this test on a windy day. Although precise environmental conditions may be unattainable, make sure that both tests are carried out under similar conditions. Attempt to complete the test on a sunny day that is not windy. Do not ride into cross traffic. Stop the test and apply the brakes if it appears that the vehicle will not stop before the intersection of California Blvd.

Equipment required:

- Speed measurement app: Speedometer (available for iOS and Android)
- Stopwatch
- Vehicles:
 - 2019 Pump My Ride upright bicycle
 - 2020 Soulenoid Cycle recumbent tricycle

Procedure:

- Charge the vehicle's accumulator to 2800 psi - Pre-charge the accumulator to 100 psi
- Verify that 1 gallon of hydraulic fluid is present in the vehicle's reservoir
- Ride the vehicle in direct-drive mode until the speedometer reads 10mph
- Turn off direct-drive mode and allow the vehicle to come to a complete stop
- When direct-drive mode is turned off, instruct a teammate to begin recording on the stopwatch
- Stop recording when the vehicle comes to a complete stop

7.11 Accumulator Charge Time

This specification refers to the time taken for the accumulator pressure to reach 2800 psi. This specification can be verified using the analog pressure gauge at the outlet of the accumulator.

Equipment required:

- Stopwatch
- Fluid powered vehicle

Procedure:

Using any method, the team will charge the accumulator, with a dedicated teammate to monitor the accumulator pressure gauge. The time elapsed to reach 2800 psi will be recorded as the accumulator charge time.

Results:

The accumulator charge time was measured three times, which is tabulated below.

Table 7.1 Accumulator charge times.

Accumulator Charge Time
3:45
3:52
4:10

From the table above, the average accumulator charge time was found to be 3:55:66.

7.12 Presentation Score

It is Soulenoid Cycle's requirement to satisfy all competition regulations and meet the judges' performance standards. This requirement will be verified by receiving feedback and guidance from industry sponsors and mentors, as well as implementing feedback from the judges after the competition's Midway Review.

Results:

Cal Poly won the award of Best Presentations. For more information, refer to the Competition Results section.

7.13 Electronics Durability

The goal of this specification is to ensure that all electrical components are protected from the elements. While environmental testing will not be conducted with actual electronics, they can be simulated.

Equipment required:

- Water, dirt, sand, etc.
- 3D printed enclosures for mechatronics parts
- Cardboard

Procedure:

- Seal cardboard inside the 3D printed enclosures with superglue; the cardboard will represent the electronics Apply dirt and water to the enclosures to simulate environmental conditions
- Sprinkle water to emulate rain
- Drop the enclosures in dirt or mud
- Subject the enclosures to light/medium impact
- Document each action with pictures and/or videos, and record visual observations during experiment
- Cut open the enclosures after testing to examine the cardboard
- Results are successful is cardboard is completely undamaged
- Results are acceptable if cardboard has a few droplets or very small damp spots
- Results are unacceptable if cardboard is wet or damaged

Results:

This page discusses water damage testing for the button and screen modules. The buttons will be used more than any other mechatronics component, and are therefore more vulnerable to wear and abuse. For the button module, three water damage scenarios were explored: light splashing, direct flow from one side, and direct flow from above. To quantify water damage, a folded piece of paper was placed inside the enclosure, instead of its actual circuitry. After each test, the paper was examined and photographed.



Figure 7.5 Button module used for testing.

The button module was placed inside a kitchen sink directly under the faucet. By hand, water was splashed and sprinkled onto the enclosure for 30 seconds to simulate light drizzling or foggy weather conditions. The wet enclosure, after splashing, is shown below.



Figure 7.6 Button module after exposure to light splashing.

The enclosure was disassembled and photographed. As shown below, the paper inside the enclosure remained completely dry.

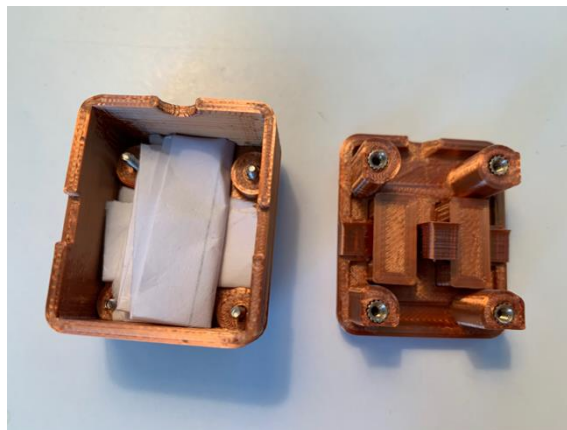


Figure 7.7 Button module successfully protects circuitry after light splashing.

The enclosure was dried before proceeding to the next test. Next, the enclosure was turned on its side and subjected to 30 seconds of direct faucet flow, which is shown in the image below.



Figure 7.8 Button module turned on its side and exposed to direct flow.

The enclosure was disassembled and photographed. As shown below, the paper still remained dry.



Figure 7.9 Button module successfully protects circuitry after faucet flow directed at its profile.

Finally, the enclosure was subjected to 30 seconds of faucet flow directly on the buttons, which is shown in the image below.



Figure 7.10 Button module exposed to direct faucet flow on the buttons.

As shown in the image below, this test thoroughly soaked the paper.

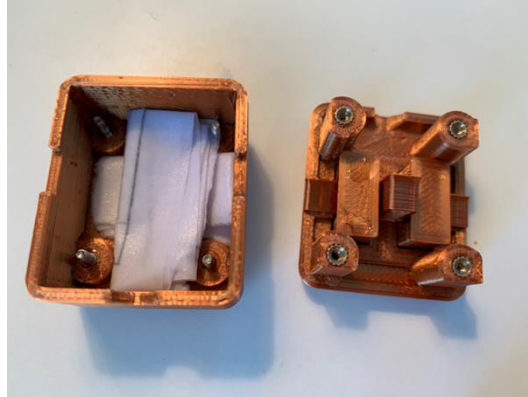


Figure 7.11 Soaked contents of the button module after direct top-down faucet flow.

These tests demonstrate that the button module is not water-tight. It would be unsuitable for use in heavy rain or other wet environmental conditions. However, the contents of the enclosure are protected from indirect splashing and water flow. This indicates that the module would not break from a single instance of splashing from the hydraulic circuit and it would be suitable to use the vehicle on a misty day. It appears that the main source of leakage is in the clearance between the buttons and the enclosure top; the indirect flow test showed that water did not leak through the side seams. To seal the top of the enclosure, a flexible silicon or rubber pad could be glued across the top of the enclosure to cover up the buttons entirely. The pad should be flexible enough to allow the user to still press the buttons. The hole in the enclosure for the wires are a clear source of leakage. An O-ring assembly at this hole, along with protecting the wires in tubing, could also improve its leak resistance.

For live animations of these water-damage tests, please refer to the online documentation wiki at: <https://jkochavi.github.io/page7.html>

7.14 Measurement Accuracy

Thus far, Simscape modeling has been valuable in estimating component performance, and improvements from altering system parameters. However, without the ability to test the vehicle, it is difficult to quantify the accuracy of the models. Soulenoid Cycle has the goal of achieving a convergence of within 10% between system models and experimental testing. This requirement will be verified by comparing the results of the sprint, endurance, and efficiency tests with model predictions. Parameters, such as weight, rolling resistance, and center of gravity will be tuned as needed.

Results:

The only measurement that could be verified for accuracy was the pressure transducer. As discussed in the mechatronics sections, the pressure transducer was calibrated to an analog pressure gauge that carries an accuracy of $\pm 1.5\%$. At the maximum accumulator pressure of 3000 psi, the analog pressure gauge could be off by as much as ± 45 psi. With an additional safety envelope of 10%, the digital pressure transducer can reasonably measure the pressure of the accumulator to ± 50 psi. For more information, refer to the Mechatronics section.

7.15 Durability: Tipping Damage

A benefit of a recumbent tricycle is that it is very hard to tip over. The vehicle can rest on 3 points of contact without a kickstand and can be left unattended without the risk of falling over. Furthermore, the frame has

two central beams spaced 7.5 inches apart, which makes it more resistant to torsional stress. Soulenoid Cycle's vehicle has the requirement of eliminating the threat of component damage from tipping. To verify this requirement, the team will rock the vehicle back and forth to search for torsional weak spots. A weak spot is defined as any location on the vehicle where rocking it can lift the vehicle off the ground. If any location on the vehicle is prone to tipping, the team will add padding to protect any vulnerable components.

8 Competition Results

The COVID-19 pandemic resulted in a virtual 2021 FPVC competition. The decision to proceed with a fully virtual competition was announced on March 8th after taking into consideration the safety of participants, the travel regulations throughout the country, and the COVID-19 restrictions in Colorado specifically, where the competition was supposed to take place. The potential for a virtual competition was a known option throughout the year.

8.1 Overview of the Virtual Competition

Each team submitted videos of each of the three challenges, Sprint, Endurance, and Efficiency, in addition to a video describing the design of their vehicle prior to the scheduled competition. Teams then presented their final vehicle over Zoom to the panel of judges, which was followed by a live Q&A. The presentation and videos were then used to judge each of the challenges and the special awards. The competition schedule is shown below:

Welcome Reception & Mentor Introduction

- Networking Reception & Recruitment Mixer
- Final Presentations
- Award Ceremony

Soulenoid Cycle focused on detailed video submissions and a thorough final presentation in order to ensure a complete understanding of the choices that were made on the vehicle. Due to the virtual nature of the competition, presentation was extremely important.

8.2 Virtual Competition Results

Soulenoid Cycle gave the final presentation on the morning of Friday, April 9th, via Zoom. The competition results were announced later that day. The overall champion awards considered the Midway Review presentation, results from each challenge, final presentations, interaction with industry mentors, and points obtained from attending industry presentations. The overall competition results are summarized in the Table 8.1.

Soulenoid Cycle was named the 2nd Place Overall Champion in addition to placing 1st in the Sprint Challenge. The team was also awarded with the Best Presentations award and the Innovative Use of Electronics award. The judges commented on the polish and professionalism of both the Midway Review and Final Presentations in addition the team's ability to effectively answer all questions during the live Q&A. The Iowa Fluid Power representatives, who sponsored the Innovative Use of Electronics award, were impressed by the interactive touchscreen display, the use of a hall-effect sensor to gather additional data, and the thorough documentation Wiki detailing the entire mechatronics system.

While Soulenoid Cycle performed well enough to earn multiple awards in other areas, they were unable to compete in the endurance challenge due to a fault with the pump selection and/or pump and crankset gearing ratio. The rider was unable to provide sufficient torque to the crankset to be able to move the vehicle for more than a few seconds at a time without becoming exhausted. The rider was therefore unable to complete the race in under ten minutes, resulting in disqualification.

Table 8.1 Awards won at the 2021 competition.

Award	Prize	Recipient
1 st Place – Overall Champion	\$3000	Michigan Technological University
2 nd Place	\$2000	California Polytechnic State University, SLO
3 rd Place	\$1000	University of Cincinnati
Best Presentations	\$2000	California Polytechnic State University, SLO
Sprint Race	\$1000	California Polytechnic State University, SLO
Efficiency Challenge	\$1000	Michigan Technological University
Endurance Challenge	\$1000	University of Akron
Best Use of Pneumatics	\$500	Murray State University
Innovative Use of Electronics	\$500	California Polytechnic State University, SLO
Best Design	\$500	University of Utah
Best Reliability and Safety	\$500	University of Cincinnati
Best Workmanship	\$500	University of Utah
Best Teamwork	\$500	Western Michigan University

9 Project Management

The project management section provides the design approach, resources, and timeline used for the project to ensure that Soulenoid Cycle's goals were met for the competition. Due to the COVID-19 pandemic, Soulenoid Cycle was unable to obtain physical access to the 2019-2020 fluid powered vehicle and begin work on the project until November of 2020. The original engineering specifications outlined in the Objectives section were optimistic in beginning in-person work on the vehicle sooner, therefore the team's goals and specifications were reevaluated to be as realistic as possible with the time that the team had. The team's focus shifted to the manufacturing of a new frame and the relocation of hydraulic components to complete a vehicle that could participate in the competition. Additional plans, such as switching to hard lines, were unfortunately unable to come to fruition due to the time constraints that were faced.

Despite the restrictions due to the pandemic, Soulenoid Cycle successfully completed this project in accordance with social distancing guidelines. Though the completion of the vehicle depended on effective collaboration among all team members, the most critical subsystems in the vehicle design were assigned to team members.

Hydraulic System: Cayla Quinn and Martin Reyes

Steering System: Kellen Giuliani

Mechatronics System: Jordan Kochavi

Frame Manufacturing: All team members

As noted in the 2020-2021 team contract, team roles were dynamic; Soulenoid Cycle was devoted to flexibility and working toward common goals.

9.1 Project Timeline

A Gantt chart is included in Appendix D that visualizes the steps that were taken to accomplish both the intermediate steps and the outcome of the project. Important project milestones include Preliminary Design Review (PDR), Critical Design Review (CDR), and the Final Design Review (FDR). The PDR, completed by June 7th, 2020, focused on Soulenoid Cycle's background research and the process of formulating the initial 2020-2021 vehicle design. The plans laid in the PDR were expected to be updated with the release of the 2021 competition rules and the team's access to on-campus manufacturing resources. The CDR, completed by October 23rd, 2020, reviewed the detailed plans for each subsystem of the vehicle and the manufacturing plan. The FDR, completed in May 2021, describes the manufacturing process, the final competition, and the competition results.

9.2 Project Management Reflection

One of Soulenoid Cycle's greatest strengths was assigning each team member a focus. This gave each member responsibility in their respective areas and allowed them to practice leadership skills when leading the rest of the team during collaborative processes. Team members communicated clearly throughout the project, increasing cohesion and aiding in the final success of the vehicle. Soulenoid Cycle also managed to stay under budget due to detailed and early planning of part orders.

The members of Soulenoid Cycle did not have much previous manufacturing experience, which caused the overestimation of what could realistically be accomplished in the time that was given. While the team did fall behind schedule, Soulenoid Cycle was still able to manufacture a working vehicle by the competition

date by working extra hours and learned a lot about manufacturing timelines in the process. One of the team's most important takeaways that was passed on to the next year's team was to plan much more time than originally thought is necessary for all manufacturing processes.

10 Conclusions and Recommendations

As discussed in the mechatronics sections, the printed circuit board could be improved by switching to smaller wires. While the 18 AWG wire is highly durable on the vehicle, several feet of the thick wire add a significant amount of weight to the electronics. Given that the entire interface is relatively low-powered, the wiring for the screen, buttons, and hall effect sensor can be switched to 24 AWG. However, the wiring for higher-current components, such as the solenoid valves, should remain as thick as possible to prevent any burnouts from too much current. Switching to smaller connectors will also reduce the overall thickness of the interface enclosure. The hinged display makes it easier to connect the wires to the PCB, however it is still inconvenient to unscrew several screw-pin connectors to install all the wires. It is recommended to make all low-voltage connections JST snap-fits with low profiles so that they can be quickly disconnected without needing a screwdriver.

An advantage of using a bi-directional, asynchronous communication bus, such as CAN, is that the network is highly scalable and can support up to 127 individual CAN nodes. Since the ECDR 0506-A and custom interface each constitute a single CAN node, 125 additional nodes can be added to the network without requiring any modification to the existing electronics.

A major opportunity to improve the mechatronics system is its battery life. The electronics currently draw power from a 5000 mAh battery. Since each of the five solenoid valves require 2000 mA to actuate, the vehicle usually runs out of power within one hour. The team had two backup batteries that were always kept charged; the battery was periodically swapped out to prevent it from dying. Switching to a larger battery would certainly alleviate these challenges, but it would also increase the weight of the vehicle. To get a better sense of when to switch out the battery, it would be beneficial to have a battery monitoring system. This system could be an additional CAN node that monitors the battery level and alerts the interface node when it needs to be charged. This system is easily achievable given the scalable nature of CAN.

Another CAN node that could be added to the system is for data storage and telemetry. While the current interface can display graphs of speed and pressure to the user, it has no way to store data. An additional CAN node with memory storage capabilities could read data from the system and store it for the user. Data storage would be highly valuable to system modeling and analyzing the performance of the vehicle.

A power switch should also be added to the vehicle. The electronics are currently powered on by plugging the battery in, which is accomplished by lifting the seat to expose the battery. While the battery uses highly durable snap-fit connections that completely cover its terminals, handling potentially high-current wires still poses a safety issue. It is also inconvenient to lift the seat to turn the vehicle on. It is recommended to add a weather-proof on-off switch to the vehicle that can be accessed while riding.

There is currently a global shortage of integrated circuits. Major electronics distributors, such as DigiKey and Mouser, are either backlogged or out of stock on several common types of electrical components. The auto industry, in particular, is responsible for much of the shortage of such components, which unfortunately include CAN transceivers and controllers. As of April 2021, the TJA1050 CAN transceiver is completely unavailable on Mouser and DigiKey. Fortunately, a second PCB was manufactured as a backup during this project, which includes the TJA1050 component. However, if a new PCB were to be designed, it should include a different transceiver that is not out of stock, such as the MCP2551.

The biggest recommendation for future work on the vehicle's mechatronics system is to continue to build on existing work and document new additions. The documentation wiki will hopefully grow as future teams add to the network.

One of the biggest criticisms from the Midway Review event was the exclusion of a hydraulic accumulator manual discharge. The current set up was only able to discharge the accumulator through boost mode. Although this could be done by riding the vehicle in boost mode until empty or lifting the rear wheel and discharging, there should be a safer alternative. Soulenoid Cycle designed a solution which required replacing a check valve (CV1) with a solenoid valve, SP08-20Y. This valve would act a typical check valve when not activated. However, by manually activating it along with the manual override on SP1, the stored accumulator energy would have discharged to the reservoir. This design also allowed the manual discharge to be independent of the mechatronic system. Due to limited space to the mounting components, the SP08-20Y valve was not installed.

Regarding vehicle performance, the aspect that could use the most improvement is the pedaling. Pedaling the crank to rotate the pump is difficult and does very little to move the vehicle. One observation noted was that applying too much torque would slip the chain from the sprocket. This could be solved by appropriate tensioning of the chain, but the amount of torque needed by the operator is still concerning. Essentially, the vehicle barely moves unless the pump rotates near its ideal operating RPM, however, getting it there requires input torque from the rider far beyond what the average person can produce for more than a couple of seconds. The other observation is that amount of fluid flowing through the pump's case drain was a lot. Soulenoid Cycle along with Dr. Widmann were not sure of the appropriate solution. The first suggestion would be to look at the pump size or orientation. The pump's 5 cc displacement might be too small to move the added weight of the vehicle. The pump may also have specific mounting instructions where it prohibits mounting the pump at an angle. The other recommendation is to investigate the gearing at the front.

The largest challenge that Soulenoid Cycle faced was the COVID-19 restrictions in place throughout the 2020-2021 project. The team had a late start in terms of manufacturing and found it difficult to coordinate adequate amounts of time in the machine shops. However, the team was grateful that Cal Poly's campus was able to partially open during Fall 2020 and Winter 2021 quarters and that they were able to manufacture at all. An applicable manufacturing lesson that the Soulenoid Cycle team members took with them upon the completion of this project is that everything takes longer than anticipated. The most important lesson that Soulenoid Cycle learned was to ask for help. The NFPA provides teams with countless resources, yet Soulenoid Cycle was slow to employ those resources in the beginning. Every industry mentor and competition staff that the team interacted with was extremely knowledgeable and was eager to help the team learn. Each member of the team grew in their technical knowledge, project management abilities, and collaboration skills during this project.

References

- [1] “Fluid Power Vehicle Challenge | Interactive Science.” *Fluid Power Challenge*, nfpahub.com/fpc/vehicle-challenge/.
- [2] Godin, Ed. “Choosing An Accumulator Takes More Than A Coin Flip.”ⁱ *StackPath*, 9 Aug. 2010, www.hydraulicspneumatics.com/technologies/accumulators/article/21883617/choosing-an-accumulator-takes-more-than-a-coin-flip.
- [3] Chowdhury, Dwaipayan Roy. “A Recumbent Trike Design with Maximum Performance and Vehicle Dynamics Analysis.” *Iarjset*, vol. 6, no. 1, 30 Jan. 2019, pp. 71–84., doi:10.17148/iarjset.2019.6112.
- [4] HYDAC Accumulators. (n.d.). *HYDAC International*. Retrieved from <http://www.hydac-na.com/sites/hydac-na/SiteCollectionDocuments/Accumulators.pdf>
- [5] Korane, Ken, et al. “Hydraulic Accumulators: How Do They Work?” *Mobile Hydraulic Tips*, www.mobilehydraulictips.com/hydraulic-accumulator-work/.
- [6] “NEMA Enclosure Types - NEMA 250-2003.” *NEMA.org*, National Electrical Manufacturers Association, Nov. 2005, www.nema.org/Products/Documents/nema-enclosure-types.pdf.
- [7] “2020 NFPA Fluid Power Vehicle Challenge Overview, Rules and Rewards”, NFPA Education and Technology Foundation, Sep. 2019.
- [8] Robot Bike Co. “Using Generative Design to Develop a Lightweight Bicycle Rocker.” GRM Consulting, [https://www.grm-consulting.co.uk/images/pdf/FY17/CASE_STUDIES/GRM-Robot-Bike-White paper.pdf](https://www.grm-consulting.co.uk/images/pdf/FY17/CASE_STUDIES/GRM-Robot-Bike-White%20paper.pdf)
- [9] “Statement of Work.” The Incompressibles, California Polytechnic State University San Luis Obispo.
- [10] “Statement of Work.” Pump My Ride, California Polytechnic State University San Luis Obispo.
- [11] “Student Success Guide.” Department of Mechanical Engineering, California Polytechnic State University San Luis Obispo.

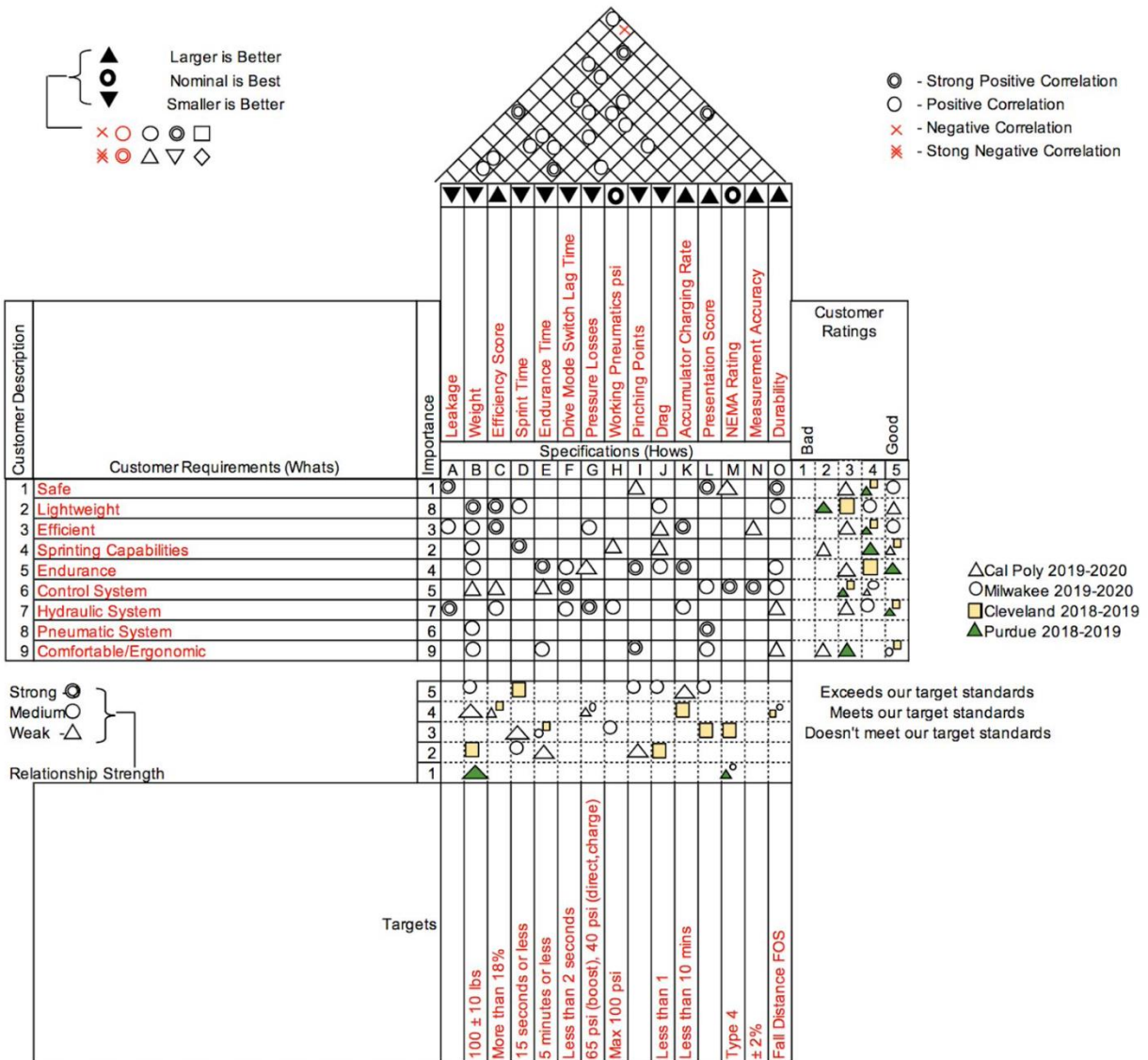
Appendix

Appendix A Customer Requirements	123
Appendix B QFD Spreadsheet.....	124
Appendix C Preliminary Interface Speed Test Data.....	125
Appendix D Gantt Chart.....	126
Appendix E Design Hazard Checklist	127
Appendix F Competition Rules	128
Appendix G Preliminary Interface Prototype Software.....	135
Appendix H Mechatronics Bill of Materials	138
Appendix I Circuit Board Schematic.....	139
Appendix J HF Impulse Software for the ECDR 0506-A	140
Appendix K Ergonomic Considerations	141
Appendix L Engineering Drawings	143
Appendix M FMEA Spreadsheet.....	163
Appendix N Feedback From Competition Judges	164
Appendix O Additional Pictures of Final Design.....	168
Appendix P Bosch Series 6 Pump Datasheet	170
Appendix Q Accumulator Datasheet	171
Appendix R Efficiency Competition Spreadsheet	172
Appendix S MSDS for the Hydraulic Fluid	173
Appendix T Simscape Block Diagram	174
Appendix U Pneumatic Braking Force Calculation	175

Appendix A Customer Requirements

Design a traditional bicycle using hydraulics as the mode of power transmission
Vehicle must be safe to ride and ship
All NFPC minimum requirements for the 2020-2021 challenge must be met Creative and innovative features must be employed
A pneumatic system must be implemented
The vehicle must weigh less than 210 pounds
The team must demonstrate hydraulics and industry knowledge
The team must give an impressive and successful performance Construction of the vehicle must remain under budget
Vehicle must win the overall competition

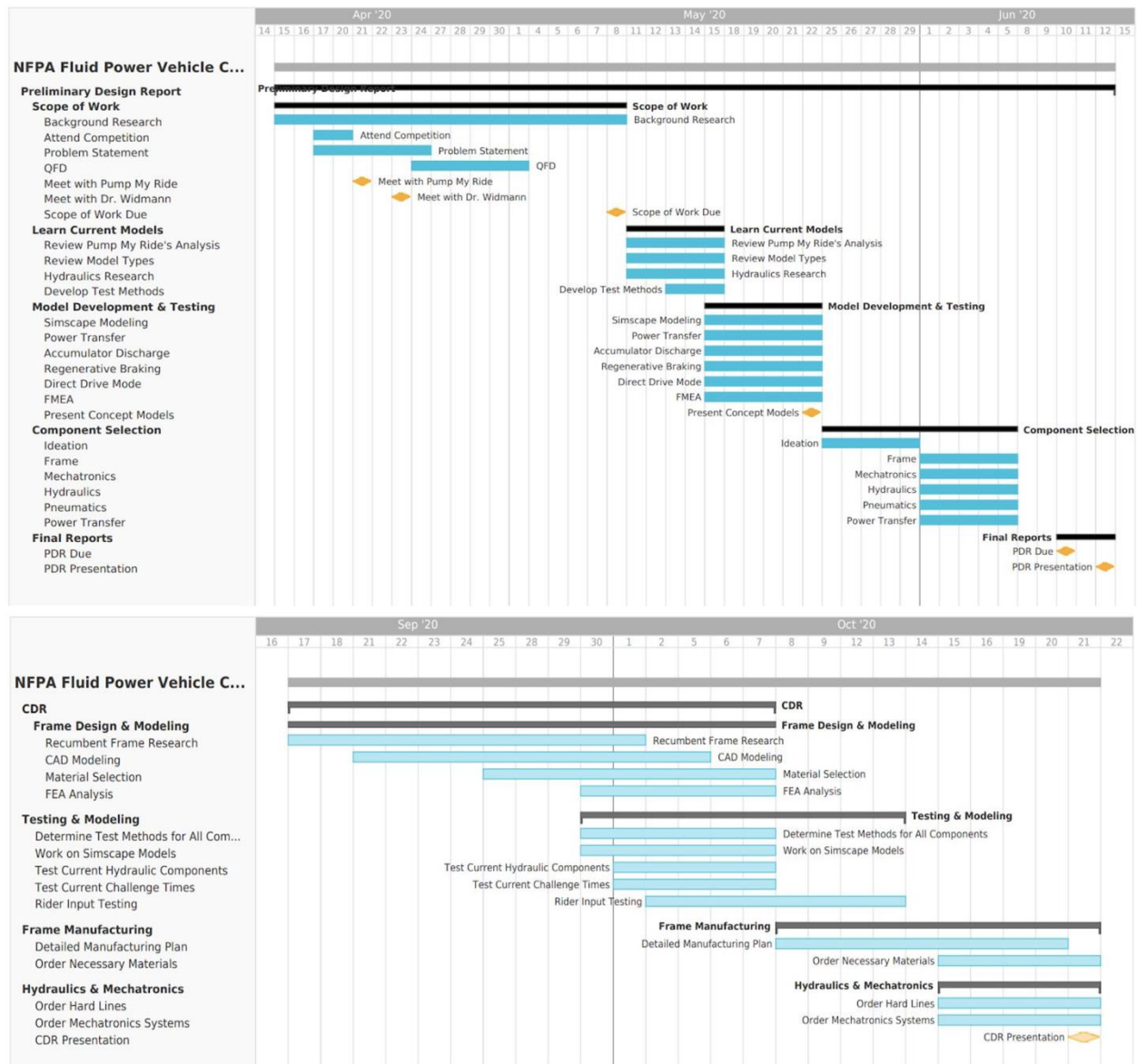
Appendix B QFD Spreadsheet



Appendix C Preliminary Interface Speed Test Data

Screen Element	Run 1 Elapsed Time [sec]	Run 2 Elapsed Time [sec]	Run 3 Elapsed Time [sec]	Average Elapsed Time [sec]
Filling entire screen solid color	3.090	3.090	3.090	3.090
Green drive mode icon	0.039	0.039	0.039	0.039
Blue virtual button	0.095	0.095	0.095	0.095
Large font text	0.148	0.148	0.148	0.148
Small font text	0.044	0.044	0.044	0.044
Thin line	0.012	0.012	0.012	0.012
Total home screen initialization time	4.073	4.073	4.073	4.073

Appendix D Gantt Chart



Appendix E Design Hazard Checklist

DESIGN HAZARD CHECKLIST		
Team:	<u>Soulenoid Cycle</u>	Faculty Coach: <u>Fabijan</u>
Y N		
<input checked="" type="checkbox"/> <input type="checkbox"/>	1. Will any part of the design create hazardous revolving, reciprocating, running, shearing, punching, pressing, squeezing, drawing, cutting, rolling, mixing or similar action, including pinch points and sheer points?	
<input checked="" type="checkbox"/> <input type="checkbox"/>	2. Can any part of the design undergo high accelerations/decelerations?	
<input checked="" type="checkbox"/> <input type="checkbox"/>	3. Will the system have any large moving masses or large forces?	
<input type="checkbox"/> <input checked="" type="checkbox"/>	4. Will the system produce a projectile?	
<input type="checkbox"/> <input checked="" type="checkbox"/>	5. Would it be possible for the system to fall under gravity creating injury?	
<input type="checkbox"/> <input checked="" type="checkbox"/>	6. Will a user be exposed to overhanging weights as part of the design?	
<input type="checkbox"/> <input checked="" type="checkbox"/>	7. Will the system have any sharp edges?	
<input type="checkbox"/> <input checked="" type="checkbox"/>	8. Will any part of the electrical systems not be grounded?	
<input type="checkbox"/> <input checked="" type="checkbox"/>	9. Will there be any large batteries or electrical voltage in the system above 40 V?	
<input checked="" type="checkbox"/> <input type="checkbox"/>	10. Will there be any stored energy in the system such as batteries, flywheels, hanging weights or pressurized fluids?	
<input checked="" type="checkbox"/> <input type="checkbox"/>	11. Will there be any explosive or flammable liquids, gases, or dust fuel as part of the system?	
<input checked="" type="checkbox"/> <input type="checkbox"/>	12. Will the user of the design be required to exert any abnormal effort or physical posture during the use of the design?	
<input checked="" type="checkbox"/> <input type="checkbox"/>	13. Will there be any materials known to be hazardous to humans involved in either the design or the manufacturing of the design?	
<input type="checkbox"/> <input checked="" type="checkbox"/>	14. Can the system generate high levels of noise?	
<input type="checkbox"/> <input checked="" type="checkbox"/>	15. Will the device/system be exposed to extreme environmental conditions such as fog, humidity, cold, high temperatures, etc?	
<input checked="" type="checkbox"/> <input type="checkbox"/>	16. Is it possible for the system to be used in an unsafe manner?	
<input type="checkbox"/> <input checked="" type="checkbox"/>	17. Will there be any other potential hazards not listed above? If yes, please explain on reverse.	
<p>For any "Y" responses, add (1) a complete description, (2) a list of corrective actions to be taken, and (3) date to be completed on the reverse side.</p>		



Appendix F Competition Rules

Norgren Event Overview

The final competition will be an exciting event where students, advisors, industry representatives, and other invited guests experience the final leg of this dynamic undergraduate engineering design challenge. Students will present and demonstrate their designs, industry representatives will judge their work, and winners will emerge.

This year, all Vehicle Challenge attendees will participate remotely but we are still expecting this to be an interactive and engaging event. Note: Virtual networking sessions are required for all student participants so teams should be aware of this when reviewing the schedule of events and updating their calendars.

Important dates and deadlines:

- Final Competition: April 7-9, 2021
- Race Footage Submitted: No later than April 6
- Proof of Working Vehicle and Vehicle Design Review Submitted: 3 business days prior to performing the races.
- Updated Resume and Portfolios Submitted: March 30
- Select the Team's Final Presentation slot: March 22

April 7

To start, teams will meet other participants and industry representatives at a virtual Welcome Reception on Wednesday, April 7th. This will be a ballroom inspired networking experience where NFPA and Norgren staff will greet participants and provide an overview of the event. One representative from each team will be asked to introduce their industry mentor by giving their name, the company they work for and one of the most helpful things your team learned from your mentor. After the Welcome Reception, Final Presentations will begin. Notice from the schedule that the presentations are back-to-back. We are asking you to be in attendance for the duration of those sessions:

- That means on the day that you are scheduled to present, log on at the "start" and log off at the announced "close". Teams are welcome to attend all presentations.
- You must be on time to keep the schedule on track.
- Do not log on at the exact start time of your presentation.

April 8

On Thursday, Final Presentations will resume. After we hear from the teams scheduled for that day, we will transition into a Networking Reception and Recruitment Mixer. This will be an engaging, 1.5-hour session in a ballroom – inspired seating arrangement pictured below and teams that have full attendance in the event will receive two points towards the competition. Like speed meetings, this event will allow HR/ Outreach representatives to exclusively connect with up to 6 to 8 students at a time in segmented Zoom breakout rooms to discuss opportunities at their companies.

Participating companies will be asked to upload their website and any other informational items in advance so that participants can visit their virtual "exhibitor booths" before the mixer. Students are encouraged to visit the booths and request individual meetings with representatives during this time. As shown above smaller virtual tables for one-on-one conversations will be available. The last 15 minutes of the event will be reserved for these one-on-one sessions and for advisors to meet with industry representatives. We recommend advisors getting to know them as they can be a source of employment for other students at your university. Resumes will be sent to industry representatives in advance, so students and advisors are encouraged to update their resumes and profiles on the Vehicle Challenge website by March 30th. These items are found in the "My Registration".

- Link to the website: <https://fpvc.secure-platform.com/a/organizations/main/home>
- Log In> Click "My Entries" > Click View "My Registration".

- There will be a yellow bar at the top, “Click Here to Make Edits”.
- Scroll through and reupload your resume or update your profile.

April 9

On Friday, we will wrap up the Final Presentations. After that, judges will meet to select the winners and all participants will come together again for the Award Ceremony.

Prior to the Final Presentations, the judges will be tasked with independently reviewing submitted footage from the Proof of Working Vehicle, Vehicle Design Review, and the races so that they can ask questions during each team’s presentation. Therefore, students must adhere to the above deadlines.

Final Competition

- Will include a safety inspection, design assessment, sprint race, efficiency challenge, endurance challenge and presentation. Each team starts with storage device void of hydraulic fluid.
- Each team will determine their own “racetrack” by finding a safe, accessible, and local space to demonstrate their vehicle performance.
- Each team will schedule their own date and time to perform the races. Race results must be recorded on the same day at or about the same time. Note: Proof of Working Vehicle needs to be submitted and approved three business days prior to race demonstration.
- Each team will need certain equipment to submit necessary data and race results for evaluation. Refer to the section “Equipment Needs” below for details and contact Stephanie at NFPA as soon as possible if obtaining this equipment provides a hardship for your team to compete. NFPA issued stipends may be used to purchase needed equipment.
- Maximum 10 minutes allowed to manually pressurize the storage device. Do not include this footage in your video submissions.
- The pre-charge of the accumulator may not exceed 50 PSI if the vehicle is being shipped. Caution: Do not empty the accumulator and let air into it.
- Teams may use a third-party hydraulic supplier to gas charge the accumulator to the safe, desired, pre-charge pressure.
- No mechanical, hydraulic, or pneumatic failures are allowed due to poor design or application of components. Vehicle failures during the Sprint Race and Efficiency Challenge will result in elimination.
- Reservoirs, components, and plumbing must meet reasonable industry standards. No duct tape or other examples of insufficient workmanship. There is zero tolerance for active leaks in the system.
- Be sure to include two pressure indicators (1) at the outlet of the accumulator with the test port and (2) before the hydraulic motor.
- The manufacturer’s size and rating of the accumulator must be easy to read. If air is used, the size of the receiver and pressure must be known.
- All course competitions will begin with a standing start. No pushing.
- The vehicle system configuration does not need to remain the same for all races. However, all components must remain in place. Teams may modify the configuration as long as there is no loss of oil during the change-over, other than a few drops.
- Drivers must maintain a safe speed and adhere to all instructions from the course marshals/university faculty. Failure to comply will result in penalties, disqualification of event races or elimination.
- The university faculty advisor is responsible for certifying all race results. A checklist will be provided. Failure to meet these requirements may result in disqualification of affected races.
- Video footage will be required for judges to accurately identify the winners of each race. The camera must stay on for the entire duration of each race or the team will be disqualified from the affected races.

- Deadline to submit video footage for all races will be April 8th if Danfoss is your competition site.
- Deadline to submit video footage for all races will be April 5th if Norgren is your competition site.
- Video footage for the races is to be submitted on the website in the form with your final presentation.
- The decisions of the judging panel are final. This includes tie breaking decisions. All ties will be broken based on adherence to the design criteria and performance.

Final Presentations

All Final Presentations will be conducted live, and teams should plan to have their cameras on during their presentation. There is no deadline to submit the Final Presentation PowerPoint. However, teams must upload the PowerPoint slides on the website prior to their scheduled time or the judges will not be able to access the form to submit scores for the team. Teams are required to use the Final Presentation Template found on the website. A YouTube link of any video(s) must be included in the speaker notes and uploaded on the website. Details to submit the PowerPoint will be provided.

Sprint Race

This event will demonstrate the ability of the vehicle to move a distance where the weight of the vehicle is proportional to the human propulsion.

- Heats of multiple bikes at a time on a 500 ft course.
- Standing start, one rider on vehicle, no pushing.
- Each team is allowed up to two attempts and must use the same rider in both attempts.
- To qualify, each team must begin at the starting line, race to the finish line, and record the results. Then, teams will reverse course beginning from the finish line, back to the starting line following the same racetrack, and record those results. Teams must use the same rider in both attempts.
- Maximum 10 minutes allowed to manually pressurize the storage device prior to each of the race attempts.
- Each team will self-report the time spent traveling to 500 ft. in both attempts. Maximum of two attempts will be allowed, one in each direction.
- To verify results, required video footage needs to include a complete view of the rider for the full duration of both the initial sprint, and the reversed return sprint.
- The submitted race result will be the average time of both attempts.
- Procedure for reporting race results and recording video:
 - Have one person at the start of the racetrack wave a flag (or their arm) to signal to the timekeeper that the race has started. This should be visible in video footage.
 - The timekeeper and videographer should be at the end of the racetrack to report the time the rider passes the 500 ft mark. The time stamp should be visible in video footage.
 - Footage may be longer than actual time it takes to perform the race. Advisors must report the duration of the race from the time of the starting flag to the time at the finish line.
 - Follow the same directions in the second attempt.
- Best time for places 1st, 2nd, and 3rd.
- Timing in Minutes: seconds: tenths of seconds: hundredths of seconds.

Efficiency Challenge

This event will demonstrate the ability of the vehicle to effectively store and most efficiently use the smallest amount of stored energy to propel the unassisted vehicle the greatest distance proportional to the vehicle's weight.

- The vehicle that goes the farthest is NOT necessarily the most efficient. Similarly, the most stored energy does not automatically indicate the winner either.
- The vehicle must travel a minimum distance of 100 ft. Braking is not required. Vehicle will go as far as it can before coming to a complete stop.
- To qualify, each team must begin at the starting line, race to the finish line, and record the results. Then, teams will reverse course beginning from the finish line, back to the starting line following the same racetrack, and record those results.
- Judges will require verification in the checklist that the accumulator is discharged at the start of this race. Here is how to verify the charge on a hydraulic accumulator:
 1. If you have the equipment and training to connect to the nitrogen side, you may simply read the nitrogen pressure when you are certain that the hydraulic side is discharged.
 2. Alternatively, if you can place a glycerin-filled pressure gauge on the hydraulic side of the accumulator and slowly discharge the accumulator, the nitrogen pre-charge is indicated momentarily on the process of slow discharge. The procedure is as follows:
 - a. Install or locate suitable pressure gauge to read pressure at the hydraulic port of the accumulator.
 - b. Apply hydraulic pressure sufficient to charge the accumulator. Typically, you would charge to full hydraulic system pressure.
 - c. Locate a bleed valve or suitable means of safely discharging the accumulator slow enough to watch the pressure sweep on a gauge.
 - d. While observing the pressure gauge, slowly discharge the accumulator and watch the pressure decrease.
 - e. At the point the accumulator runs out of oil there will be an immediate drop to zero on the pressure gauge. The pressure immediately before the rapid drop indicates the nitrogen pre-charge on the accumulator.
 - f. This procedure can be repeated to visually verify again if needed.
 - g. [Here is an example.](#)
- The vehicle, designated rider, and safety gear will be weighed in advance of the race and will be self-reported by each team.
- Each team must use the same rider in both attempts.
- Standing start, one rider on vehicle. There can be no assistance in making the machine move on its own. No windshields or wiggling of handlebars is allowed. Rider must remain on the vehicle for the entire event. If a foot touches the ground, this distance will be measured from the starting point.
- Rider will not be allowed to operate the pedals or any other mechanical input device from the start of the event until the vehicle comes to rest. Braking is allowed for energy recovery, but not required.
- 10 minutes will be allotted to charge the accumulator. No prior charging will be allowed. All charging will be human powered only.
- The vehicle's pre-charge pressure used in the calculation below will be the pre-charge that is requested by the team. **Caution –No air enters the accumulator, only nitrogen enters that accumulator.**
- Teams may use a third-party hydraulic supplier to gas charge the accumulator to the safe, desired, pre-charge pressure.

- The volume of the storage device used in the calculation will be as stated on the vessel by the manufacturer (Pressure storage devices manufactured other than by Iowa Fluid Power or SunSource must be approved by the Technical Liaison).
- The winner will be determined by the following parameters and equation:
 - Column B = gas pre-charge pressure in pounds per square inch (PSI) (Note: The minimum accumulator gas pre-charge pressure during filling will be 100 PSI)
 - Column C = Maximum system pressure that the accumulator is charged to.
 - Column D = Volume of the accumulator (Maximum 231 in³).
 - Column E = weight of the vehicle and rider in pounds.
 - Column F = total distance traveled from starting point in feet.
 - Refer to the Excel spreadsheet for the scoring ratio.
- This calculation is an efficiency ratio and will provide an objective measurement to judge vehicle/system efficiency. It quantifies the winning vehicle as providing the most work with the smallest amount of stored energy.
- Each team will self-report the data needed to complete the equation. The submitted race result will be the average of both attempts.
- In the simplest terms, the vehicle that completes the challenge with the least amount of energy per pound of weight, wins.
- Procedure for reporting race results and recording video:
 - Have one person at the start of the racetrack wave a flag (or their arm) to signal to the timekeeper that the race has started. This should be visible in video footage.
 - The timekeeper and videographer should be at the 100 ft mark and if applicable, after that point, follow the rider on foot from a safe distance until their stopping point to record the distance and time. The time stamp should be visible in video footage.
 - Follow the same directions in the second attempt.

Endurance Challenge

This event will demonstrate the reliability, safety, replicability, and durability of the fluid power system design and assembly.

- The course may consist of laps in a slalom fashion and will total no more than 1 mile or (5280 feet). Maximum time to complete will be 30 minutes.
- Each team must define a course that is 2640 feet in length.
- To test the regenerative braking circuits of the vehicles, the course will require at least one stop and restart of the vehicle.
- To qualify, the rider must pedal the vehicle to recover as much energy as possible, make a complete stop at 2640 ft (½ mile), turn around to reverse course and restart the final ½ mile by accelerating with only the accumulator for at least the **first 10 feet**, and finish the race by returning to the original starting line.
- Video footage must capture the complete stop (both feet on the ground, no push off), the turn around and return start off stored energy. Teams will be disqualified from the Endurance race for not verifying their regenerative braking ability in video footage. This could be a short clip from a second camera.
- No hydraulic pressure in accumulators in advance of the race.
- Judges will require video verification in the checklist that the accumulator is discharged at the start of this race. Refer to the efficiency race above to read how to verify the charge on a hydraulic accumulator.
- Standing start, one rider on vehicle, no pushing.

- Teams are allowed up to two drivers, as an option, although not a requirement to complete the course. For safety, the vehicle will come to a complete stop to change drivers, no pushing.
- Driver changes will only be allowed at the 2640, half mile point.
- The clock will keep running during any stops, even if the team switches riders.
- If vehicle breaks down during the Endurance Challenge. The team will have 15 minutes to repair. The clock is not stopped for repairs.
- Procedure for reporting race results and recording video:
 - Have one person at the start of the racetrack wave a flag (or their arm) to signal to the timekeeper that the race has started. This should be visible in video footage.
 - The timekeeper and videographer should stay at the starting line of the racetrack for the duration of the race to report the time the rider passes the 1-mile mark. The time stamp should be visible in video footage.
 - Footage may be longer than actual time it takes to perform the race. Advisors must report the duration of the race from the time of the starting flag to the time at the finish line.
- Best time for places 1st, 2nd, and 3rd. Timing in minutes: seconds: tenths of seconds.

Advisor Checklist

Each university team advisor is required to email Stephanie the advisor checklist no later than April 6 to certify the teams race results. Students do not submit this form.

- If the team thinks that their entry qualifies for any of the awards, they are welcome to describe why, in 100 words or less, for each category. If an award is not applicable, leave it blank. There is also a "Note to Judges." This is an additional opportunity to share anything that you think the judges should know when considering your overall participation in the event.
- This portion of the checklist is optional. All other fields are considered required.

Proof of Working Vehicle & Vehicle Design Review

It is required that teams demonstrate your vehicle is in working condition by submitting a YouTube video link, indicating your intent to participate in final event. **The video must also capture all components and design elements and must be no longer than 6 minutes. Footage needs to be captured in this order:**

1. Confirm that the vehicle is safe and operational with a team member riding it at least ½ a block or better.
2. Verify stored energy working off the accumulator.
3. Confirm the use of pressure indicators and test point.
4. For judges to adequately review the Vehicle Design, video footage should showcase and verbally describe these criteria in the following order:
 - Quality of vehicle design associated with reliability.
 - Quality of vehicle design associated with operator safety and comfort.
 - Quality of vehicle design associated with originality and uniqueness.
 - Refer to the FPVC assessment rubric for more detail on criteria.
 - Missing footage will result in a score of zero for the affected criteria.

Your proof of a working vehicle must be received **and approved three business days prior to race demonstration**. Teams can manage who can view content through privacy settings of YouTube videos. [Learn how here](#). Teams are also required to submit one photo of only their vehicle for judges to refer to during the final competition.

Equipment needs

- Each team needs a way to display a date and time stamp in their video footage. (smart phone options available that include date/time)
 - [Option to add a time stamp to an iPhone.](#)
 - [Option to add a time stamp to an Android.](#)
- Each team needs a way of measuring distance in feet.
 - A measuring wheel can be used to do this. [Here is an option.](#)
- Each team needs a way to weigh the vehicle and the rider separately.
- Each team needs a camera (mobile phone quality is fine) capable of zooming to capture detailed races elements.

Awards

- All \$14,000 in cash prizes will be distributed directly to the team participants for the winners of all award categories.
- Student Teams will select the Best Design award. One person from each team will be responsible for nominating another team for Best Design. Teams may not vote for themselves. Details to vote will be provided.

Appendix G Preliminary Interface Prototype Software

```
// Soulenoid Cycle
// Preliminary Display Interface
// Date Created: 05/14/20
// Date Installed: 06/04/20
// Date Modified: 06/06/20
#include <Adafruit_GFX.h>
#include <Adafruit_ILI9341.h>
#include <URTouCh.h>
#define t_SCK 3
#define t_CS 4
#define t_MOSI 5
#define t_MISO 6
#define t_IRQ 7
#define TFT_RST 8
#define TFT_DC 9
#define TFT_CS 10
#define TFT_MISO 12
#define TFT_MOSI 11
#define TFT_CLK 13
// General Adafruit graphics library
// Library specific to ILI9341 display module // Touch screen library
// SPI pin
// SPI pin
// SPI pin
// SPI pin
// SPI pin
// Reset pin
// SPI pin
// SPI pin
// SPI pin
// SPI pin
Adafruit_ILI9341 tft = Adafruit_ILI9341(TFT_CS, TFT_DC, TFT_MOSI, TFT_CLK, TFT_RST, TFT_MISO); // Instantiate //screen object
URTouCh ts(t_SCK, t_CS, t_MOSI, t_MISO, t_IRQ); //touch object
// Some global variables
uint8_t loading;
int x;
int y;
uint8_t screen;
uint8_t driveMode[2];
second number is current drive mode.
uint8_t UdMode;
class Button { public:
{
// Instantiate
// Array, stores current drive-mode and previous drive-mode. First number is previous, // Boolean flag - raised when the drive-mode needs to be updated on
the display
// Virtual button class
// Public attributes
// Array, stores coordinates to check for press
// Boolean flag - raised when screen page is done initializing // Stores x-coordinate of where the screen was touched
// Stores y-coordinate of where the screen was touched
// Screen state variable
int coord[4];
// Function, displays button at a location.
// Parameters: Coordinates [x,y], width, height, text, button color, text size, x and y offset for text
//placement
// This function is action-based; it does not return any values and is entirely self-contained
void displayButton(int x, int y, int w, int h, String text, uint16_t color, int textSize,int xoff, int yoff)
int dx = (2*x+w)/2 + xoff;
int dy = (2*y+h)/2 + yoff;
coord[0] = x;coord[1] = y;coord[2]=x+w;coord[3]=y+w; tft.fillRect(x,y,w,h,color); tft.setTextColor(ILI9341_BLACK); tft.setCursor(dx,dy);
tft.setTextSize(textSize);
tft.print(text);
// Calculate x-coordinate of center of button // Calculate y-coordinate of center of button // Update coordinate array based on parameters // Write a
filled rectangle to the screen
// Set text color to black
// Set cursor to center of button // Set text size to parameter value // Print text to screen
}
// Function, checks if the button is pressed
// Parameters: Coordinates [x,y]
// This function returns a boolean value, either true or false based boolean isPressed(int x, int y) {
on entered parameters
Define boolean to store press status If the user touched a location within
Then set pressStat to TRUE Otherwise... the user didn't press the
Sp set pressStat to FALSE Output pressStat
boolean pressStat;
// //
// // //
if (x>coord[0] && x<coord[2] && y>coord[1] && y<coord[3]) { //the coordinates of the button...
pressStat = true;
}
else { //button
pressStat = false; return pressStat;
}
};
Button D,B,C,R,check,pressure,flow,data,Home; // Instantiate 8 virtual buttons // Function, init sequence for Arduino bootloader
// A setup() function is required for void setup() {
Serial.begin(9600); // refers to a baud rate.
tft.begin();
tft.setRotation(3); // orientation of the display
ts.InitTouch(); ts.setPrecision(PREC_EXTREME); screen = 0;
driveMode[0] = 0; driveMode[1] = 1;
}
// Function, main code execution loop
all Arduino boards
// Begin serial connection through USB port for debugging to PC. "9600"
// Initialize LCD display
// Rotate screen origin 270 degrees, just has to do with the physical
// Initialize the touch interface
// Set touch sensitivity to high
// Initialize display page to 0 (load the home screen) // Initialize drive mode to Direct Drive
// A loop() function void loop() {
ts.read();
x = ts.getX(); y = updateScreen(x,y); delay(10);
for Arduino bootloader is required for all Arduino boards
}
// Function, display void updateScreen(int x,
if (screen == 0) { mainScreen(x,y);
```

```

}
else if (screen == 1){
checkScreen(x,y);
}
else if (screen ==
flowScreen(x,y);
2){
// If display state = 0, then // Execute home page state
// If display state = 1, then // Execute check screen state
// If display state = 2, then // Execute flow screen state
proceed proceed proceed proceed
to home page state to check screen to flow screen
to pressure screen to data screen
// Initialize state, execute if // Clear screen by filling with // Display all virtual buttons at
// Set text size // Set cursor
// Print large text // Set cursor
// Print large text // Set cursor
// Reduce text size // Print small text // Set cursor
// Print small text // Set cursor
// Print small text // Draw table outline
}
else if (screen ==
3){ pressureScreen(x,y);
// If display state = 3, then // Execute pressure screen state
ts.getY();
// Check the touch screen for presses
// If the screen is touched, store touched coordinates // Update the screen
// 10 millisecond delay for stability
hub
int y) {
}
else if (screen == 4){
dataScreen(x,y);
} }
// Function, main screen
void mainScreen(int x, int y) {
if (!loading) { loading not complete
tft.fillScreen(ILI9341_WHITE); white background
D.displayButton(250,50,30,23,"D",ILI9341_GREEN,2,-5,-7); desired coordinates
C.displayButton(250,100,30,23,"C",ILI9341_GREEN,2,-5,-7); B.displayButton(250,150,30,23,"B",ILI9341_GREEN,2,-5,-7);
R.displayButton(250,200,30,23,"R",ILI9341_GREEN,2,-5,-7); check.displayButton(160,133,60,30,"Check",ILI9341_CYAN,1,-13,-3);
data.displayButton(160,188,60,30,"Data",ILI9341_CYAN,1,-13,-3); flow.displayButton(86,188,60,30,"Flowrates",ILI9341_CYAN,1,-26,-3);
pressure.displayButton(11,188,60,30,"Pressures",ILI9341_CYAN,1,-26,-3); tft.setTextSize(2);
tft.setCursor(0,10);
tft.print(" SPEED ACCUMULATOR MODE"); tft.setCursor(0,100);
tft.print(" (mph)
tft.setCursor(0,230);
tft.setTextSize(1);
tft.print(" Soulenoid Cycle, Cal Poly SLO FPV"); tft.setCursor(4,126);
tft.print("Error Status:");
tft.setCursor(4,136);
tft.print("NONE"); tft.drawFastVLine(240,0,240,240); tft.drawFastVLine(100,0,120,122); tft.drawFastHLine(0,120,240,120); tft.drawFastHLine(0,175,240,175);
state of display task
(psi)");
// If display state = 4, then proceed // Execute data screen state
tft.drawFastHLine(0,225,240,225);
UdMode = 1; //on screen
loading = 1;
}
// Home page hub, wait for virtual button presses if (D.isPressed(x,y) && driveMode[2]!=1) {
// Raise flag to update drive mode // Loading complete
//mode is not yet selected...
driveMode[0] = driveMode[1]; driveMode[1] =
//accordingly UdMode = 1;
//accordingly }
else if (C.isPressed(x,y) && driveMode !=2) { //drive mode is not yet selected...
driveMode[0] = driveMode[1]; driveMode[1] = //accordingly
UdMode = 1; //accordingly
}
else if (B.isPressed(x,y) && driveMode !=3) { //drive mode is not yet selected...
driveMode[0] = driveMode[1]; driveMode[1] = //accordingly
UdMode = 1; //accordingly
}
else if (R.isPressed(x,y) && driveMode !=4) { //drive mode is not yet selected...
driveMode[0] = driveMode[1]; driveMode[1] = //accordingly
UdMode = 1; //accordingly
}
else if (check.isPressed(x,y)){ //pressed...
screen = 1; loading = 0;
}
else if (flow.isPressed(x,y)){
screen = 2; loading = 0;
}
else if (pressure.isPressed(x,y)){ //pressed...
screen = 3; loading = 0;
}
else if (data.isPressed(x,y)){
screen = 4; loading = 0;
}
}
if (UdMode == 1) { //updated on the display
displayDriveMode(1,driveMode[0]); //white circle to the display
displayDriveMode(2,driveMode[1]); //at the new location
UdMode = 0;
1;
2;
3;
4;
// IfD //
//
// Else //
//
// Else //
//
// Else //
//
// Else
//
// Else //
//
// Else
//
// Else //
//
}

```

```

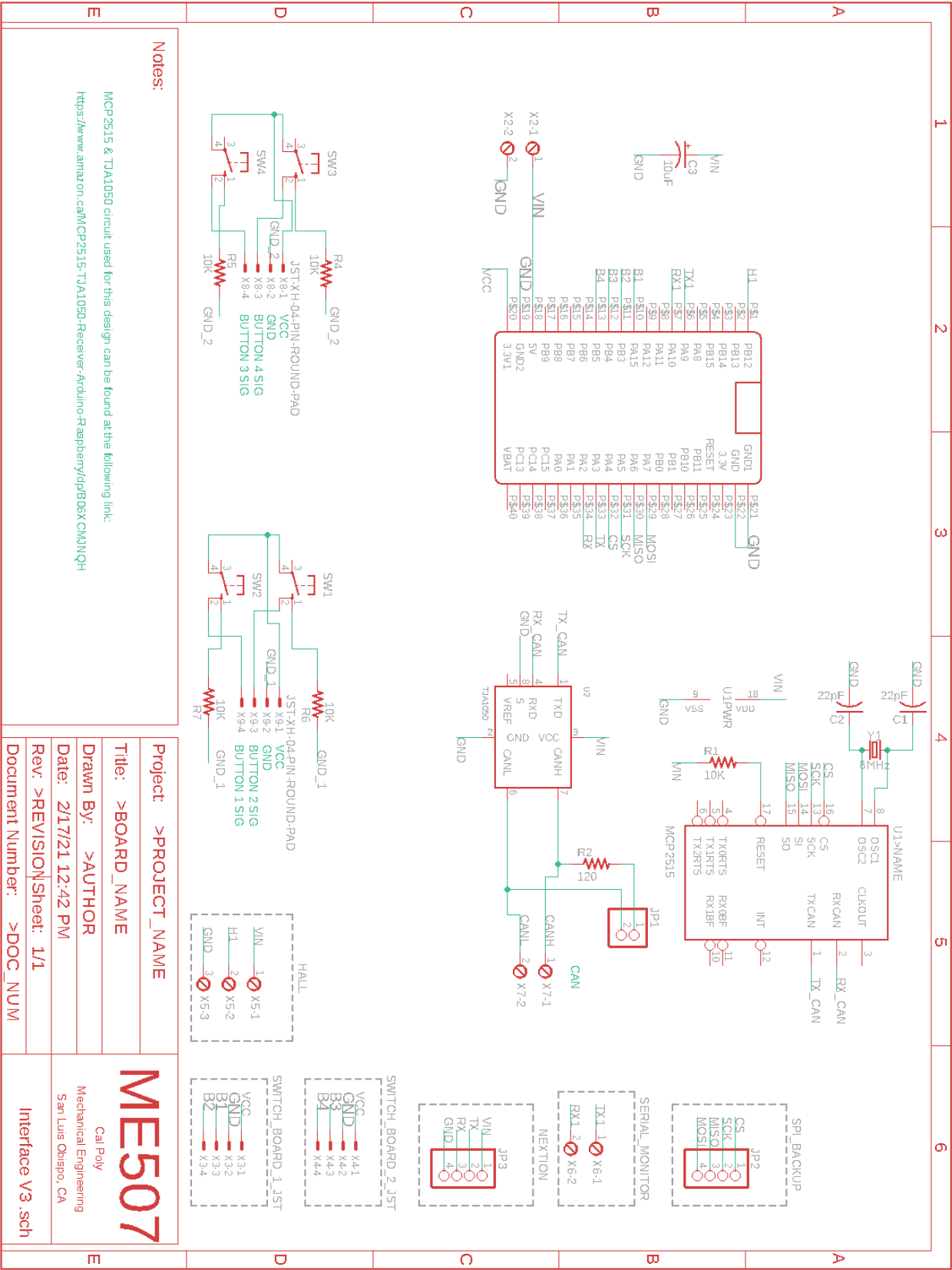
is pressed and that drive Set the drive mode
Raise display flag
if C is pressed and that Set the drive mode Raise display flag
if B is pressed and that Set the drive mode Raise display flag
if R is pressed and that Set the drive mode Raise display flag
if check button is
Change screen state variable Flag to initialise screen
if flow button is pressed... Change screen state variable Flag to initialize screen
if pressure button is
Change screen state variable Flag to initialize screen
if data button is pressed... Change screen state variable Flag to initialize screen
} }
// If the drive mode needs to be
// Clear the drive mode by writing a // Write a red circle to the display // Lower flag
// Initialize screen // Fill white
// Display home button // Set text size
// Set cursor
// Print large text
// Draw title border
// Flag that initialization is done
// If home button is pressed...
// Change screen state variable // Flag to initialize screen
// Function, check errors screen of display task void checkScreen(int x, int y) {
if (!loading) {
tft.fillScreen(ILI9341_WHITE); Home.displayButton(5,204,60,30,"Home",ILI9341_CYAN,1,-13,-3); tft.setTextSize(2);
tft.setCursor(0,10);
tft.print(" MANAGE ERRORS"); tft.drawFastHLine(0,25,320,25);
loading = 1;
}
if (Home.isPressed(x,y)) {
screen = 0; loading = 0;
} }
// Function, display flow rates screen of display task void flowScreen(int x, int y) {
if (!loading) {
tft.fillScreen(ILI9341_WHITE); Home.displayButton(5,204,60,30,"Home",ILI9341_CYAN,1,-13,-3); tft.setTextSize(2);
tft.setCursor(0,10);
tft.print(" FLOWRATE MONITORING"); tft.drawFastHLine(0,25,320,25);
loading = 1;
}
if (Home.isPressed(x,y)) {
screen = 0;
loading = 0; }
}
void pressureScreen(int x, int y) {
if (!loading) {
tft.fillScreen(ILI9341_WHITE); Home.displayButton(5,204,60,30,"Home",ILI9341_CYAN,1,-13,-3); tft.setTextSize(2);
tft.setCursor(0,10);
tft.print(" PRESSURE MONITORING"); tft.drawFastHLine(0,25,320,25);
loading = 1;
}
if (Home.isPressed(x,y)) {
screen = 0;
loading = 0; }
}
void dataScreen(int x, int y) {
if (!loading) {
tft.fillScreen(ILI9341_WHITE); Home.displayButton(5,204,60,30,"Home",ILI9341_CYAN,1,-13,-3); tft.setTextSize(2);
tft.setCursor(0,10);
tft.print(" MANAGE DATA LOGGING"); tft.drawFastHLine(0,25,320,25);
loading = 1;
}
if (Home.isPressed(x,y)) {
screen = 0;
loading = 0; }
}
// Function, updates drive mode indicator on display // Takes two parameters: an action, and a drive-mode // For action: 1 = clear, 2 = new
void displayDriveMode(int action,int driveMode) {
uint16_t color; if (action == 1) {
color = ILI9341_WHITE;
}
else if (action == 2) {
color = ILI9341_RED;
}
if (driveMode == 1) { location with appropriate color
tft.fillCircle(300,60,10,color); }
else if (driveMode == 2) { tft.fillCircle(300,110,10,color);
}
else if (driveMode == 3) {
tft.fillCircle(300,160,10,color); }
else if (driveMode == 4) { tft.fillCircle(300,210,10,color);
} }
// Initialize screen // Fill white
// Display home button // Set text size
// Set cursor
// Print large text
// Set text size // Set cursor
// Print large text
// Set text size // Set cursor
// Print large text
// Define 16 bits to store color // If action = 1, need to clear // So set color to white
// Else if action = 2, need to write // So set color to red
// Draw circle at drive mode

```

Appendix H Mechatronics Bill of Materials

Component Name & Description	Qty	Price/Item	Subtotal
C0805 Surface Mount Capacitor 22pF	2	\$ 0.18	\$ 0.36
R0805 Surface Mount Resistor 10K	5	\$ 0.10	\$ 0.50
R0805 Surface Mount Resistor 120	1	\$ 0.10	\$ 0.10
Tantalum Capacitor 10uF	1	\$ 0.47	\$ 0.47
8 MHz Crystal (22pF load)	1	\$ 0.18	\$ 0.18
Momentary Push Button 6mm	4	\$ 0.18	\$ 0.72
JST-XH 2.54mm Pitch Connector	4	\$ 0.21	\$ 0.84
2.54mm Pin Headers 4x	2	\$ 0.44	\$ 0.88
2.54mm Pin Headers 2x	1	\$ 0.13	\$ 0.13
3.81mm Screw Pin Terminal 2x	3	\$ 1.28	\$ 3.84
3.81mm Screw Pin Terminal 3x	1	\$ 1.94	\$ 1.94
2.54mm Pin Header Jumper	1	\$ 0.10	\$ 0.10
TJA1050 CAN Transceiver SOIC-8	1	\$ 0.99	\$ 0.99
MCP2515 CAN Controller	1	\$ 1.78	\$ 1.78
STM32 Development Board	1	\$ 6.85	\$ 6.85
Total Cost of PCB Manufacturing	1	\$ 32.40	\$ 32.40
Nextion Display	1	\$ 28.99	\$ 28.99
Total			\$ 81.07

Appendix I Circuit Board Schematic



[illegible]

Appendix K Ergonomic Considerations

In order to determine the proper seat angle on the vehicle, Soulenoid Cycle gathered via Zoom to test different incline angles with a reclining chair. The materials used were a black reclining chair, and a large fan, pictured below in Figure J1.



Figure K1. Materials used for ergonomic analysis.

The large fan was positioned in front of the chair and switched on at its highest setting. A teammate sat in the chair and experimented with different incline angles, observing the effects of the fan. They observed that when completely reclined, they barely felt the wind produced by the fan, although they had to strain in order to look straight ahead. On a recumbent tricycle, the rider still needs to be able to look forward to the road to safely drive the vehicle; the seat angle should not strain the rider. The teammate adjusted their seat until they observed a balance of comfort and wind resistance. After finding a comfortable position, the teammate stood up from the chair, leaving it in its reclined position. A profile picture of the chair was taken and imported into Fusion 360, where it was scaled and dimensioned to find the seat angle. The dimensions of the chair are shown below in Figure J2.



Figure K2. Comfortable recline position after ergonomic testing. J-1

To find the seat angle, both the seat bottom and seat back were measured on the actual recliner chair. Those dimensions are 22 inches and 27 inches, respectively. In Fusion 360, a new sketch was created as an overlay on the profile picture, and two lines of lengths 22 and 27 inches were drawn. The profile picture was scaled until the chair matched the sketched dimensions, and then the seat angle was measured relative to the horizontal. The seat angle was measured to be 42.1 degrees, which is consistent with Ricky Horwitz's guidance for recumbent seat inclines. For simplicity, Soulenoid Cycle rounded to 40 degrees as a selected seat incline. Although the leg angle was measured to be 9.9 degrees, Soulenoid Cycle chose a leg angle of 15 degrees to lower the center of gravity of the vehicle. In other words, a steeper leg incline allows the seat to rest closer to the ground, below the front two wheels. A leg angle of 15 degrees is also consistent with Horwitz's recommended range of 10-20 degrees.

After determining an appropriate seat angle, the team proceeded to design a frame on paper based solely on the constraint of the seat angle. The sketch, shown below in Figure J3, is drawn at a 1:13 scale on 8.5x11 inch printer paper. The 27 and 22 inch dimensions of the recliner, a seat incline of 40 degrees, and a leg incline of 15 degrees, were drawn at 1:13 scale on the paper. Next, the chosen wheelbase of 64 inches governed the rest of the dimensions. The sketch in Figure J3 became the basis of Soulenoid Cycle's final frame design.

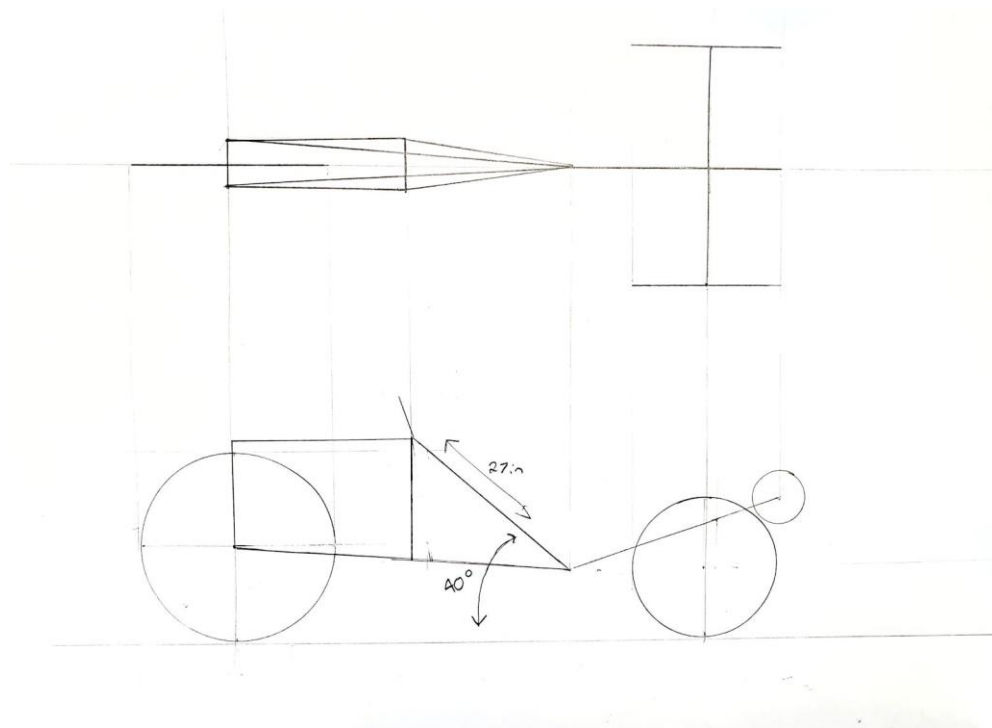
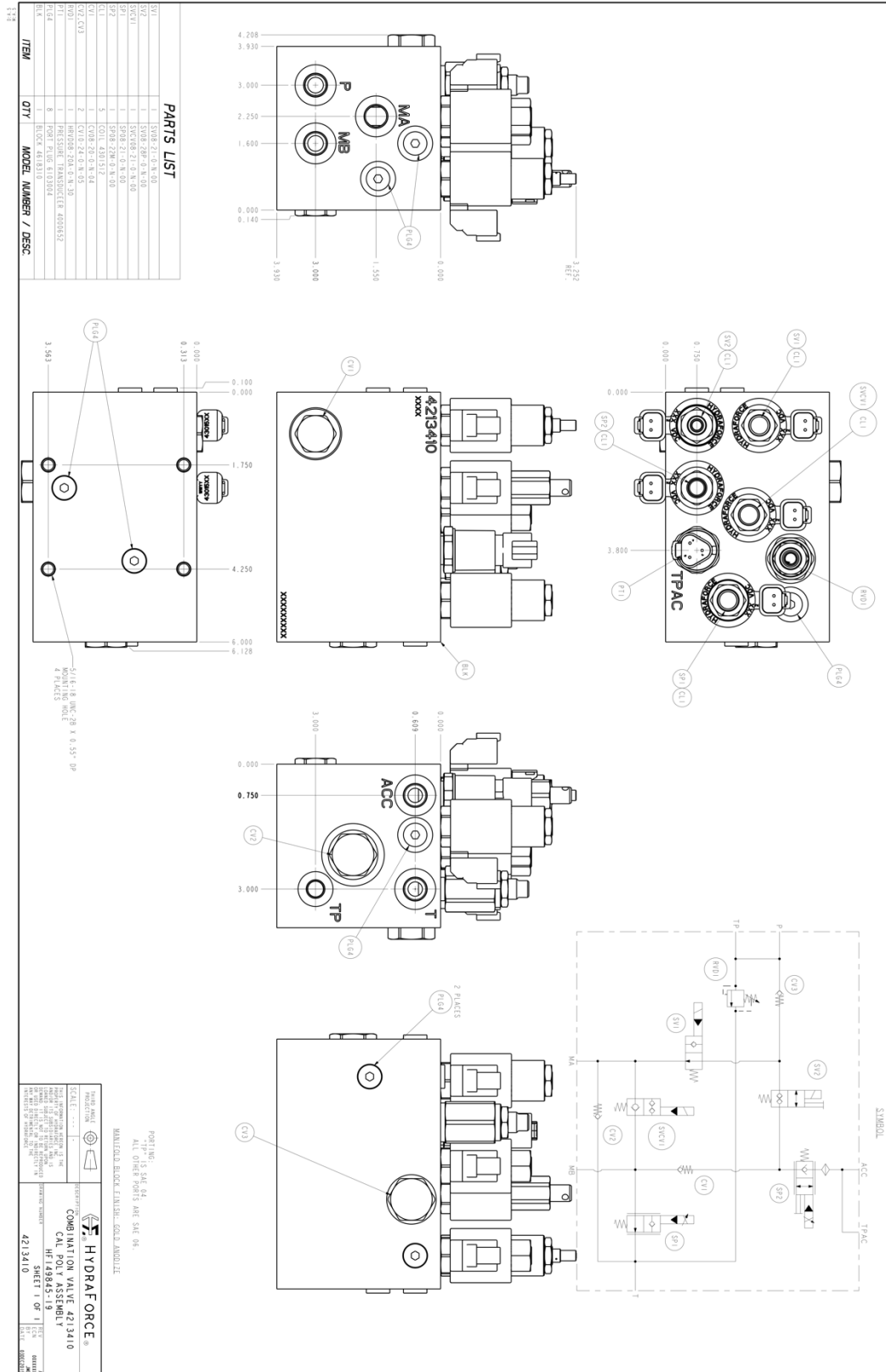
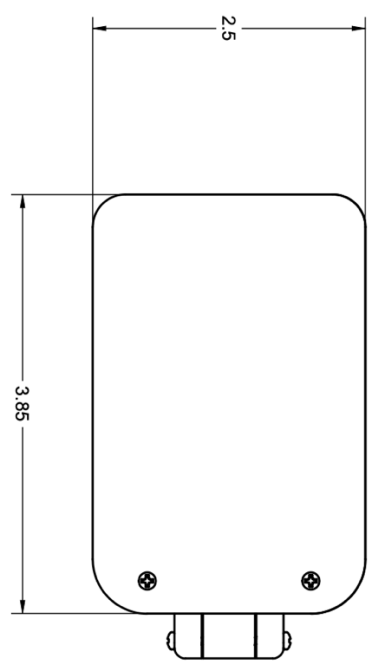
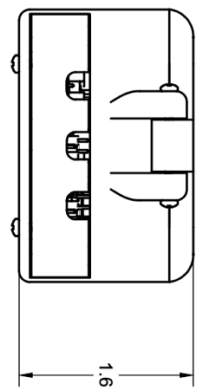
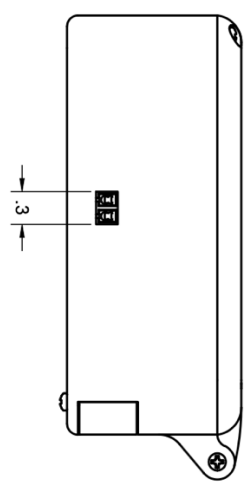
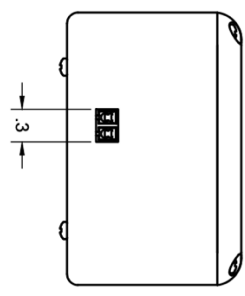
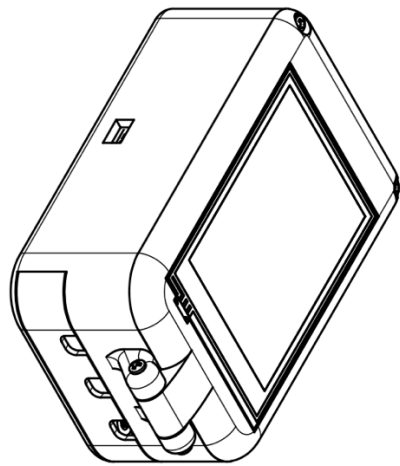
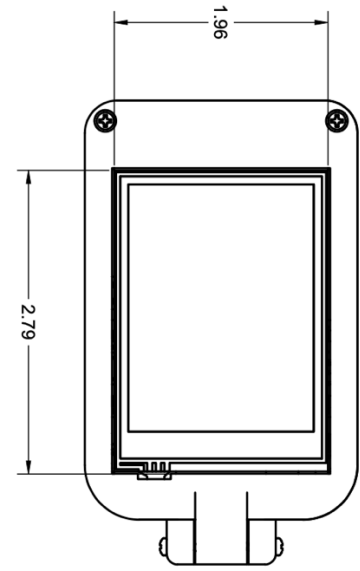


Figure K3. Frame concept based on results of ergonomic analysis.

Although not completely precise, this simple test allowed Soulenoid Cycle to investigate the comfort of different seat angles, and verify that their chosen angle of 40 degrees would be both comfortable and practical.

Appendix L Engineering Drawings





Notes:

- All dimensions in inches.
- Drawings for reference only, see 3D models to export for 3D printing.

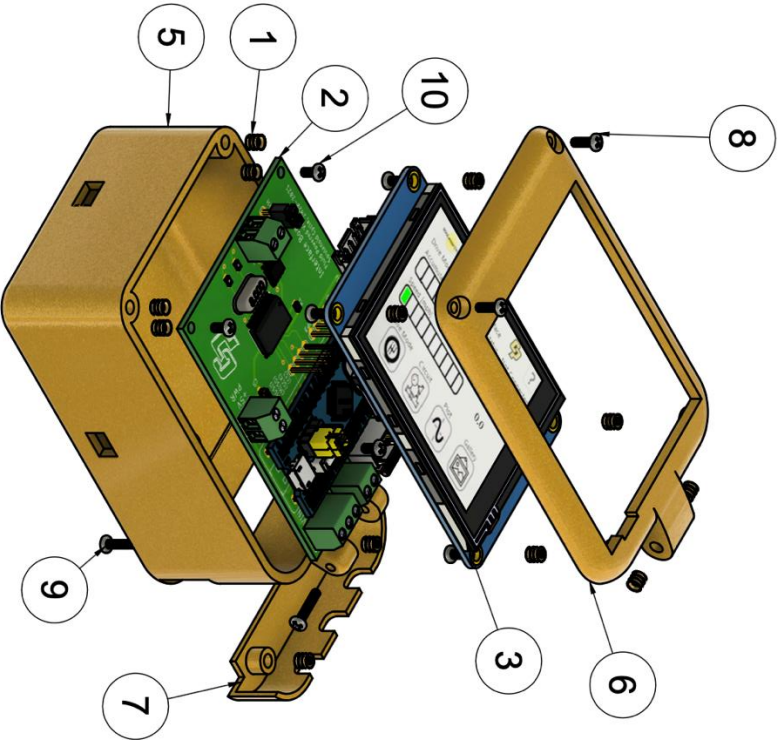
PROJECT		Senior Project	
TITLE		Solenoid Cycle Mechanics CAN Interface	
APPROVED	SIZE	CODE	DWG NO
CHECKED	B		
DRAWN	Jordan Kochavi	4/28/21	SCALE 1:1
WEIGHT		SHEET 1/2	
REV			

10	7	92000A011	92000A011 V1	
9	4	92000A017	92000A017 V1	
8	2	92000A013	92000A013 V1	
7	1	PORT CAP	PORT CAP	
6	1		TOP	
5	1		BOTTOM	
4	1	DS1071-1X4	DS1071-1X4 V2	
3	1	NEXTION NX3224T028	NEXTION NX3224T028 V4	
2	1	FINAL CIRCUIT BOARD	FINAL CIRCUIT BOARD V41	
1	13		M2 THREADED INSERT	HEAT-SET THREADED INSERT FOR 3D PRINTED PARTS.
ITEM	QTY	PART NUMBER	PART NAME	DESCRIPTION

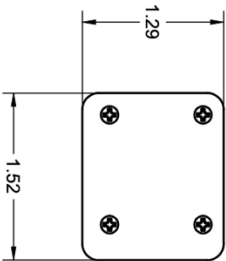
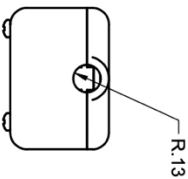
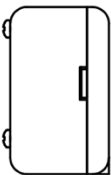
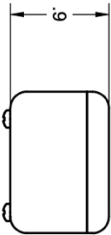
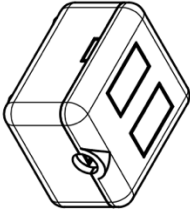
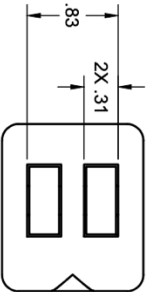
PARTS LIST

Notes:

- Ignore Item 4 (it is specific to the circuit board assembly).
- The 3D models of the screws used in this assembly were downloaded from McMaster, although it is recommended to purchase an assorted M2 screw kit from Amazon or Home Depot.
- Parts were 3D printed on a Bibo 2 Touch with 20% infill, 0.2 mm layer height, 50 mm/s.



PROJECT			
Senior Project			
TITLE			
Soulenoid Cycle Mechatronics CAN Interface			
APPROVED	SIZE	CODE	DWG NO
CHECKED	B		
DRAWN	Jordan Kochavi	4/28/21	SCALE 1:1
		WEIGHT	SHEET 2/2
			REV

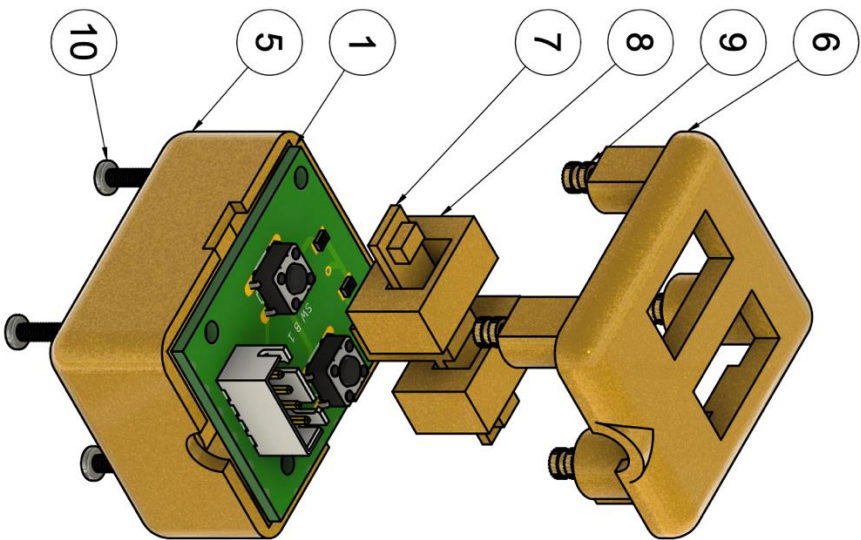


Notes:

- All dimensions in inches.
- Drawings for reference only, see 3D models to export for 3D printing.

PROJECT		Senior Project	
TITLE		Handlebar Buttons	
APPROVED	SIZE	CODE	DWG NO
CHECKED	B		
DRAWN	Jordan Kochavi	5/3/21	SCALE 1:1
		WEIGHT	SHEET 1/2
			REV

- Notes:
- Ignore items 2, 3, 4, as they pertain to the printed circuit board.
 - Recommended print settings are 20% infill, 50 mm/s, 0.2mm layer height.



10	4	92000A013	STEEL	
9	4	M2 THREADED INSERT	STEEL	
8	2	PRESSER	STEEL	
7	1	SANDWICH	STEEL	
6	1	TOP	STEEL	
5	1	BOTTOM	STEEL	
4	2	PUSH TACTILE BUTTON SPST-NO 6X6MM L=5MM OMRON B3F-1020	GENERISCH	
3	1	B4B-XH-A	STEEL	
2	2	R0805	STEEL	
1	1	BUTTON CIRCUIT BOARD	STEEL	
ITEM	QTY	PART NUMBER	DESCRIPTION	MATERIAL

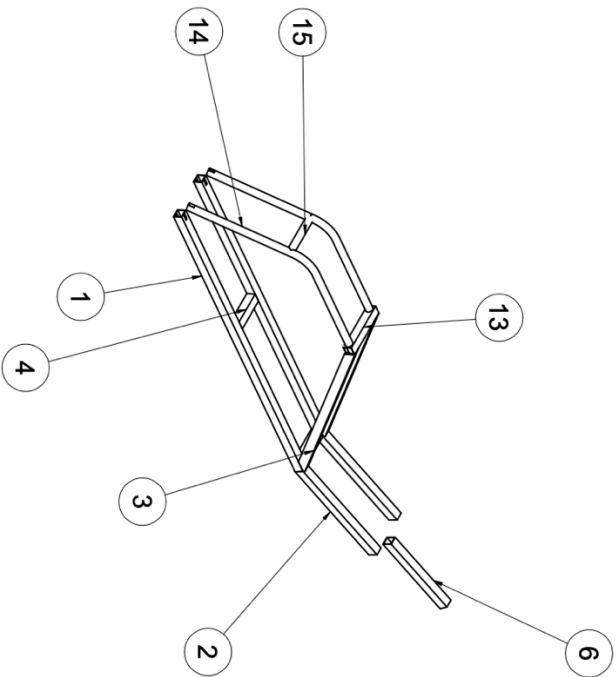
PARTS LIST

PROJECT
Senior Project
TITLE
Handlebar Buttons

APPROVED	SIZE	CODE	DWG NO	REV	
CHECKED	B				
DRAWN	Jordan Koochavi	5/3/21	SCALE 2:1	WEIGHT	SHEET 2/2

NOTES:

- FOR ALL SHEETS:
- UNITS IN INCHES
- TOLERANCES:
- LINEAR ± 0.1
- ANGLES $\pm 1^\circ$



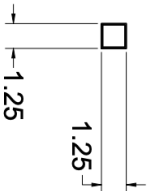
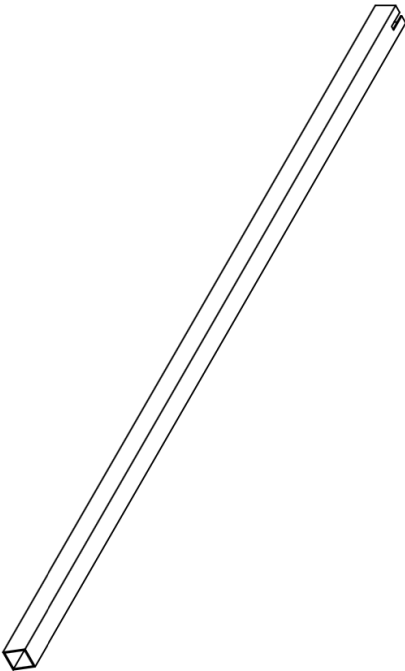
15	1	P6	ROUND TUBING	STEEL ASTM A572
14	2	P8	ROUND TUBING	STEEL ASTM A572
13	1	P5	ROUND/SQUAR E INTERSECT	STEEL ASTM A572
6	1	P7		STEEL ASTM A572
4	2	P4	SQUARE TUBING	STEEL ASTM A572
3	2	P3	SQUARE TUBING	STEEL ASTM A572
2	2	P2	SQUARE TUBING	STEEL ASTM A572
1	2	P1	SQUARE TUBING	STEEL ASTM A572
ITEM	QTY	PART NUMBER	DESCRIPTION	MATERIAL

PARTS LIST

PROJECT				
Soulenoid Cycle FPV				
TITLE				
Frame Assembly				
APPROVED	SIZE	CODE	DWG NO	REV
CHECKED	C		1.1	1
DRAWN	Jordan Kochavi	10/20/20	SCALE 1:5	WEIGHT
				SHEET 1/9

NOTES:

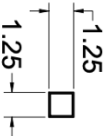
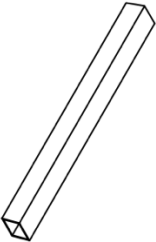
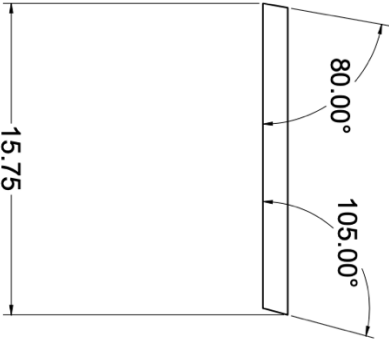
- ALL DIMENSIONS IN INCHES
- MILL SLOT
- MAKE ANGLED CUTS ON CHOP SAW



PROJECT		Soulenoid Cycle FPV Frame	
TITLE		P1 Detailed Drawing	
Angled Cuts			
APPROVED	SIZE	CODE	REV
CHECKED	C	1.2	1
DRAWN	Jordan Kodhani	10/20/20	SCALE 1:4
		WEIGHT	SHEET 2/9

NOTES:

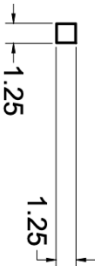
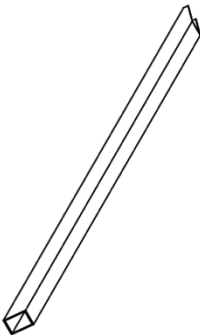
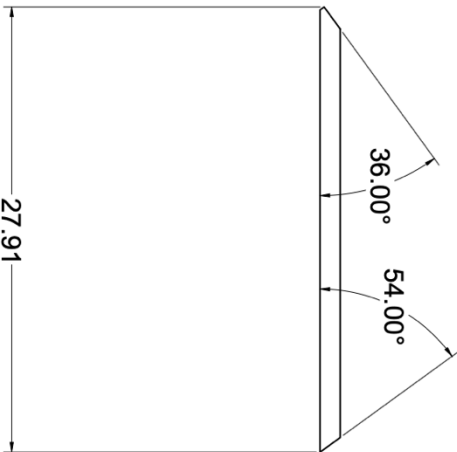
- ALL DIMENSIONS IN INCHES
- MAKE ANGLED CUTS ON CHOP SAW



PROJECT		Soulenoid Cycle FPV Frame	
TITLE		P2 Detailed Drawing	
		Angled Cuts	
APPROVED	SIZE	CODE	DWG NO
CHECKED	C	1.3	
DRAWN	Jordan Kochavi	10/20/20	SCALE 1/4
		WEIGHT	SHEET 3/9
			REV
			1

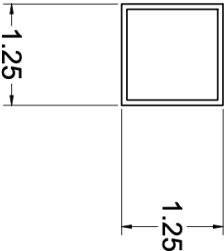
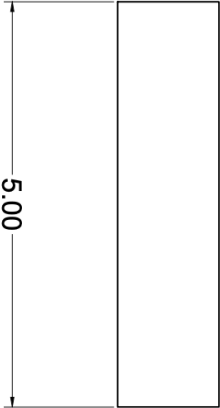
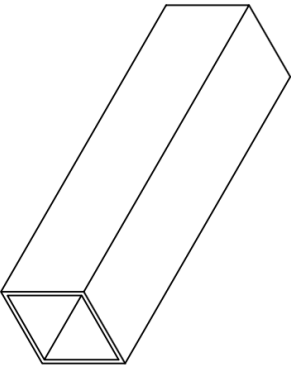
NOTES:

- ALL DIMENSIONS IN INCHES
- MAKE ANGLED CUTS ON CHOP SAW



PROJECT		Solenoid Cycle FPV Frame	
TITLE		P3 Detailed Drawing	
Angled Cuts			
APPROVED	SIZE	CODE	REV
CHECKED	C	1.4	1
DRAWN	Jordan Koshavi	10/20/20	SHEET 4/9

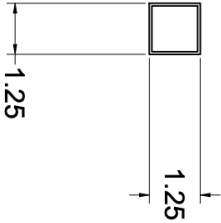
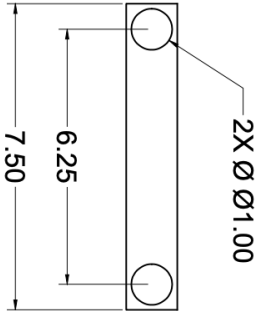
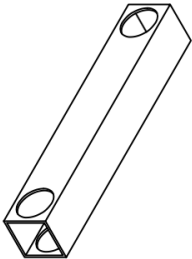
- NOTES:
- ALL DIMENSIONS IN INCHES
 - MAKE ALL CUTS ON CHOP SAW



PROJECT		Soulenoid Cycle FPV Frame	
TITLE		P4 Detailed Drawing	
Angled Cuts			
APPROVED	SIZE	CODE	REV
CHECKED	C	DWG NO	1
DRAWN	Jordan Kochani	10/20/20	SCALE 1:1
		WEIGHT	SHEET 5/9

NOTES:

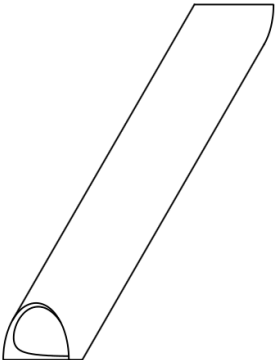
- ALL DIMENSIONS IN INCHES
- MAKE ALL CUTS ON CHOP SAW



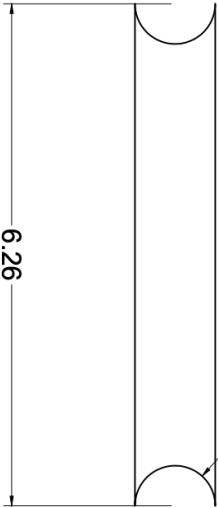
PROJECT		Soulenoid Cycle FPV Frame	
TITLE		P5 Detailed Drawing	
Angled Cuts			
APPROVED	SIZE	CODE	DWG NO
CHECKED	C		1.6
DRAWN	Jordan Kodhani	10/20/20	SCALE 1:2
		WEIGHT	SHEET 6/9
			REV
			1

NOTES:

- ALL DIMENSIONS IN INCHES
- MAKE ALL CUTS ON CHOP SAW



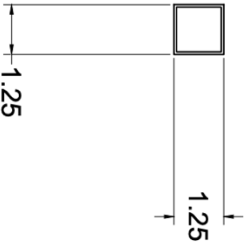
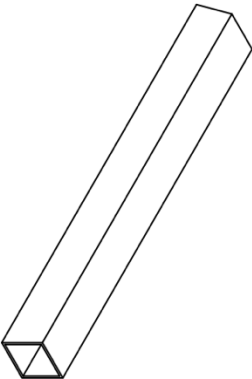
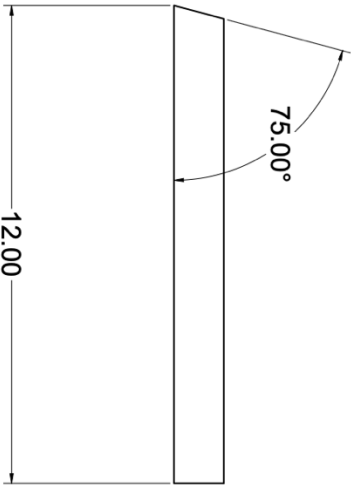
2X Ø1.00



Ø1.00

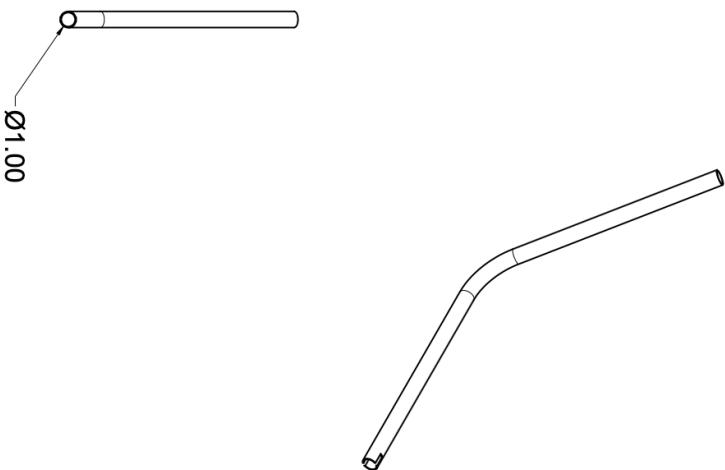
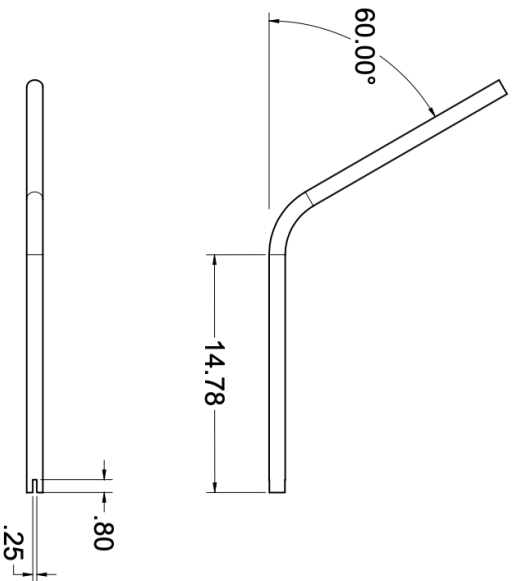
				PROJECT
				Soulenoid Cycle FPV Frame
				TITLE
				P6 Detailed Drawing
				Angled Cuts
APPROVED	SIZE	CODE	DWG NO	REV
CHECKED	C		1.7	1
DRAWN	Jordan Kochavi	10/20/20	SCALE 1:1	WEIGHT
				SHEET 7/9

- NOTES:
- ALL DIMENSIONS IN INCHES
 - MAKE ALL CUTS ON CHOP SAW

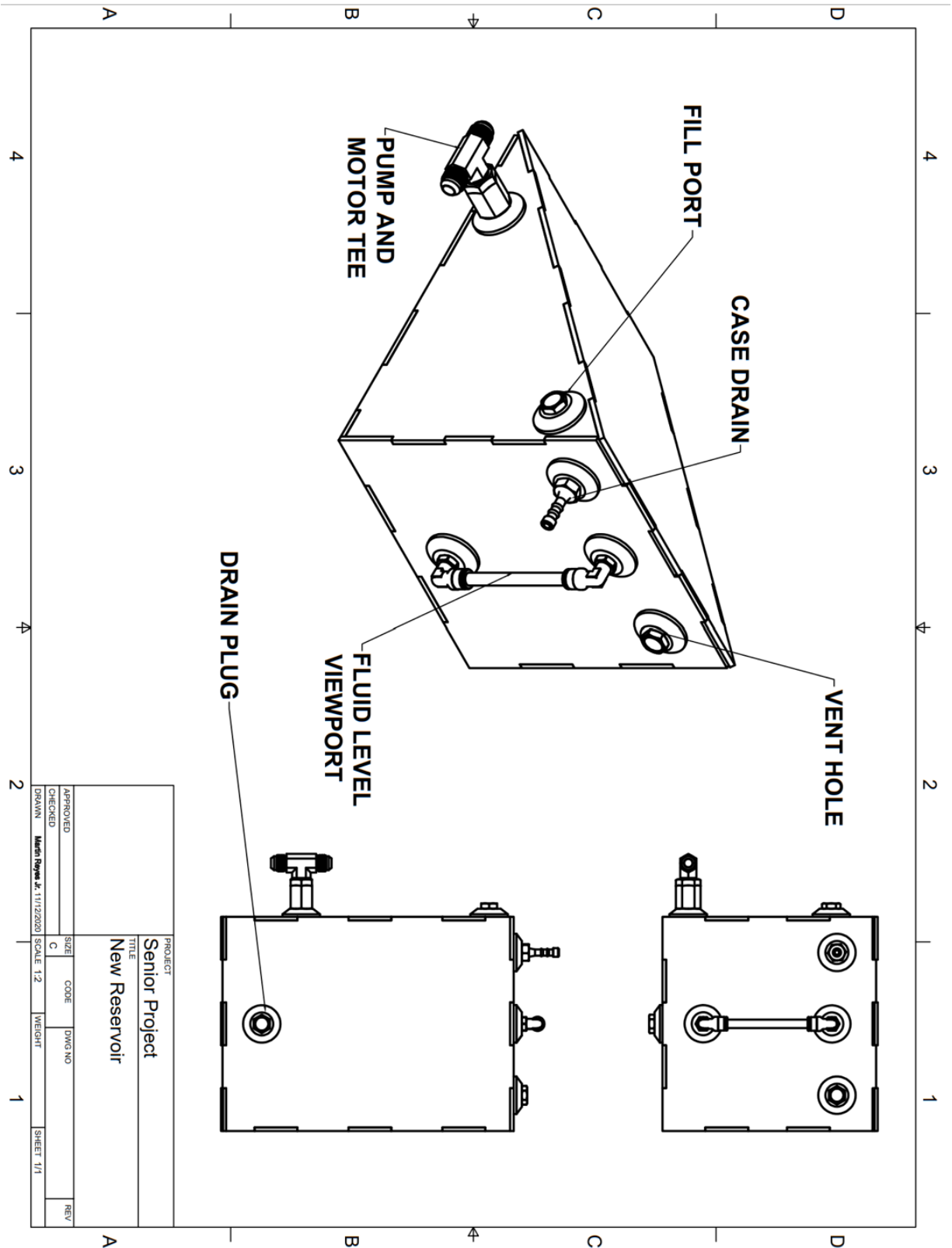


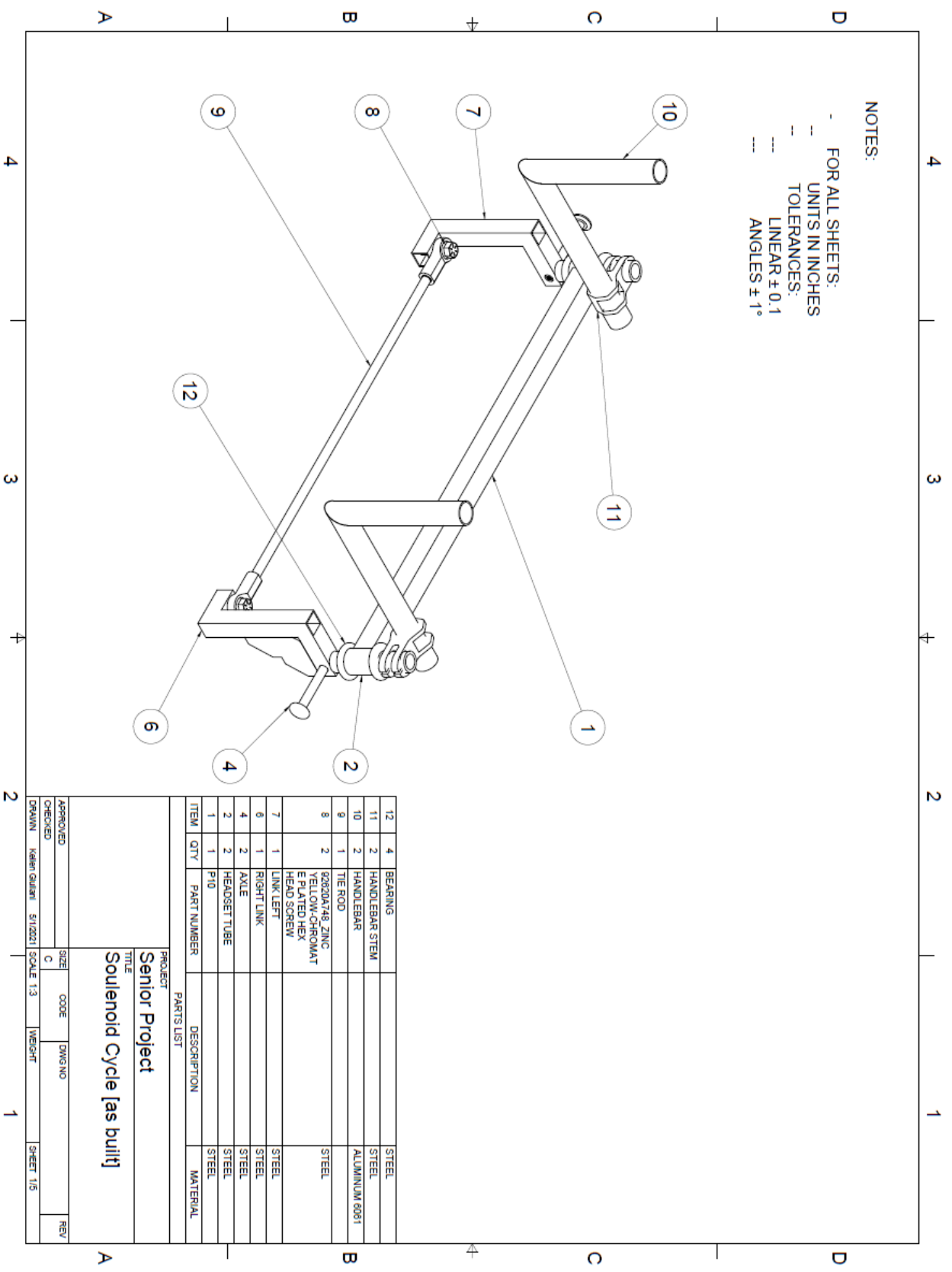
PROJECT		Soulenoid Cycle FPV Frame	
TITLE		P7 Detailed Drawing	
Angled Cuts			
APPROVED	SIZE	CODE	DWG NO
CHECKED	C		1.8
DRAWN	Jordan Kochavi	10/20/20	SCALE 1:2
		WEIGHT	SHEET 8/9
		REV	1

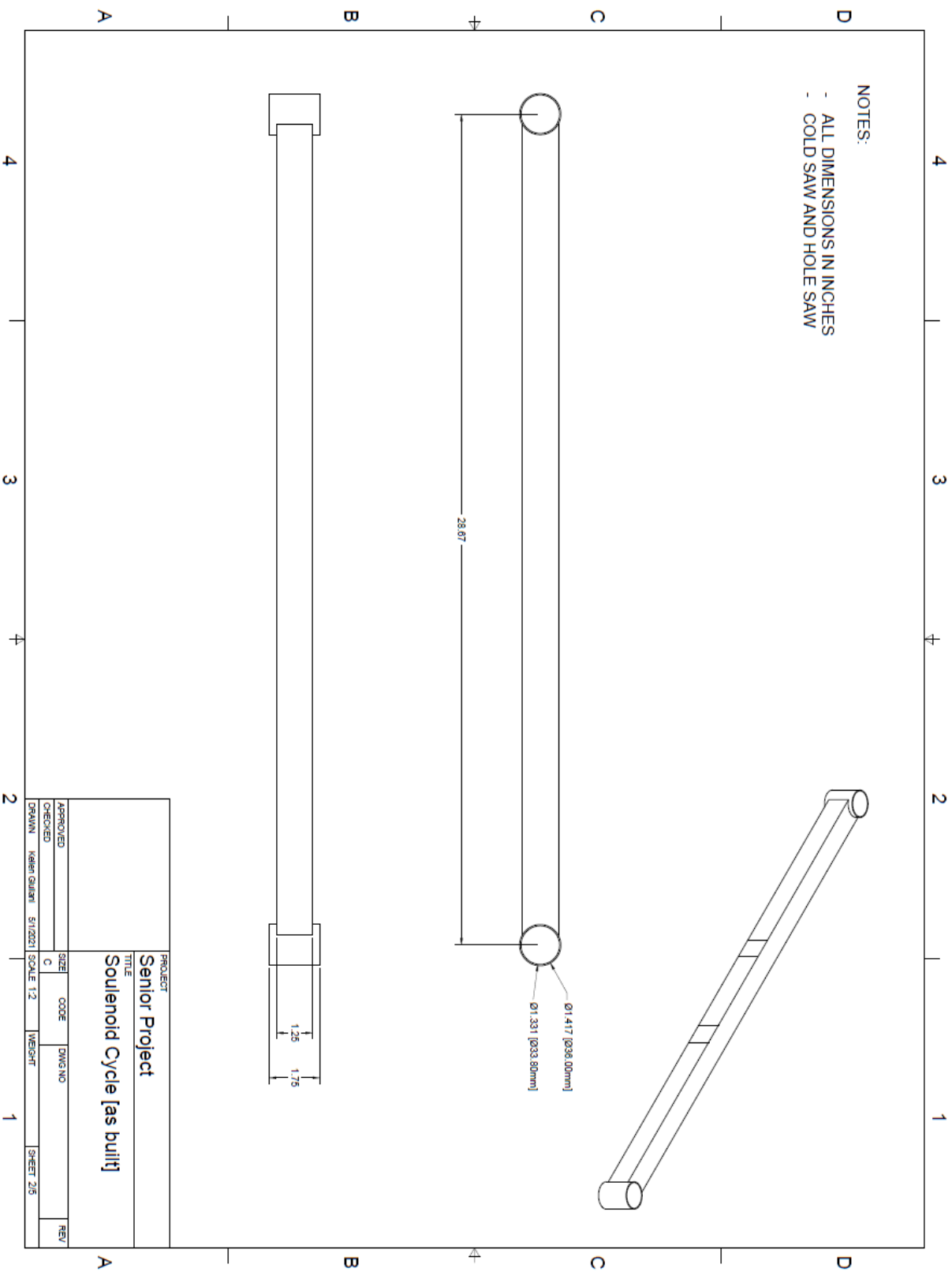
- NOTES:
- ALL DIMENSIONS IN INCHES
 - MAKE ALL CUTS ON COLD SAW
 - USE TUBE BENDER, 4 INCH RADIUS
 - USE ANGLE GRINDER FOR SLOT
 - TOTAL TUBE LENGTH 32.25 IN

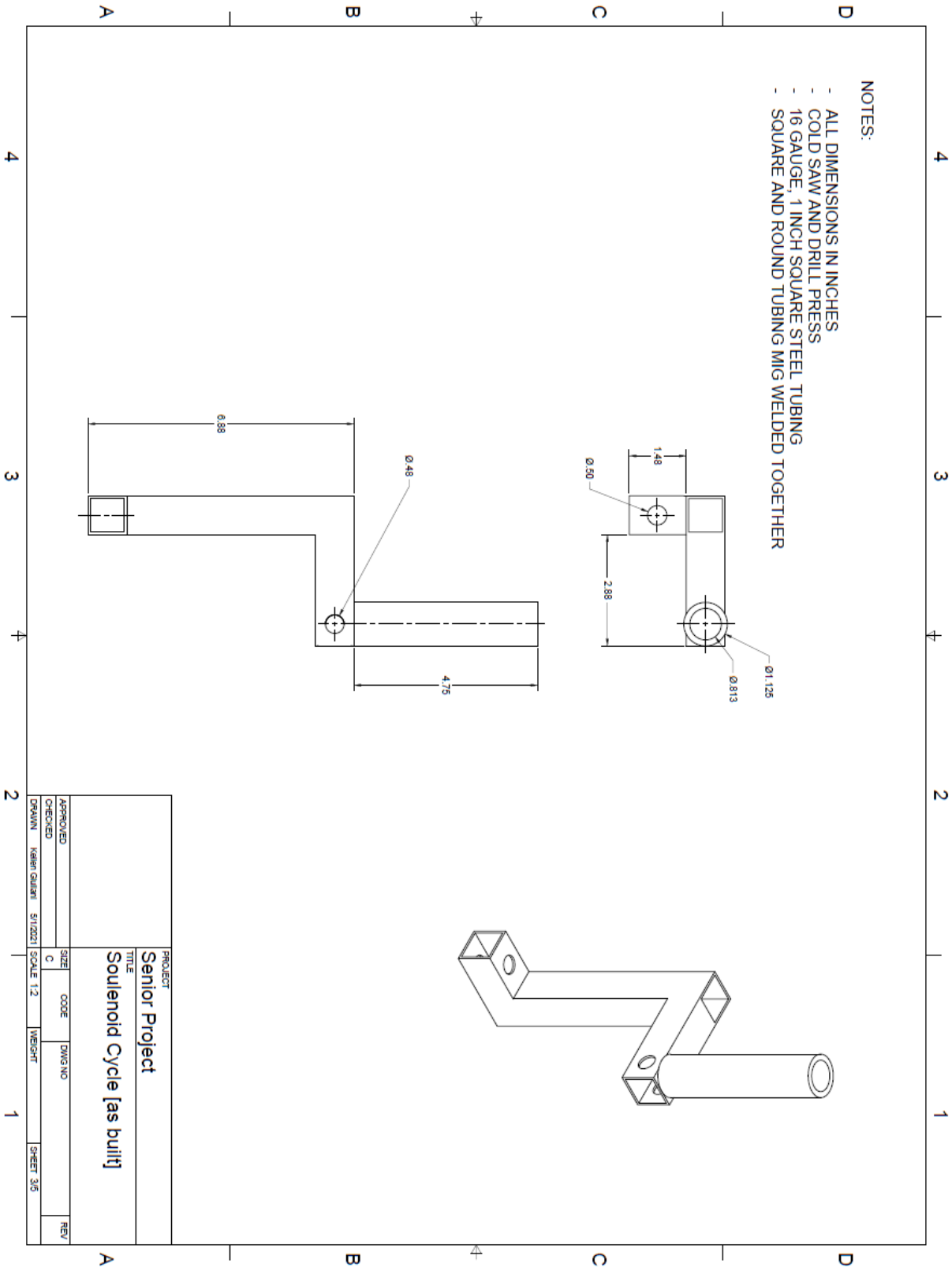


PROJECT		Solenoid Cycle FPV Frame	
TITLE		P8 Detailed Drawing	
Angled Cuts			
APPROVED	SIZE	CODE	REV
CHECKED	C	DWG NO	1
DRAWN	Jordan Kochavi	10/20/20	SCALE 1:5
		WEIGHT	SHEET 9/9

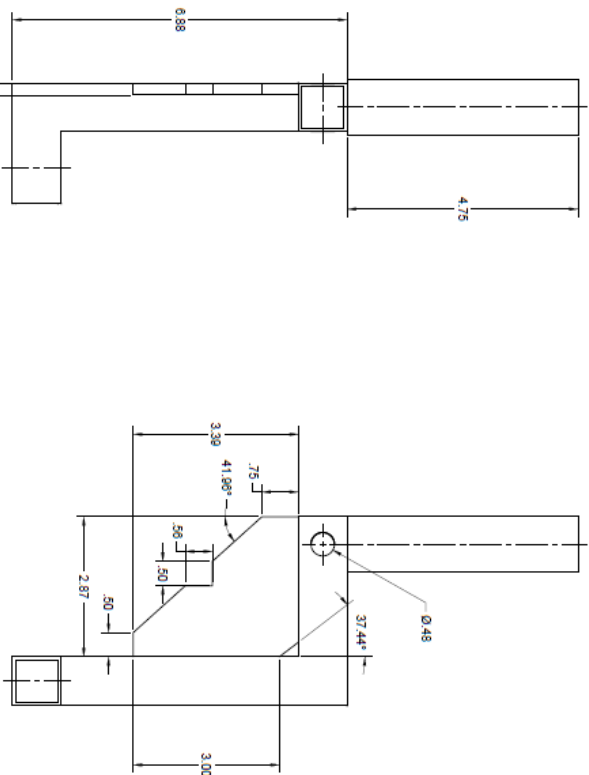
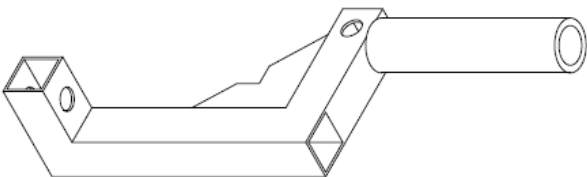
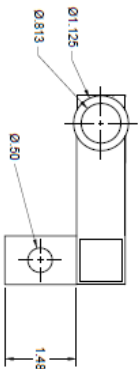






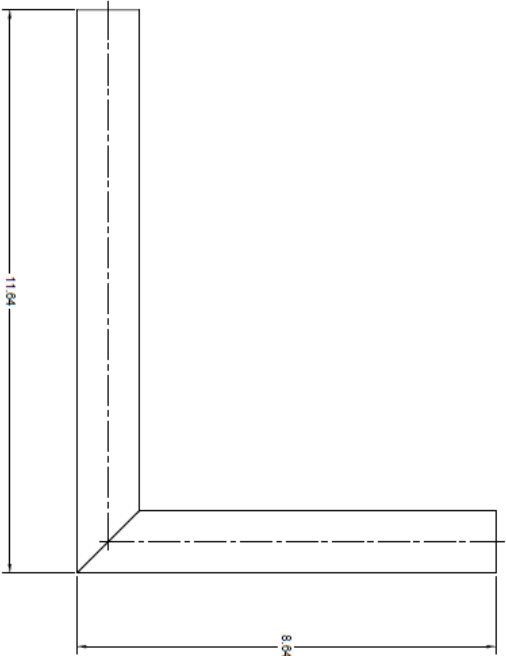
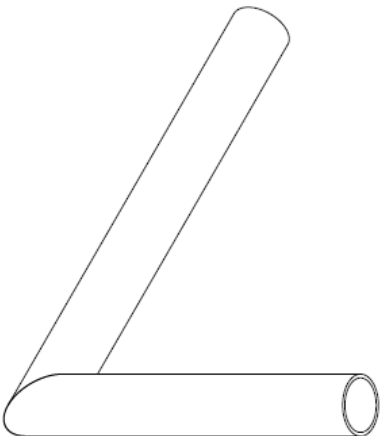
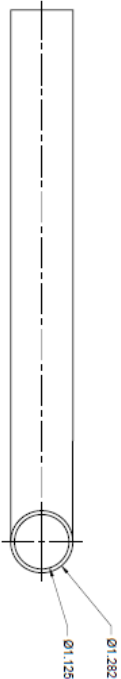


- NOTES:
- ALL DIMENSIONS IN INCHES
 - COLD SAW AND DRILL PRESS
 - 16 GAUGE, 1 INCH SQUARE STEEL TUBING
 - SQUARE AND ROUND TUBING MIG WELDED TOGETHER
 - TRIANGULAR PIECE CUT FROM $\frac{1}{4}$ INCH STEEL PLATE



PROJECT		Senior Project	
TITLE		Solenoid Cycle [as built]	
APPROVED	SIZE	CODE	DWG NO
CHECKED	C		
DRAWN	KEVIN GILMAN	5/1/2021	SCALE 1:2
WEIGHT		SHEET 4/5	

- NOTES:
- ALL DIMENSIONS IN INCHES
 - CUT TUBE ON BAND SAW BAND SAW AT 45°
 - TIG WELDED
 - 6061 T6 ALUMINUM TUBING



PROJECT		Senior Project	
TITLE		Solenoid Cycle [as built]	
APPROVED	SIZE	CODE	DWG NO
CHECKED	C		
DRAWN	KEVIN GILBERT	5/1/2021	SCALE 1:1.5
WEIGHT		SHEET 5/5	

Appendix M FMEA Spreadsheet

System / Function	Potential Failure Mode	Potential Effects of the Failure Mode	Severity	Potential Causes of the Failure Mode	Current Preventative Activities	Occurrence	Current Detection Activities	Detection	RPN	Recommended Action(s)	Responsibility & Target Completion Date
Frame / Stability	Bike, components, or rider tip or fall while riding	a) Injure rider b) Break or damage components	10	1) Steering difficulties 2) Rider cannot control the drive mode 3) Unbalanced weight distribution of rider/components	1) Iterate on steering angles 2) Default coast mode 3) Model to confirm overall weight balance	3	Testing done by rider	3	90	Add rider safety instructions	Cayla Q. 2/15
Hydraulics / Fluid Movement	Fluid losses or internal leakages	a) Safety concerns for rider. b) Poor performance in challenges	5	1) Too many fittings 2) Broken connections 3) Line length or surface roughness too large	1) Fluid analysis with hand calculations and modeling 2) Performance testing 3) Safety checks before every ride	8	Testing comparison to calculations and models & component checks	4	160	Create hydraulic safety checklist for riders to complete prior to each ride	Martin R. 2/15
Mechatronics / Fluid Coordination	No response or late response from electronics system	a) Unable to move or control bike b) Cannot use fluid power system c) Unable to switch drive modes d) Increase in racing time	5	1) Damage to electronic circuit 2) Latency issues 3) Sensors unresponsive	1) Electronic components either shielded beneath seat or in a protective enclosure 2) PCB design analysis	2	Mechatronics circuit design to be checked and tested	2	20	Test an electronic "malfunction" to ensure that coast mode is activated so that the rider is in control	Kellen G. & Jordan K. 2/25

Appendix N Feedback From Competition Judges

NFPA Fluid Power Vehicle Challenge SCORING RUBRIC

Team: Cal- Poly

MIDWAY REVIEW
Design objectives are clearly stated and appropriate to the competition.
Vehicle design clearly supports the design objectives and is of obvious quality.
Hydraulic and Pneumatic circuit designs are complete and reflects an understanding of fluid power components and systems.
Selection of hardware is complete and is appropriate to the design objectives.
Analyses have been performed and their results have been incorporated into vehicle and/or circuit designs.
Prototype vehicle assembly has begun.
Presentation is completed on time and demonstrates team synergy.

JUDGES COMMENTS:
<p>*Nice job to all of you with your presentation. Air tank to regulator to 3 way valve to cylinder. Mount the cylinder as close to the cylinder as possible to save air. HydraForce is a good choice for controls. Lots of great thinking and planning but remember to keep it simple when possible. *Wonderful initiative on the mechatronics side of the build. I am glad to see schools seeing the power of controls for this project. Industry is almost always paired with a controller in the end solution. Manual controls are going away more and more. Teams typically struggle with the controls side and end up with relays and buttons. Glad to see you are so far into the development. Please consider a way to release accumulator to tank without using the motor. This is a 'safety' setup in my opinion. You can get a push/pull poppet that when open will simply not let your accumulator hold energy and also allows you to release it should the need arise to de-energize the system immediately. *WOW... great work. If this was an investor pitch, I'd be sending money! Relatively small team, so they have been each doing a lot of work. Tubing is OD, not ID sizing. Pneumatic brake should be fail-safe. *1. Need to justify the 70% - 30% weight distribution between front and back wheels. 2. Pneumatic circuit needs to have a 3/2 valve in order for air to be exhausted. 3. Consider the spring return cylinder to be a spring advance type to require the braking function to be engaged without air pressure. This has advantages and disadvantages. State your reason for a decision. 4. All circuit designs are hard to read. Put only one circuit on a slide and use all of the space available. *Wow, what a nice start... keep up the great job guys! *One schematic per slide, tube is sized by OD not ID, use 3 way solenoid valve in pneumatic circuit, consider adding a pressure regulator in the pneumatic circuit.</p>

OVERALL SCORE:
3.97/5

NFPA Fluid Power Vehicle Challenge
SCORING RUBRIC

FINAL PRESENTATION
Summary of midway presentation is succinct and well organized.
Vehicle construction was completed on-time and performed mostly by the team members.
Vehicle testing was performed and improvements were made based on results.
Final vehicle brought to competition appears reliable, safe and of quality craftsmanship.
Lessons learned are clearly stated and appropriate to the design/build experience described.
Presentation is completed on time and demonstrates good team synergy.

JUDGES COMMENTS:
Construction was largely done by the machine but some assistance was required. Vehicle was well designed, but gear ratio did not allow for easy continuous use of the vehicle. Challenges reflected were not specific to the project, but were valuable lessons.* Nice job with the CAN system and great overall effort.* Having the schematic available on the display screen was a clever and practical solution- very nice!* Above and beyond with the control system and documentation. Well done!* Pneumatic system was not installed on the vehicle. Symbol of filter above the servo valve is not right. You cannot have flow through the filter in both directions.

OVERALL SCORE:
4.53/5

NFPA Fluid Power Vehicle Challenge
SCORING RUBRIC

VEHICLE INSPECTION	
Quality of vehicle design associated with reliability . The vehicle is robust and durable, but not too heavy.	
Quality of vehicle design associated with operator safety and comfort . The vehicle is ergonomic and easy to use.	
Quality of vehicle design associated with originality and uniqueness . The vehicle incorporates innovative concepts and could be marketable as a production vehicle.	
JUDGES COMMENTS:	
OVERALL SCORE:	
4.37/5	

NFPA Fluid Power Vehicle Challenge
SCORING RUBRIC

FPVC Mentorship
Introduction and initial discussion about vehicle design.
Discussion about component design.
Discussion about assembly and testing
Final discussion on adjustments

JUDGES COMMENTS:

OVERALL SCORE:
3/4

INDUSTRY PRESENTATIONS	
Danfoss	.5
Norgren	.5
Recruitment Mixer	2

OVERALL SCORE:
3/1

Appendix O Additional Pictures of Final Design





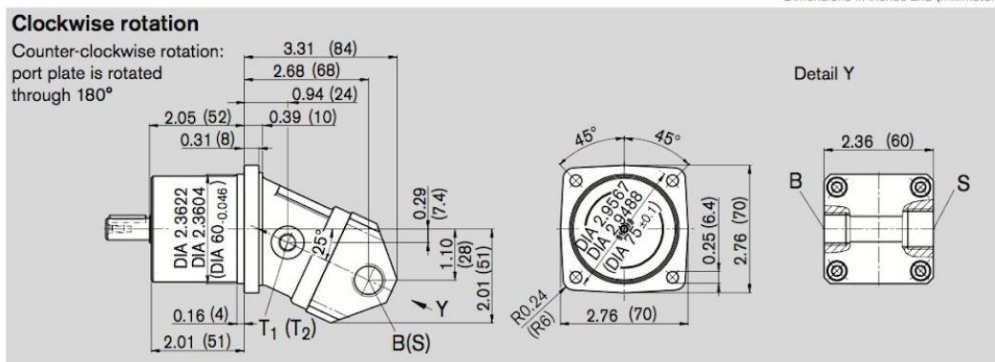
10/28 Bosch Rexroth Corp. AA2FO | RA 91 401/07.05

A2F	5	/	60		-		7
01	02		03	04		05	06

Service line ports		
06	Threaded ports A und B at side, metric	7

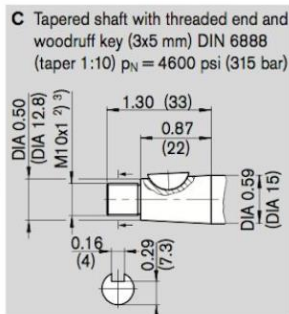
"with FKM-seals"

Please request a certified installation drawing
before finalizing your design.
Dimensions in inches and (millimeters)



B Parallel keyed shaft
DIN 6885 – A4x4x20 (mm)
 $p_N = 3000$ psi (210 bar)

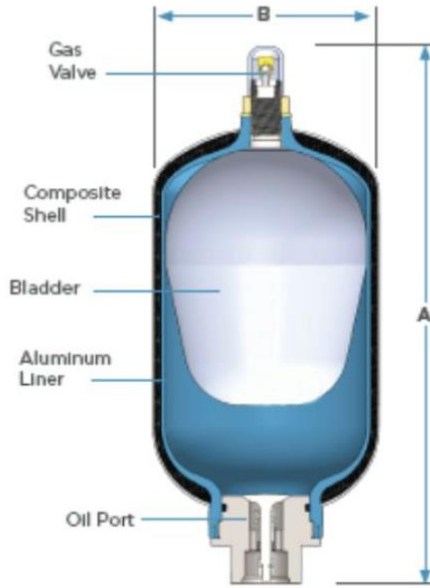
Technical drawing of a parallel keyed shaft (B) showing dimensions in inches and millimeters. The drawing includes a side view and a cross-sectional view. Key dimensions are: overall length 0.53 (13.5), diameter at the left end 0.473 (12.017), diameter at the keyway 0.472 (12.007), keyway width 0.13 (3.2), key height 0.095 (2.4), and diameter at the right end 0.59 (15.0). The keyway is labeled M4x0.71. The shaft is labeled DIN 6885 – A4x4x20 (mm) and $p_N = 3000$ psi (210 bar). The keyway is labeled R0.02 (R0.4).



B (A)	Service line port	M18x1.5; DIN 3852	100 lb-ft ³⁾ (140 Nm) 0.47 (12) deep
S	Suction port	M22x1.5; DIN 3852	155 lb-ft ³⁾ (210 Nm) 0.55 (14) deep
T ₁ , T ₂	Case drain ports	M10x1; DIN 3852	20 lb-ft ³⁾ (30 Nm) 0.31 (8) deep

¹⁾ centering bore according to DIN 332 (thread according to DIN 13), tightening torque see safety instructions
²⁾ thread according to DIN 3852, max. tightening torque: 20 lb-ft (30 Nm)
³⁾ please observe the general notes for the max.tightening torques on page 28

MICROMAX SERIES BLADDER ACCUMULATOR



Steelhead Composites Micromax series lightweight 3,000 psi (207 bar) to 5,000 psi (345 bar) bladder accumulators come in 1.0 gallon (4 liter) and 1.3 gallons (5 liter) capacities. These small and lightweight composite accumulators are a superior alternative to steel accumulators for any weight-restricted uses, mobile and industrial applications where access is remote, elevated or limited.

SPECIFICATIONS

- Type 3 Pressure Vessel
- Operating Pressure: 3000 psi (206 bar)-5,000 psi (345 bar)
- Minimum Burst Pressure: 3x Max Operating Pressure
- Fluid Connection: Industry standard port options available
- Operating Temperature Range: -4° to 160°F (-20° to 71° C)
- Liner: Impermeable 6061-T6 Aluminum
- Structural: Carbon fiber and epoxy composite
- Bladder: Buna-Nitrile (other materials available)

NOMINAL VOLUME GAL (L)	OPERATING PRESSURE PSI (BAR)**	DIMENSION A IN (MM)	DIMENSION B IN (MM)	WEIGHT LBS (KGS)
1 (4)	3,000 (206)	15.7 (399)	6.5 (165)	10.8 (5)
1.3 (5)	3,000 (206)	19.4 (493)	6.5 (165)	12.8 (6)
2.5 (10)	3,000 (206)	28.7 (729)	6.5 (165)	17.7 (8)

RUGGED 5,000 PSI MICROMAX				
NOMINAL VOLUME GAL (L)	OPERATING PRESSURE PSI (BAR)**	DIMENSION A IN (MM)	DIMENSION B IN (MM)	WEIGHT LBS (KGS)
1 (4)	5,000 (345)	15.7 (399)	6.7 (170)	13.2 (6)
1.3 (5)	5,000 (345)	19.4 (493)	6.7 (170)	14.3 (6.5)

**Additional pressures available upon request.

Visit www.steelheadcomposites.com/about/lunch-learn/ to request a lunch and learn

CONTACT STEELHEAD COMPOSITES



720.524.3360



500 Corporate Circle, Suite O
Golden, CO 80401



www.steelheadcomposites.com



SHC/REV03/022117

Copyright © 2016 Steelhead Composites All Rights Reserved

Appendix R Efficiency Competition Spreadsheet

School	Precharge PSI	Max Pressure PSI	Accumulator Volume (in ³)	Weight Pounds	Distance Feet	Precharge PSIA	Max PSIA	Useable Volume (in ³) V1 - V2	Energy Out (lb Ft.) Weight x Ct (0.025) x Dis. (Ft)	Neutron-Meters	Average PSI	Input Energy (lb Ft.) Ave. PSI x in ³ of useable oil / 12	Joules	Eff (%) W/O Wind or Hill
Example	1,000.00	3,000.00	231.00	300.00	13,543.40	1,014.70	3,014.70	153.25	20,315.10	27,628.54	1,585.78	20,251.61	27,461.21	1.00
CP Pump W/ Ride	200.00	2,800.00	231.00	260.00	5,000.00	214.70	2,814.70	213.38	6,500.00	8,840.00	961.51	17,097.30	23,183.96	0.38
CP Souleiroid Cycle	200.00	2,795.00	231.00	260.00	5,600.00	214.70	2,809.70	213.35	7,280.00	9,900.80	960.05	17,068.75	23,145.25	0.43

Appendix S MSDS for the Hydraulic Fluid



Product Name: MOBIL EAL 224H
Revision Date: 06 Sep 2019
Page 1 of 10

SAFETY DATA SHEET

SECTION 1

PRODUCT AND COMPANY IDENTIFICATION

PRODUCT

Product Name: MOBIL EAL 224H
Product Description: Plant/Vegetable Oil
Product Code: 201560105010, 601831-00, 973407
Intended Use: Hydraulic fluid

COMPANY IDENTIFICATION

Supplier: EXXON MOBIL CORPORATION
22777 Springwoods Village Parkway
Spring, TX 77389 USA
24 Hour Health Emergency 609-737-4411
Transportation Emergency Phone 800-424-9300 or 703-527-3887 CHEMTREC
Product Technical Information 800-662-4525
MSDS Internet Address www.exxon.com, www.mobil.com

SECTION 2

HAZARDS IDENTIFICATION

This material is not hazardous according to regulatory guidelines (see (M)SDS Section 15).

Other hazard information:

HAZARD NOT OTHERWISE CLASSIFIED (HNOC): None as defined under 29 CFR 1910.1200.

PHYSICAL / CHEMICAL HAZARDS

No significant hazards.

HEALTH HAZARDS

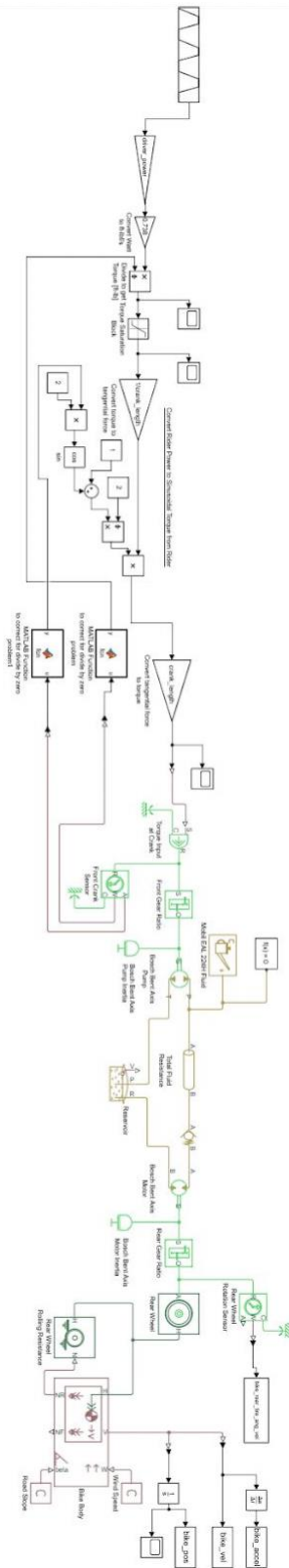
High-pressure injection under skin may cause serious damage. Mildly irritating to skin. May be irritating to the eyes, nose, throat, and lungs.

ENVIRONMENTAL HAZARDS

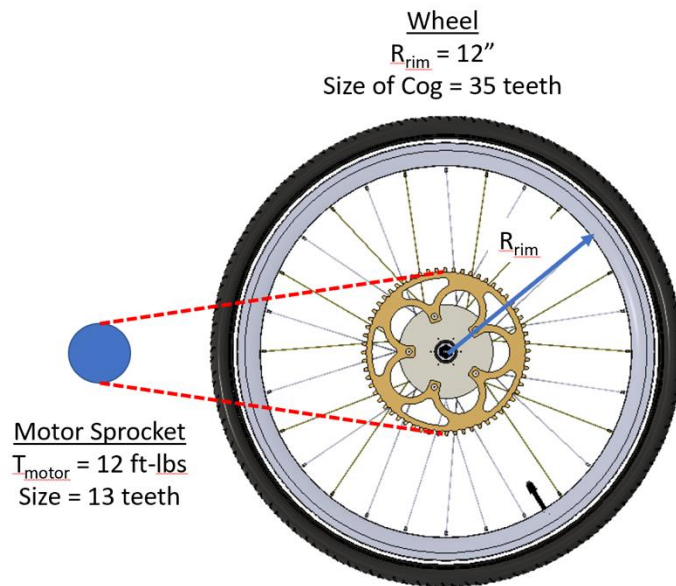
No significant hazards.

NFPA Hazard ID:	Health: 1	Flammability: 1	Reactivity: 0
HMIS Hazard ID:	Health: 1	Flammability: 1	Reactivity: 0

Appendix T Simscape Block Diagram



Appendix U Pneumatic Braking Force Calculation



$$T_{wheel} = T_{motor} * \frac{\text{wheel cog size}}{\text{motor sprocket size}}$$

$$T_{wheel} = 12 \text{ ft-lb} * \frac{35}{13}$$

$$T_{wheel} = 32.31 \text{ ft-lb}$$

$$F_{Brake} = T_{wheel} * R_{rim}$$

$$F_{Brake} = (32.31 \text{ ft-lb}) \left(\frac{12}{12} \right) \text{ ft}$$

$$\boxed{F_{Brake} = 32.31 \text{ lb}}$$